POLITECNICO
MILANO 1863

**DIPARTIMENTO DI ELETTRONICA
INFORMAZIONE E BIOINGEGNERIA**

DOCTORAL PROGRAMME IN BIOENGINEERING

ANTICIPATORY POSTURAL ADJUSTMENT OF GAIT INITIATION IN SUBJECTS WITH NEURO-DEGENERATIVE DISEASES: EXPERIMENTAL STUDY AND DYNAMIC MODEL SIMULATIONS

Doctoral Dissertation of:
Mariangela DIPAOLA

Supervisor:
Prof. Carlo A. FRIGO

Co-supervisor:
Prof. Ioannis U. ISAIAS
Julius-Maximilians-Universität Würzburg
and Dept. of Neurology, University Hospital Würzburg (Germany)

Tutor:
Prof. Silvia FARÈ

The Chair of the Doctoral Program:
Prof. Andrea ALIVERTI

Cycle XXVIII

INDEX

ABSTRACT

Anticipatory postural adjustments (APAs) represent a *feedforward* organization of a coherent set of motor commands (synergistic muscular activity) that are seen prior to an action producing a mechanical postural perturbation. Accordingly, APAs are fundamental in facilitating the set-up of the necessary condition of the forthcoming movement. This is clearly the case of gait initiation, during which the propulsive forces for the intended gait speed are generated. The study of APAs at gait initiation can therefore help understanding postural stability problems related to neurodegenerative diseases. In particular, in patients with great impairments due to disease severity, gait initiation is one of the few tasks available to investigate their locomotor behavior.

This thesis collects computational simulations and experimental analyses of gait initiation patterns in adults with neurodegenerative diseases (i.e. Parkinson's disease and Progressive Supranuclear Palsy). We have also investigated in healthy subjects the parameters of gait initiation that are influenced by anthropometrical measurements (e.g. distance between the feet) to better match patients and controls for comparisons.

Patients showed several abnormalities in APAs production and execution and lead to relevant advances in our understanding of motor control towards new patient-tailored rehabilitation and pharmacological strategies. Particularly helpful to the interpretation of data was the evaluation of the synergic activity of distal postural muscles (i.e. tibialis anterior and soleus muscles) that resulted variably desynchronized, segmented and delayed in most of the patients.

Finally, the development of a dynamic musculoskeletal model provided further information on the cause-effect relationships between the entity and the timing of the dorsiflexion of the ankle and the related displacement of the body mass. The simulation of pathological patterns of muscular activation further contributed to the interpretations of the results of the experimental section.

INTRODUCTION

Anticipatory postural adjustments (APAs) were first described by Belen'kii et al. (1967) who found that during movements, such as raising one arm while standing, the first muscles to be activated were the muscles of the leg involved in postural control, approximately 50-100 ms prior to the prime mover activation (Belen'kii, Gurfinkel, & Pal'tsev, 1967). These muscular activities were called "anticipatory" because their onset occurs prior to any movement itself (Massion, 1992). Quantitative characterization of the APAs (both as anticipatory muscular synergies as well as associated mechanical effects) may provide relevant information on the underlying motor programs, and how they are organized by the nervous system.

APAs are present also at gait initiation (Carlsöö, 1966; Mann, Hagy, White, & Liddell, 1979), they must be activated to shift the weight toward the stance leg, allowing the swing leg to be unloaded, and generating the propulsive forces necessary to start walking and reach the intended gait speed. The initiation of gait is interesting paradigm to study the control of human locomotion (Carlsöö, 1966), in particular from the perspective of the transition from upright posture to steady state walking. For this reason, APAs at gait initiation have been extensively investigated in healthy subjects and in patients with different neurological disorders. Indeed, an accurate study of the gait initiation could help us to understand the control of balance and investigate postural stability problems related to neurodegenerative diseases.

In the first part of the present work, we aimed to explore the alteration of gait initiation in patients with Parkinson's disease (PD) and Progressive Supranuclear Palsy (PSP). We selected these patients as they invariably suffer from impaired postural control along with disease progression, with often dramatic consequences (e.g. falls, fractures, hospitalization, loss of independence, etc.) (Hill, Stuart, Lord, Del Din, & Rochester, 2016; Michalowska, Fiszer, Krygowska-Wajs, & Owczarek, 2005). APAs were in this case interpreted as feed-forward commands aimed at minimizing the equilibrium disturbance associated with the movement performance (Massion, 1992). The great differences in gait initiation patterns seen in patients, prompted us to explore, in healthy subjects, the contribution of initial standing conditions (e.g. distance between the feet) and anthropometrical measurements on APAs measurements.

The impact of postural perturbations on APAs at gait initiation has been sparingly addressed (Dalton, Bishop, Tillman, & Hass, 2011; Rocchi et al., 2006), but it plays a relevant role, particularly in patients with movement disorders. Surprisingly, to our knowledge no study took into account the influence of the body size and lower limbs positioning at gait initiation. Still, these parameters could significantly alter APAs measurements and lead to bias in the interpretation of data.

We addressed this topic in the second part of this study. In particular, we investigated the variation of APAs measurements with respect to the distance between the feet expressed as percentage of an anthropometric measurement, i.e. the distance between anterior superior iliac spines (IFD%). This parameter was then used to compare patients with a selected group of matched healthy subjects.

In the third part of this study, we implemented a musculoskeletal model to simulate muscular activation and replicate synergies of lower limb muscles in standing position. This tool was used to provide further information on the cause-effect relationships between the altered muscle synergic activities observed in patients. The dynamic simulations, indeed, allowed us to reproduce the main muscular synergies of APAs at gait initiation, and to perform "what if?" studies by simulating the excitation pattern of a muscle and observing the resulting motion of the body center of mass.

AIM OF THE STUDY

The principal aim of this study was to investigate APAs at gait initiation as a surrogate marker of *feedforward* motor control in patients with neurodegenerative disorders. We combined experimental analyses and computational simulations to identify reliable APAs measurements to support the clinical follow-up and to develop new patient-tailored rehabilitation and pharmacological strategies.

OBJECTIVES

- To describe the changes of the biomechanical measurements of APAs at gait initiation due to anthropometric measurements (i.e. the distance between the feet at gait initiation).
- To investigate gait initiation abnormalities in neurodegenerative diseases compared with matched control groups (i.e. Parkinson's disease, Progressive Supranuclear Palsy).
- To implement a musculoskeletal model of muscular synergies of lower limb muscles in the standing position.

GAIT INITIATION IN PARKINSON'S DISEASE AND PROGRESSIVE SUPRANUCLEAR PALSY

Introduction

APAs at gait initiation are characterized by two sub-phases: a release phase or *imbalance* phase and an *unloading* phase (Mickelborough, Van Der Linden, Tallis, & Ennos, 2004) (Figure 1). During the imbalance phase, a bilateral relaxation of the soleus muscle (SOL) and a subsequent activation of the tibialis anterior (TA) (Cook & Cozzens, 1976; Elble, Moody, Leffler, & Sinha, 1994) move the centre of pressure (CoP) backward and toward the swing (leading) foot to produce a forward displacement of the body centre of mass (CoM) and, consequently, a postural inclination which allows a more effective propulsion of the body by contraction of calf muscles. The following unloading phase is characterized by a sharp reversal of CoP motion medially toward the stance (trailing) foot. With regards to the electromyography (EMG), the combined effect of SOL and TA aims to produce a dorsiflexion moment at the ankles and consequently a backward displacement of the CoP (Kirker, Simpson, Jenner, & Wing, 2000). The resulting misalignment between CoP and CoM produces a moment of force applied to the body and thus a rotation of the body forward and over the feet. The hip abductor muscles further contribute to the control of motion in the frontal plane during unloading phase (Winter, MacKinnon, Ruder, & Wieman, 1993; Winter, Prince, Frank, Powell, & Zabjek, 1996). The amplitude of SOL inhibition and TA activation is related to the pre-existing postural setting as well as the expected amount of perturbation of the equilibrium of the body caused by the subsequent movement. The relative timing between SOL inhibition and TA activation, and the consequent amplitude and the duration of APAs, inversely correlate with the velocity of steady-state gait (at the end of the first step) (Breniere & Do, 1986).
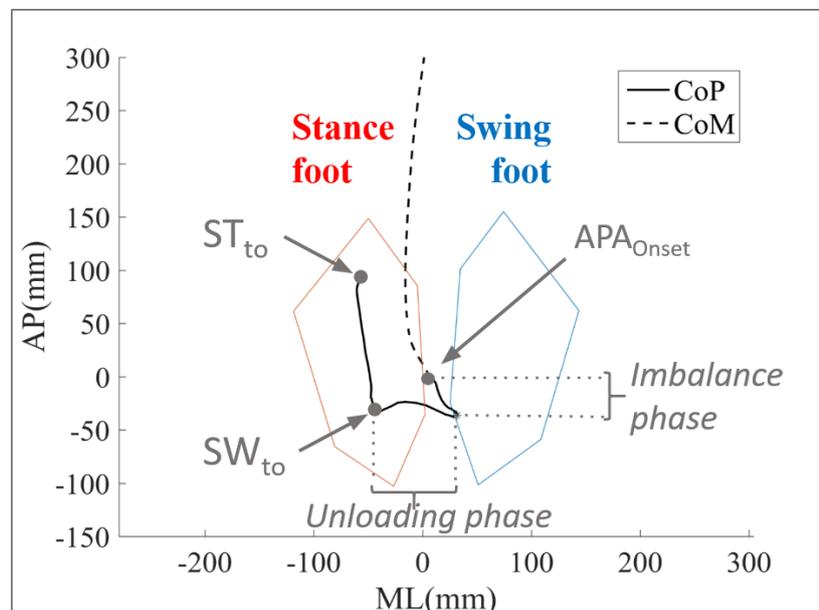

Figure 1. The CoP and CoM displacement during gait initiation in a healthy subject. Imbalance phase, from the instant APA_{Onset}, at which the CoP start moving backward, to the instant of heel-off of the swing foot (SW_{ho}). Unloading phase, from SW_{ho} to toe-off of the swing foot (SW_{to}). ST_{to} is the instant of toe-off of the stance foot.

Parkinson's disease: incidence, main symptoms, incidence and etiology

Parkinson's disease has been traditionally defined as a clinico-pathological entity associated, at autopsy, with neuronal loss and the presence of eosinophilic intracytoplasmic Lewy bodies in specific central and autonomic nervous structures, in particular the substantia nigra (dopaminergic). However, the pathology is usually much more widespread, also involving serotonergic raphe nuclei, the cholinergic nucleus basalis of Meynert, the cerebral cortex, the hypothalamus, the dorsal motor nucleus of vagus, the olfactory tract and sympathetic ganglia.

The incidence is 20 new cases per 100.000 population per year, with a prevalence of 187 cases per 100.000 population. For the population over 40 years of age, the prevalence rate is 347 per 100.000.

Although few genetic mutations (alpha-synuclein and LRKK2) can cause dominantly inherited or sporadic parkinsonism accompanied by Lewy bodies, the etiology of idiopathic PD is still largely unknown.

Akinesia is the defining, obligatory and principal disabling feature of PD. Almost all patients also display muscular rigidity to passive movement across a joint and up to 80% also display tremor at rest. In addition, flexed posture may be evident early in the disease, and postural instability is typically a late feature in PD. A host of other non-motor features (e.g. depression, anxiety, pain, sleep disruption and urinary urgency) may also occur and can be greatly disabling for PD patients.

The Hoehn and Yahr scale (HY) is a widely used clinical rating scale. At stage I, the patient has only unilateral involvement, with minimal or no functional impairment; at stage II, symptoms are bilateral without impairment of balance; at stage III, the first signs of impairment of righting reflexes appear; at stage IV, the patients are markedly incapacitated but still able to walk and stand unassisted; at stage V, the patient is confined to bed or wheelchair unless aided. The disease severity is instead evaluated by means of the Unified Parkinson's Disease Rating Scale (UPDRS).

Gait and gait initiation abnormalities in patients with Parkinson's disease at an early disease stage

At an early stage of PD (HY stage I or II), biomechanical measures of gait are usually reported as normal, with the exception of increased stride duration, difficulties in shifting between gait velocities and different phase lags between rotations of upper and lower body segments (Van Emmerik, Wagenaar, Winogrodzka, & Wolters, 1999; Winogrodzka, Wagenaar, Booij, & Wolters, 2005). Similarly, APAs at gait initiation are usually preserved in PD patients at an early clinical stage. However, the backward displacement of the CoP can be reduced during the imbalance phase and the swing phase of the first step can be prolonged (Carpinella et al., 2007). An impaired feedforward motor processing together with an adaptive strategy to minimize postural instability (Vaugoyeau et al., 2003) (Halliday et al., 1998) might explain these abnormalities. Still, the evaluation of EMG profiles usually show the typical pattern of healthy subjects (Crenna et al., 2006).

Gait abnormalities in patients with advanced Parkinson's disease

Several experimental studies have been performed to describe gait abnormalities in patients with PD. The majority of these studies focused on steady-state walking in advanced stages of the disease. The main findings can be summarized as follow:

- shortened stride length, prolonged stance and double support phases, reduced velocity (Ferrarin et al., 2002, 2005; Kimmeskamp & Hennig, 2001; Mitoma, Hayashi, Yanagisawa, & Tsukagoshi, 2000; Morris, Iansek, Matyas, & Summers, 1994a, 1996; Morris, Huxham, McGinley, Dodd, & Iansek, 2001; Morris, McGinley, Huxham, Collier, & Iansek, 1999; Nieuwboer et al., 1999; Vieregge, Stolze, Klein, & Heberlein, 1997). Of note, cadence can be normal, or slightly increased, as a possible adaptation to stride length reduction (Kimmeskamp & Hennig, 2001; Morris, Iansek, Matyas, & Summers, 1994a, 1996; Morris et al., 2005);
- trunk flexed forward with limited torsion and lateral bending (Mitoma et al., 2000; Morris et al., 2001);
- the range-of-motion (ROM) of lower and upper limbs is usually reduced (Ferrarin et al., 2005b; Mitoma et al., 2000; Morris et al., 2001; Morris et al., 1999 and 2005);
- the peaks of ground reaction forces at heel-strike and push-off as the peak of power production at lower limb joints are reduced (Ferrarin, Rizzone, Lopiano, Recalcati, & Pedotti, 2004; Kimmeskamp & Hennig, 2001; Mitoma et al., 2000; Morris et al., 1996, 1999; Nieuwboer et al., 1999).

Very few studies investigated energetic expenditure in PD patients, with unclear results mainly because PD patients were evaluated exclusively under the effect of dopaminergic medications (Maggioni et al., 2012), which can greatly varies between patients, or because patients were investigated when walking on a treadmill (Christiansen, Schenkman, McFann, Wolfe, & Kohrt, 2009), a condition that alters locomotion (Carpinella, Crenna, Rabuffetti, & Ferrarin, 2010; Cavagna, Heglund, & Taylor, 1977). To further describe, gait abnormalities in PD patients, with particular attention to their effect on energy expenditure, we have completed a study on mechanical energy recovery and its correlations with spatio-temporal gait parameters in PD patients at different disease stages (Dipaola et al., 2016, abstract below and full text in Appendix A).

Dipaola M, et al. (2016)
Mechanical Energy Recovery during Walking in Patients with Parkinson Disease
PLoS ONE 11(6): e0156420. doi:10.1371/journal.pone.0156420
Abstract – The mechanisms of mechanical energy recovery during gait have been thoroughly investigated in healthy subjects, but never described in patients with Parkinson disease (PD). The aim of this study was to investigate whether such mechanisms are preserved in PD patients despite an altered pattern of locomotion. We consecutively enrolled 23 PD patients (mean age 64±9 years) with bilateral symptoms (H&Y ≥III) if able to walk unassisted in medication- off condition (overnight suspension of all dopaminergic drugs). Ten healthy subjects (mean age 62±3 years) walked both at their 'preferred' and 'slow' speeds, to match the whole range of PD velocities. Kinematic data were recorded by means of an optoelectronic motion analyzer. For each stride we computed spatio-temporal parameters, time-course and range of motion (ROM) of hip, knee and ankle joint angles. We also measured kinetic (Wk), potential (Wp), total (WtotCM) energy variations and the energy recovery index (ER). Along with PD progression, we found a significant correlation of WtotCM and Wp with knee ROM and in particular with knee extension in terminal stance phase. Wk and ER were instead mainly related to gait velocity. In PD subjects, the reduction of knee ROM significantly diminished both Wp and WtotCM. Rehabilitation treatments should possibly integrate passive and active mobilization of knee to prevent a reduction of gait-related energetic components.

Gait initiation failure in advanced Parkinson's disease patients

Postural instability is a predominant clinical sign in advance stages of PD (Player, 2001) and it is a primary risk factor for falling (Matinolli et al., 2007). Falls in PD lead to severe injuries and fractures, which often result in hospitalization (Temlett & Thompson, 2006), reduced mobility and poor quality of life (Player, 2001). Gait initiation has been intensively studied in PD patients to describe the pathophysiological mechanisms of loss of postural control. Many authors focused on APAs (Burleigh-Jacobs, Horak, Nutt, & Obeso, 1997; Crenna et al., 2006; Crenna, Frigo, Giovannini, & Piccolo, 1990; Gantchev, Viallet, Aurenty, & Massion, 1996; Halliday, Winter, Frank, Patla, & Prince, 1998) mainly describing:

- the absence or reduction of anterior-posterior and lateral displacement of the CoP (Burleigh-Jacobs et al., 1997)
- a reduction of first step length and velocity (Crenna et al., 2006)
- desynchronized, segmented or absent muscular synergies associated with APAs (Crenna et al., 1990; Gantchev et al., 1996). It is of relevance to note that during locomotion the muscular (synergic) activity is preserved thus excluding a primary muscular disorder.

The abnormal APAs found in the advanced PD has been explained either with a deficient or ineffective commands for motor units recruitment (Gantchev et al., 1996; Vaugoyeau, Viallet, Mesure, & Massion, 2003) or as the results of impairments in proprioceptive-motor integration (Dietz, Swinnen, Heuer, Massion, & Casaer, 1994; Schieppati, Hugon, Grasso, Nardone, & Galante, 1994; Tatton, Eastman, Bedingham, Verrier, & Bruce, 1984). Proprioceptive inflow is involved in the internal representation of body geometry, including orientation of body axis (Vaugoyeau et al., 2003). This internal representation is reconstructed on the basis of a set of sensory-motor information, which play a central role in the maintenance of upright standing and in the transition position of the body from different equilibrium conditions. An altered proprioceptive processing might therefore explain the postural instability, documented in PD patients during forward and backward leaning (Schieppati et al., 1994) as well as the prolonged APAs and the reduction of backward shift of the CoP during the imbalance phase at gait initiation.

Progressive Supranuclear Palsy: main symptoms, incidence and etiology

Progressive supranuclear palsy (PSP) is neurodegenerative disease mainly characterized by axial akinesia and rigidity, early falls (classically backwards without warning) and a characteristic supranuclear gaze palsy (paresis) that is necessary for the clinical diagnosis and which gives the disease its name (Golbe, 2001; Maher & Lees, 1986). Besides motor symptoms, cognitive and behavioral abnormalities play an important role in the course of the disease. In particular, motor perseveration, slowness in thinking, impaired attention, impaired abstract thoughts, decreased verbal fluency as well as frontal behavioral disturbances have been reported.

The prevalence of PSP is about 5/100,000, mean age at onset is 63 years, never starting before 40, and mean survival is 7 years.

The pathology of PSP is unknown and involves neuronal loss and gliosis, with straight neurofibrillary tangles and tufted astrocytes particularly in substantia nigra, dentate nucleus, pallidum, subthalamic nucleus and, to a variable degree, cerebral cortex.

Gait abnormalities and gait initiation failure in patients with Progressive Sopranuclear Palsy

The mechanisms underlying postural instability in PSP are unclear. The relative paucity of information regarding postural control and gait function in PSP has been a limiting factor to define the pathophysiological mechanisms of falls in PSP and consequently to design of disease-specific therapeutic options. Besides our work, only one study investigated gait initiation of PSP patients (Amano et al., 2015) describing several abnormalities. In particular, during the imbalance phase, PSP patients move the CoP anteriorly and toward the stance foot, instead of posteriorly and toward the swing foot. Such a locomotor behavior rises however some difficulties in explaining how the CoM can be accelerated towards the stance foot, which were not clearly addressed by the authors. Indeed, Winter et al. (Winter, 1995) showed that the CoM acceleration is proportional to the distance between CoP and CoM (see also Martin et al., 2002). Furthermore, in the study of Amano and coll. it was not clear how the APAs phases very identified and there is no mention of the effect of the wide base of support adopted by PSP patients.

Materials and Methods

Participants

To investigate gait initiation differences in patients with parkinsonism, we enrolled 17 PD and 14 PSP patients (of 30 recruited) able to walk unassisted for at least three steps in medication-off condition (overnight suspension of all dopaminergic drugs). All patients had stable dopaminergic treatment for at least six months and were evaluated in the morning after overnight suspension of all dopaminergic drugs.

The diagnosis of PD was made according to the UK Brain Bank criteria and patients were evaluated with the Unified Parkinson Disease Rating Scale motor part (UPDRS-III). All PD patients improved (>20% at UPDRS-III score) after intake of 150-200 mg of L-Dopa (acute challenge test), thus further supporting the clinical diagnosis of idiopathic PD. PD patients with cognitive decline (Mini-Mental State Examination <27) or any other signs of neurological or psychiatric

disease other than PD were excluded. Patients with PD were divided into two groups according to the HY stage: mild group (PD$_M$: HY stage I or II), and severely affected group (PD$_S$: HY stage III or IV).

The diagnosis of PSP was established by a fellowship-trained movement disorders neurologist at the Parkinson Institute, Pini-CTO in Milan (Italy), using the National Institute of Neurological Disorders and Society for Progressive Supranuclear Palsy criteria for PSP (Litvan et al., 1996). We have enrolled only patients with PSP-P (parkinsonism) (other variants were excluded). The PSP rating scale (PSPRS) was adopted to clinically assess the subjects. Subjects who underwent major surgery (e.g. orthopedic surgery) were excluded. The local institutional review board (Section of Human Physiology, Department of Pathophysiology and Transplantation, University of Milan) approved the study and the consent procedure. All participants signed a written informed consent. All efforts were made to protect patient privacy and anonymity.

Experimental protocol

Participants were instructed to stand on a force platform located in the center of the walkway, standing in self-selected upright standing position, and to start walking spontaneously after a vocal prompt. The task was repeated three to five times, according to patients' capabilities. With regards to PSP patients, we have excluded the trials in which the patients were not able to stand unassisted in the upright position or lost their stability before the execution of the third step after gait initiation.

The leading limb and the initial feet position were self-selected, thus avoiding the bias of imposing a not-preferred (unnatural) posture or a masking-effect of disease-related abnormalities.

Recording system

Kinematic data were recorded using an optoelectronic system (SMART-E, BTS Bioengineering, Italy), consisting of six video cameras (sampling rate: 60 Hz; calibrated volume 4x2x1.5m). The position body segments of the subjects was determined by means of 29 retro-reflective markers (diameter: 15 mm) according to a published protocol (Carpinella et al., 2007). During the static calibration trial, eight additional "technical" markers were attached on the following bony landmarks on both sides of the body: greater trochanter, medial femoral condyle, medial malleolus, and first metatarsal head. The position of these points, not visible to the cameras during gait initiation, was computed offline by means of technical reference systems, assuming their relative position in relation to local reference frames was fixed. Anthropometric parameters of each subject were computed from the positions of the markers recorded during the calibration trial, and used for the estimation of internal joint centers, thus enabling calculation of lower limb kinematics.

The position of the CoP was measured by means of a dynamometric platform (KISTLER, GmbH, Winterthur, Switzerland) embedded in the floor (sampling rate 960 Hz).

In ten PD_M, seven PD_S and ten PSP patients we have also recorded surface electromyography (EMG) of the tibialis anterior (TA) and soleus (SOL) muscles bilaterally by means of a wireless system (FREEEMG 1000, BTS Bioengineering, Italy). Myoelectric signals were collected by pre-amplified Ag/AgCl electrodes (diameter: 25 mm, bipolar configuration, interelectrode distance: 20 mm) at a sampling frequency of 960 Hz and with a resolution of 16 bit and band-pass filtered ($f_{high-pass}$= 10 Hz, $f_{low-pass}$ =200 Hz). A digital zero-phase shift eight-order Butterworth high-pass filter with a cutoff frequency of 20 Hz was applied in order to remove movement artifacts. For limiting the passband, a high-pass filter of 300 Hz was also used, than the signal was rectified, and finally a low-pass filter of 3 Hz was used for smoothing the envelope (D. A. Winter & Yack, 1987).

Data Processing

We used ad-hoc algorithms to compute the whole body CoM trajectory (Dipaola et al., 2016, Appendix A). The CoM was computed with segmental analysis, estimating the position of the CoM of each body segment and the mass of each body segment from the anthropometric tables and regression equations provided by Zatsiorsky and Seluyanov (Zatsiorsky & Seluyanov, 1983). CoP data were under-sampled to 60 Hz to be time-synchronized to CoM data. Superimposition of CoM and CoP in the ground level plane was obtained by removing the respective average values computed in a steady state time window of 30 sec, before any occurrence of voluntary movement, so that CoP and CoM had common spatial origins, the same of CoP ones. Both CoP and CoM were expressed in the coordinate system integral with the subject's base of support defined by the external markers placed on both feet.

Events identification and parameters evaluated

During standing, the inter foot distance (IFD) was measured as the distance between the centers of the ankles estimated from the position of the markers on lateral and medial malleolus. The IFD was then expressed as a percentage of the distance between anterior superior iliac spines (ASIS) calculated by means of markers positioned on these anatomical landmarks. The normalized value of the inter foot distance is as IFD%.

The temporal transition between standing, APAs (imbalance and unloading phases) and first step are described in Figure 1.

The parameters extracted to describe the APAs were:
- the duration of imbalance and unloading phase
- the antero-posterior (AP) and medio-lateral (ML) shift of the CoP (%FL)

- the AP and ML mean velocity of the CoP (%FL/s). The AP displacements were considered positive if CoP moved forward and negative if went backward. ML displacements were positive if CoP moved toward the swing foot and negative when moved toward the stance foot.

For the first stepping phase, the parameters extracted were:
- the duration of the swing phase
- the length and the velocity of the first step of the swing foot. The length of the first step was defined as the measure of the anterior displacement of the ankle marker of the swing foot, from the initial standing position to next heel strike. The velocity of the first step was defined as the maximum value of the time derivative of the ankle marker displacement. Spatial parameters of the stepping phase were normalized on the basis of body height (%BH)
- the forward velocity of CoM at ST_{to}
- the forward velocity and acceleration of CoM at SW_{to}, that is the end of the unloading phase.

As surrogate measures of the efficiency of gait initiation, we evaluated:
- the magnitude (%FL) and the orientation (°) of the CoP-CoM vector with respect to the progression line at the end of imbalance phase and at the end of unloading phase (Isaias et al., 2014, Appendix B). These measurements are in our opinion of particular relevance as the CoP-CoM vector in the frontal and sagittal plane is directly influenced by the activity of the hip adduction/abduction muscles and the activity of inversion/eversion muscles at the ankle, respectively (D. A. Winter, 1995; David A. Winter, Patla, Ishac, & Gage, 2003).

Of note, angles were positive if opened toward swing foot and negative if opened toward the stance foot (Figure 2) so that in healthy subjects the angle was positive at the end of the unloading phase and negative at the end of imbalance phase.
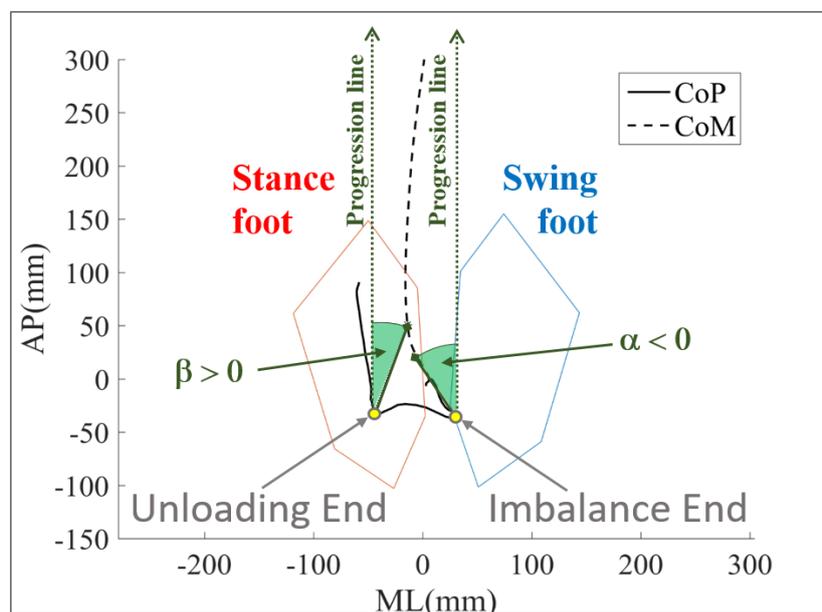

Figure 2. The orientation of the CoP-CoM vector with respect to the progression line at the end of imbalance phase and at the end of unloading phase, with the sign of the angles.

Statistics
Statistical analysis was performed using JMP statistical package (version 12.0, SAS Institute, Inc., Cary, NC, USA). Differences among groups were analyzed with Steel Dwass test. Correlations were investigated with a multivariate analysis on all trials (Spearman correlation coefficient). Given the great intra- and inter-subject

variability in the measurement of APAs at gait initiation, we have set for studies on patients a statistical threshold of p<0.01.

Results

Demographic and clinical data of the three groups were shown in Table 1. Biomechanical measurements are listed in Table 2 and 3.

Of note, the distance between the feet was larger in PSP than PD patients. There was no difference instead between PD_M and PD_S.

We found several differences in APAs at gait initiation (Figure 3). The imbalance phase was significantly longer in PSP than in PD groups (Table 3). In this phase, the CoP displacement and velocity were reduced in both directions (i.e. AP and ML) in PSP and PD_S when compared to PD_M.

The unloading phase was prolonged in PSP. The lateral displacement of the CoP during the unloading phase was greater in PSP than in PD. Furthermore, in PD at the end of the unloading phase the CoP displaced backward from its position at the beginning of the unloading phase, and slightly forward in PSP. The velocity of the CoP was slower in PSP particularly in ML direction.

With regards to the CoP-CoM vectors, both PD_S and PSP showed a decreased magnitude of both vectors when compared to PD_M (Table 4). The inclination of the CoP-CoM vector at the end of the imbalance phase was significantly greater in PD_S and PSP, while at the end of APAs it was strongly different among all the groups and, particularly, it was smaller in PD_M and greater in PSP. Accordingly, the velocity and the acceleration of CoM at the end of unloading phase, the velocity of CoM at stance toe off and the peak velocity of the first step were all significantly different among groups. The first step length was significantly reduced in PD_S and PSP compared to PD_M.

Table 1. Demographic and clinical data.
LEDD = L-Dopa Equivalent Daily Dose; UPDRS-III = Unified Parkinson's Disease Rating Scale motor part (III) in meds-off state; BMI = Body mass index. Disease duration was from motor symptoms onset. Values are means and standard deviation.

	PD_M	PD_S	PSP
N. (male/female)	10 (8/2)	7 (4/3)	15 (6/9)
N. of trials	31	19	35
Age (years)	62 ± 9	65 ± 8	65 ± 4
Weight (kg)	76.04 ± 14.4	71.4 ± 12.7	72.9 ± 8.5
Height (m)	1.68 ± 0.1	1.66 ± 0.1	1.62 ± 0.1
BMI	26.6 ± 3.6	26.1 ± 5.4	27.6 ± 4.1
Disease duration (years)	5 ± 2	12 ± 3	6.5 ± 2.5
UPDRS-III	19.8 ± 8.9	28.4 ± 9.2	
L-Dopa daily dose	325.0 ± 143.6	557.1 ± 225	
LEDD	443.3 ± 142.4	690.4 ± 205.6	

Discussion

When comparing patients with PD and PSP we first noticed a significant difference in the base of support during standing before gait initiation (Table 1).

A wide base of support is *per se* suggestive at a clinical level of balance problems. Given also the unknown relationship between IFD% and APAs measurements, we could not normalize for such value and directly draw any conclusion from the direct comparison of these patients groups. We therefore decided to investigate the influence of IFD% on gait initiation in healthy subjects. Of note, PD_M and PD_S likely did not differ for IFD% and these two groups were directly comparable (see also "Discussion", Chapter III).

Table 2. Inter-foot distance and CoP-heels distance during standing in PD_M, PD_S and PSP.
Superscript letters indicate statistically significant differences (p<0.01) between PD_M and PSP (a), PD_S and PSP (b). No significant difference was present between PD_M and PD_S. See text for statistical analysis. Abbreviations: FL: foot length.

	PD_M			PD_S			PSP		
	10th	**Median**	90th	10th	**Median**	90th	10th	**Median**	90th
IFD% (%)	34.3	**53.18 [a]**	63.02	39.66	**53.04 [b]**	71.02	55.18	**70.73 [a b]**	90.81
CoP-heels distance (%FL)	31.59	**41.78**	49.87	35.84	**39.66**	50.83	34.83	**39.99**	48.33

Table 3. Spatio-temporal parameters related to APAs in PD_M, PD_S and PSP.
Superscript letters indicate statistically significant differences (p<0.01) between PD_M and PSP (a), PD_S and PSP (b), PD_M and PD_S (c). See text for statistical analysis. Abbreviations: FL: foot length; AP: anterior-posterior; ML: medio-lateral.

	PD_M			PD_S			PSP		
	10th	**Median**	90th	10th	**Median**	90th	10th	**Median**	90th
Imbalance Parameters									
Duration (s)	0.2	**0.28 [a]**	0.35	0.21	**0.28**	0.46	0.25	**0.33 [a]**	0.88
AP avg. CoP displacement (%FL)	-25.8	**-13 [a, c]**	-2.54	-11.54	**-2.23 [c]**	1.57	-5.98	**-3.18 [a]**	6.01
ML avg. CoP displacement (%FL)	5.83	**15.86 [a, c]**	21.73	1.74	**6.26 [c]**	16.26	1.43	**7.33 [a]**	15.43
AP avg. CoP velocity (%FL/s)	13.15	**42 [a, c]**	102.1	0.33	**11.17 [c]**	48.37	3.16	**11.09 [a]**	19.15
ML avg. CoP velocity (%FL/s)	19.63	**55.38 [a, c]**	78.6	5.91	**19.25 [c]**	60.41	1.86	**18.96 [a]**	50.2
Unloading Parameters									
Duration (s)	0.2	**0.32 [a]**	0.53	0.23	**0.35 [b]**	1.35	0.33	**0.62 [a, b]**	1.37
AP avg. CoP displacement (%FL)	-11.4	**-3.44**	10.75	-13.3	**-8.17**	0.87	-14.52	**0.31**	17.83
ML avg. CoP displacement (%FL)	-27.5	**-48.75**	-60.7	-34.93	**-44.35 [b]**	-57.47	-39.18	**-56.47 [b]**	-70.88
AP avg. CoP velocity (%FL/s)	1.436	**20.24**	44.59	1.85	**16.67**	49.86	1.55	**11.28**	44.32
ML avg. CoP velocity (%FL/s)	74.84	**157.99 [a]**	248.3	33.77	**110.53**	190.05	45.6	**95.23 [a]**	160.07

Table 4. Parameters related to the APAs end and first step in PD_M, PD_S and PSP.
Superscript letters indicate statistically significant differences (p<0.01) between PD_M and PSP (a), PD_S and PSP (b), PD_M and PD_S (c). See text for statistical analysis. Abbreviations: BH: body height; AP: anterior-posterior; ML: medio-lateral; Imb.: Imbalance.

|	PD_M			PD_S			PSP		
	10th	**Median**	90th	10th	**Median**	90th	10th	**Median**	90th
CoP-CoM vector									
Magnitude at Imb. end (%BH)	1.5	**3.71 [a, c]**	5.68	0.44	**2.1 [c]**	3.22	0.55	**1.6 [a]**	2.96
Orientation at Imb. end (°)	-32.5	**-43.62 [a, c]**	-62.24	-34.83	**-60.61 [c]**	-80.78	-41.19	**-70.29 [a]**	-86.34
Magnitude at Unl. end (%BH)	3.95	**5.93 [a, c]**	8.51	3.42	**4.47 [c]**	6.96	2.37	**3.72 [a]**	5.6
Orientation at Unl. end (°)	18.77	**27.74 [a, c]**	44.56	29.43	**40.62 [b, c]**	63.12	35.74	**55.43 [a, b]**	73.53
CoM parameters									
AP velocity at ST_to (%BH/s)	29.06	**48.23 [a, c]**	66.39	10.3	**31.21 [b, c]**	36.6	4.7	**17.4 [a, b]**	31.42
AP velocity at Unl. end (%BH/s)	9.72	**13.03 [a, c]**	19.58	5.11	**8.28 [c]**	13.71	1.52	**6.51 [a]**	11.51
AP acceleration at Unl. end (%BH/s^2)	25.58	**49.64 [a]**	77.78	26.3	**35.9 [b]**	61.87	3.18	**23.36 [a, b]**	49.33
First step									
Swing duration (s)	0.5	**0.6 [a]**	0.75	0.47	**0.62 [b]**	0.75	0.65	**0.82 [a, b]**	1.34
Length (%BH)	18.15	**29.69 [a, c]**	37.61	10.44	**19.87 [c]**	24.65	3.17	**18.07 [a]**	28.74
Peak velocity (%BH/s)	67.74	**90.43 [a, c]**	124.18	50.6	**70.83 [b, c]**	95.37	20.12	**50.94 [a, b]**	82.89

11
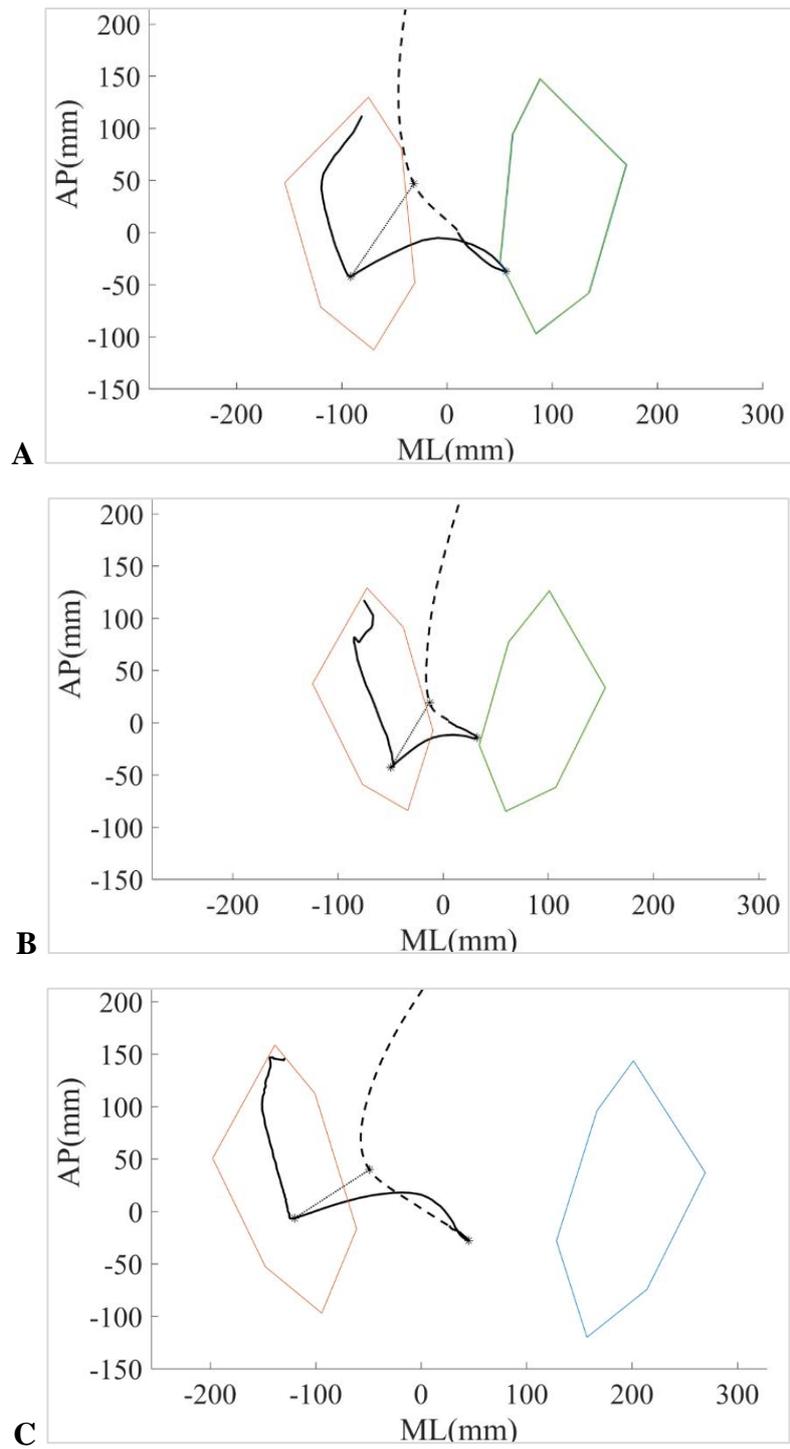
Figure 3: CoP and CoM displacements in the transverse plane in one representative PD_M subject (A), one representative PD_S subject (B) and one representative PSP subject (C). Plain line was for CoP and dotted line for CoM.

CHAPTER II

THE ANTICIPATORY POSTURAL ADJUSTMENTS OF GAIT INITIATION IN HEALTHY SUBJECTS: THE EFFECT OF INTERFOOT DISTANCE

Introduction

Despite its great relevance, the effect of posture, and feet positioning in particular, on APAs production at gait initiation has been poorly investigated. Dalton and coll. evaluated the influence of the position of the swing limb foot on the gait initiation in a group of patients with Parkinson's disease (Dalton et al., 2011). They found that, when translating the swing foot posteriorly to the stance foot by half the foot length, the magnitude of the propulsive force and the resulting CoM velocity throughout the stepping phase were significantly increased. Rocchi and coll. have also shown that the widening of the initial base of support leads to greater loading of the swing limb and to an increased step velocity in subjects with PD (Rocchi et al., 2006). They found a larger backward displacement of the CoP when the feet where wide apart (26 cm) rather than at a narrow distance (5 cm). Of relevant note, in these studies the authors did not take into account the mass distribution of the subjects, which could lead to a bias in the interpretation of data. Given also our previous experience with PD and PSP patients (cfr. Chapter I), we found mandatory at this point to analyze the influence of the variation of the inter foot distance normalized for pelvis width on gait initiation performance.

Materials and Methods

Participants

Eight healthy subjects (mean age 62 ± 4 years, weight 80.7 ± 5.9 kg, height 1.7 ± 0.05 m).

Experimental protocol

Subjects were instructed to stand on a force plate and to start walking spontaneously after a vocal prompt. The leading limb and the initial position of the feet were self-selected. All subjects started walking five times with a preferred distance between the feet and five times with a wide base of support (the distance between the ankle joint centers was increased by 80% respect to preferred position). The initial stepping limb was self-selected.

Recording system, data processing, events identification and parameters evaluated

Recording system, data processing, events identification and the parameters evaluated were already described in Chapter I.

Statistics

As in Chapter I.

Results

At APA_{Onset}, the distance of the CoP from line connecting the heels negatively correlated with its displacement during the imbalance phase ($\rho= -0.49$): the more distant (posterior) the CoP was from the line connecting the heels, the less it moved backward during the imbalance phase. Furthermore, the backward position of the CoP during standing was correlated with the swing duration ($\rho= -0.32$), the first step length and velocity ($\rho= 0.47$ and $\rho= 0.56$, respectively), and the magnitude of the CoP-CoM vector at the end of unloading phase ($\rho= 0.48$). Of note, the distance between the CoP and the heels during standing did not differ between preferred (44.68%FL) and wide (45.13%FL) distance between the feet.

The IFD% positively correlated with the lateral displacement of the CoP during imbalance ($\rho= 0.4$) and unloading phase ($\rho= 0.8$) (Figure 4, top and middle respectively). IFD% correlated positively also with the first step length ($\rho= 0.38$) (Figure 4, bottom). We also found a positive correlation between IFD% and the magnitude of the vector at the end of imbalance ($\rho= 0.46$) and unloading phase ($\rho= 0.41$), and between IFD% and the orientation of the vector with respect to the progression line at the end of unloading phase ($\rho= 0.64$) but not at the end of the imbalance phase (Figure 5).
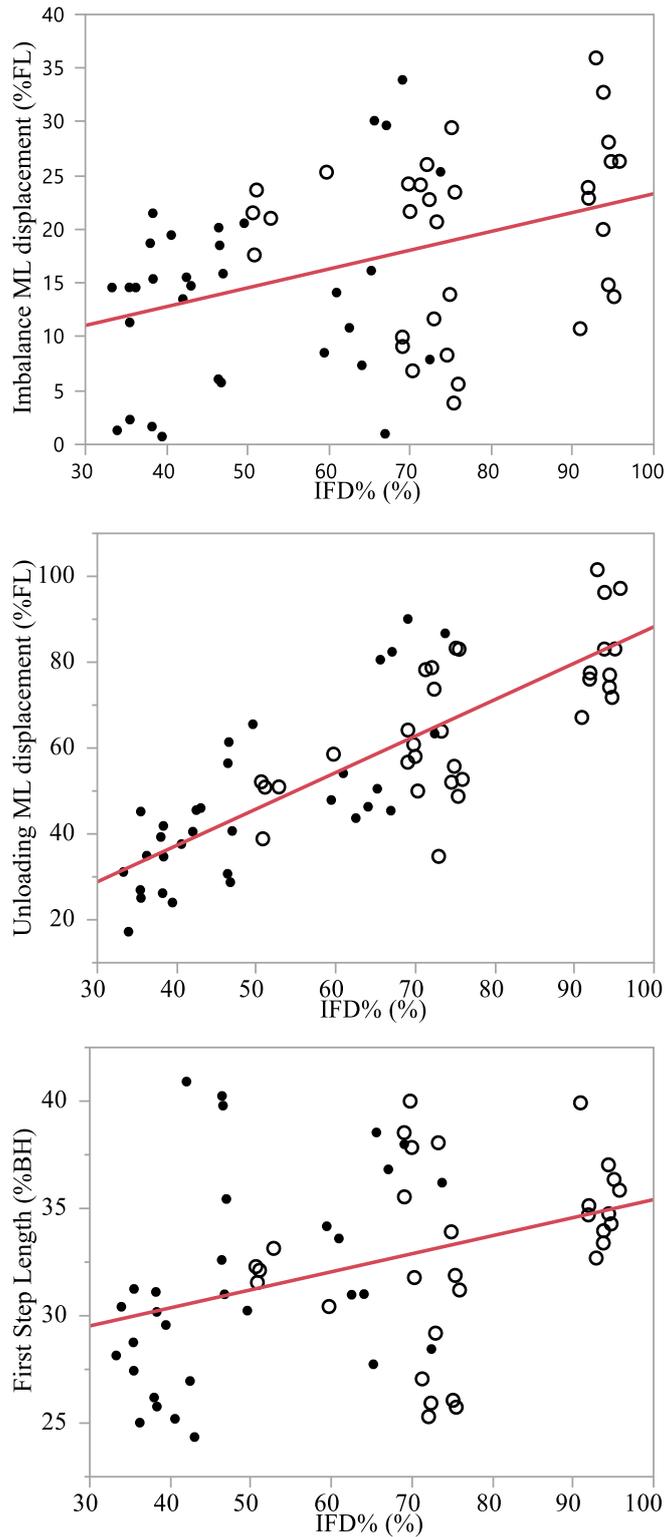
Figure 4. *Linear fit of the relationship between the imbalance ML displacement of CoP and the IFD% (top), the unloading ML displacement of CoP and the IFD% (middle) and the the first step of the swing foot and the IFD% (bottom).*
Black circles represent trials starting from preferred foot position (4 trials per subject), empty circles indicates trials in which subjects start walking from an 80% larger base of support (4 trial per subject).

.
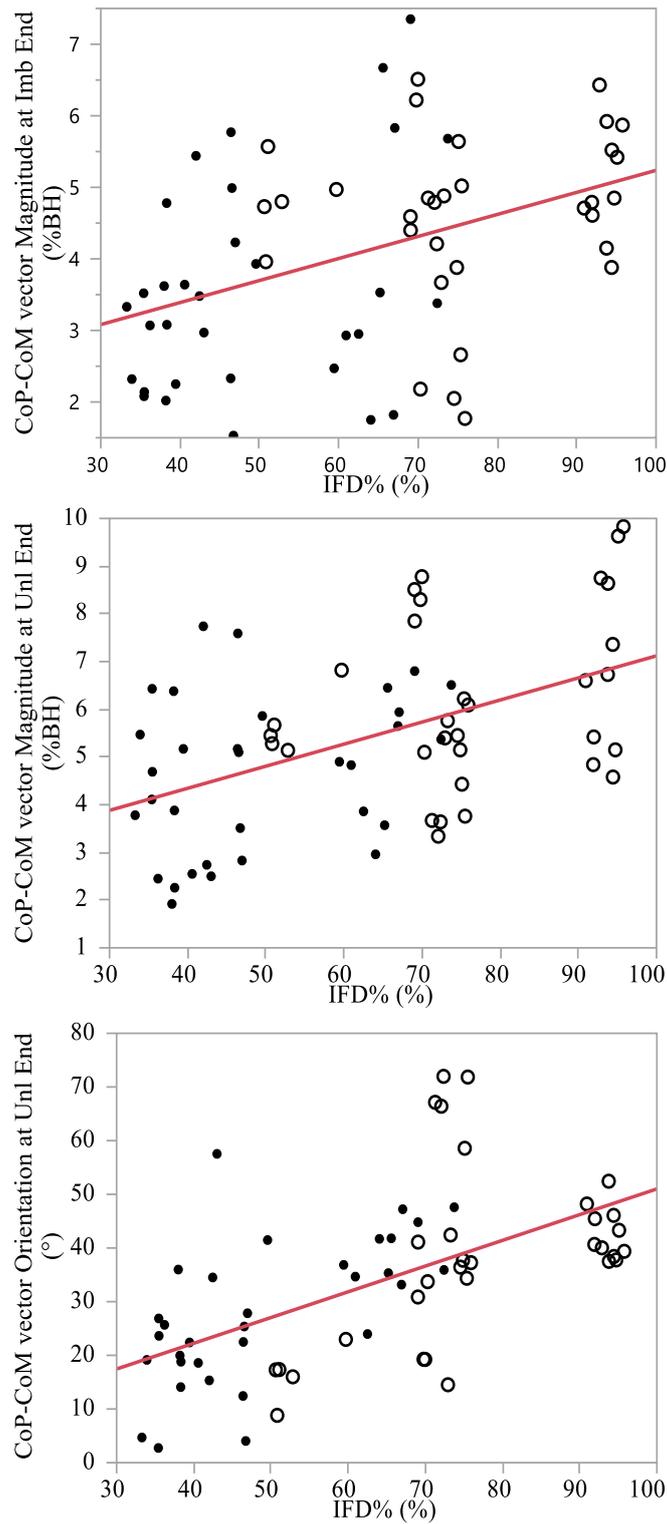
Figure 5. *Linear fit of the relationship between the magnitude of the CoP-CoM vector and the IFD% at the end of imbalance phase (top) and at the end of unloading phase (middle) and linear fit of the relationship between the orientation of the CoP-CoM vector at the end of unloading phase and the IFD% (bottom). Black circles represent trials starting from preferred foot position (4 trials per subject), while empty circles indicates trials in which subjects start walking from an 80% larger base of support (4 trials per subject).*

Discussion

In agreement with previous findings (Rocchi et al., 2006), we confirmed that the ML displacement of the CoP during APAs at gait initiation is strongly influence by the IFD%. More importantly, the AP displacement of the CoP does not seem to be influenced by the IFD%, thus providing a robust measurement, in particular for pathological conditions characterized by a wide base of support. Of note, Rocchi and coll. reported a larger backward displacement of the CoP when starting to walk with a wide (26 cm) rather than a narrow (5 cm) distance between the feet. The discrepancy with our findings could be mainly due to the normalization. Indeed, in the study of Rocchi and coll. the subjects were not evaluated when starting from their preferred distance between the feet, the position of the feet was imposed in parallel and the distance between the feet was fixed and not related to any anthropometrical measurement (Rocchi et al., 2006).

The length of the first step increased with the increment of IFD%, thus meaning that the initial stance condition directly influences the stepping phase. Of note, we cannot exclude that a increased step length when starting to walk with a wide IFD% was merely related to the unusual (not preferred) standing posture.

The magnitude and the orientation of the CoP-CoM vector at the end of APAs positively correlated with the IFD%. The forward velocity and acceleration of the CoM at the end of each APAs phases (i.e. imbalance and unloading) was instead not influenced by IFD%. These findings suggest that the evaluation of the CoM is a valuable measurement at the end of APAs, whereas the CoP-CoM vector is greatly influenced by the initial condition of stance and cannot be considered significant to further interpret the modulation of the CoM during gait initiation. On the other hand, the orientation of the CoP-CoM vector at the end the imbalance phase was not influenced by the initial condition of stance.

In conclusion, our results suggest the importance of the initial stance conditions when investigating APAs at gait initiation. The AP displacement of the CoP during the imbalance phase, as well as the forward velocity and acceleration of the CoM, and the orientation of CoP-CoM vector at the end of imbalance phase are the most reliable measurements as not influenced by the distance between the feet.

CHAPTER III

EXPERIMENTAL STUDY ON GAIT INITIATION IN NEURODEGENERATIVE DISEASES: PARKINSON'S DISEASE AND PROGRESSIVE SOPRANUCLEAR PALSY

Introduction
In this chapter, we reanalyzed the biomechanical measurements of PD and PSP patients (cfr. Chapter I) and compared them with selected groups of healthy control subjects matched for IFD% (cfr. Chapter II). Unfortunately, only few PD and PSP patients matched for IFD% and a comparison between the two diseases could be only indirectly attempted. Of relevant note, we did not force the patients to start walking with an imposed feet position, thus avoiding the bias of imposing a not-preferred (unnatural) posture or a masking-effect of disease-related abnormalities.

Material and methods
Participants
We selectively enrolled 17 PD and 14 PSP patients able to walk unassisted for at least three steps in medication-off condition (overnight suspension of all dopaminergic drugs) and 13 age-matched healthy subjects as controls (HC). Clinical and demographic characteristic are listed in Table 1 of Chapter I.
The local institutional review board (Section of Human Physiology, Department of Pathophysiology and Transplantation, University of Milan) approved the study and the consent procedure. All participants signed a written informed consent. All efforts were made to protect patient privacy and anonymity.

Experimental protocol
Please refer to Chapter I and II. Of relevant note to this part of the study, the leading limb and the initial feet position were self-selected, thus avoiding the bias of imposing a not-preferred (unnatural) posture or a masking-effect of disease-related abnormalities. We selected the trails of HC that were included between the 25th and 75th percentile of all IFD% of all recordings of each group of patients. Therefore, PD$_M$, PD$_S$ and PSP were compared to a different subgroup of trials of HC.

Recording system, data processing, events identification and parameters evaluated
Recording system, data processing, events identification and the parameters evaluated were already described in Chapter I and II.

Statistics
As in Chapter I.

Results
Patients with Parkinson's disease at an early stage
Demographic and clinical data are listed in Table 5. PD$_M$ showed only minimal differences in comparison to HC. During standing, in PD$_M$ the position of the CoP (AP coordinate) was more posterior (closer to the heels) than in HC (Table 6). At the end of the unloading phase, in PD$_M$ the CoP positioned backward from its original position (at the beginning of the unloading phase) and therefore nearer to the line connecting the heels, whereas in HC it was always placed forward (Table 7). The CoP displacement and EMG activity during gait initiation in HC and PD$_M$ are shown in Figure 6 and in Figure 7, respectively. A fragmented activity of TA between the imbalance and the unloading phases, as well as a delayed SOL activity, may have accounted for such a displacement of the CoP during the unloading phase (Figure 7).
Concerning the CoP-CoM vectors, the magnitude at the end of the unloading phase was significantly reduced in PD$_M$ in comparison with HC (Table 8).

Table 5. Demographic and clinical data. *Disease duration was calculated from motor symptoms onset. Values are means ± standard deviation. Abbreviations: BMI = Body mass index; HC= healthy controls; HY = Hoehn and Yahr stage; LEDD = L-Dopa Equivalent Daily Dose; UPDRS-III = Unified Parkinson's Disease Rating Scale motor part (III) in meds-off state; PD_M = patients with mild Parkinson's disease (HY stage I-II).*

	HC	PD_M (HY: I-II)
N. (male/female)	8 (7/1)	10 (8/2)
N. of trials	33	31
Age (years)	62 ± 4	62 ± 9
Weight (kg)	80.7 ± 5.9	76.04 ± 14.4
Height (m)	1.7 ± 0.05	1.7 ± 0.1
BMI	26.6 ± 2.6	26.6 ± 3.6
Disease duration (years)		5 ± 2
UPDRS-III		19.8 ± 8.9
L-Dopa daily dose		325.0 ± 143.6
LEDD		443.3 ± 142.4

Table 6. Inter-foot distance and CoP-heels distance during standing. *Superscript asterisk indicate statistically significant differences at p<0.01 between groups. See text for statistical analysis.*

	HC			PD_M		
	10th	Median	90th	10th	Median	90th
IFD% (%)	45.21	50.03	58.53	34.3	53.18	63.02
CoP-heel distance (%FL)	39.57	46.44 *	53.1	31.59	41.78 *	49.87

Table 7. Spatio-temporal parameters related to APAs phases. *Superscript asterisk indicate statistically significant differences at p<0.01 between groups. See text for statistical analysis.*

	HC			PD_M		
	10th	**Median**	90th	10th	**Median**	90th
Imbalance Parameters						
Duration (s)	0.236	**0.28**	0.421	0.2	**0.27**	0.35
AP avg. CoP displacement (%FL)	-16.86	**-10.24**	-3.50	-25.81	**-13.03**	-2.54
ML avg. CoP displacement (%FL)	5.8	**16.74**	23.26	5.83	**15.86**	21.73
AP avg. CoP velocity (%FL/s)	14.12	**33.13**	58.65	13.15	**42**	102.1
ML avg. CoP velocity (%FL/s)	17.13	**50.19**	91.4	19.63	**55.38**	78.6
Unloading Parameters						
Duration (s)	0.23	**0.33**	0.48	0.20	**0.32**	0.53
AP avg. CoP displacement (%FL)	-6.41	**2.23 ***	18.54	-11.36	**-3.44 ***	10.75
ML avg. CoP displacement (%FL)	-28.64	**-46.64**	-70.33	-27.5	**-48.75**	-60.72
AP avg. CoP velocity (%FL/s)	1.71	**6.6**	32.99	1.436	**20.24**	44.59
ML avg. CoP velocity (%FL/s)	63.39	**124.37**	245.2	74.84	**157.99**	248.3

Table 8. Parameters related to the APAs end and first step in PD_M and HC with comparable IFD%. *Superscript asterisk indicate statistically significant differences at p<0.01 between groups. See text for statistical analysis. Abbreviations: AP: anterior-posterior; BH: body height; Imb.: Imbalance; ML: medio-lateral; Unl.: unloading.*

	HC			PD_M		
	10th	**Median**	90th	10th	**Median**	90th
CoP-CoM vector						
Magnitude at Imb. end (%BH)	1.71	**3.75**	4.95	1.51	**3.71**	5.68
Orientation at Imb. end (°)	-36.92	**-52.09**	-68.90	-32.55	**-43.62**	-62.24
Magnitude at Unl. end (%BH)	2.95	**4.9 ***	6.12	3.95	**5.93 ***	8.51
Orientation at Unl. end (°)	9.22	**25.37**	53.70	18.77	**27.74**	44.56
CoM parameters						
AP velocity at ST_{to} (%BH/s)	29.65	**42.82**	57.1	29.06	**48.23**	66.39
AP velocity at Unl. end (%BH/s)	8.58	**13.52**	17.52	9.72	**13.03**	19.58
AP acceleleration at Unl. end (%BH/s²)	18.08	**44.88**	57.52	25.58	**49.64**	77.78
First step						
Swing duration (s)	0.54	**0.65**	0.88	0.50	**0.6**	0.746
Length (%BH)	23.67	**30.24**	38.02	18.15	**29.69**	37.61
Peak velocity (%BH/s)	71.03	**95.86**	124.15	67.74	**90.43**	124.18
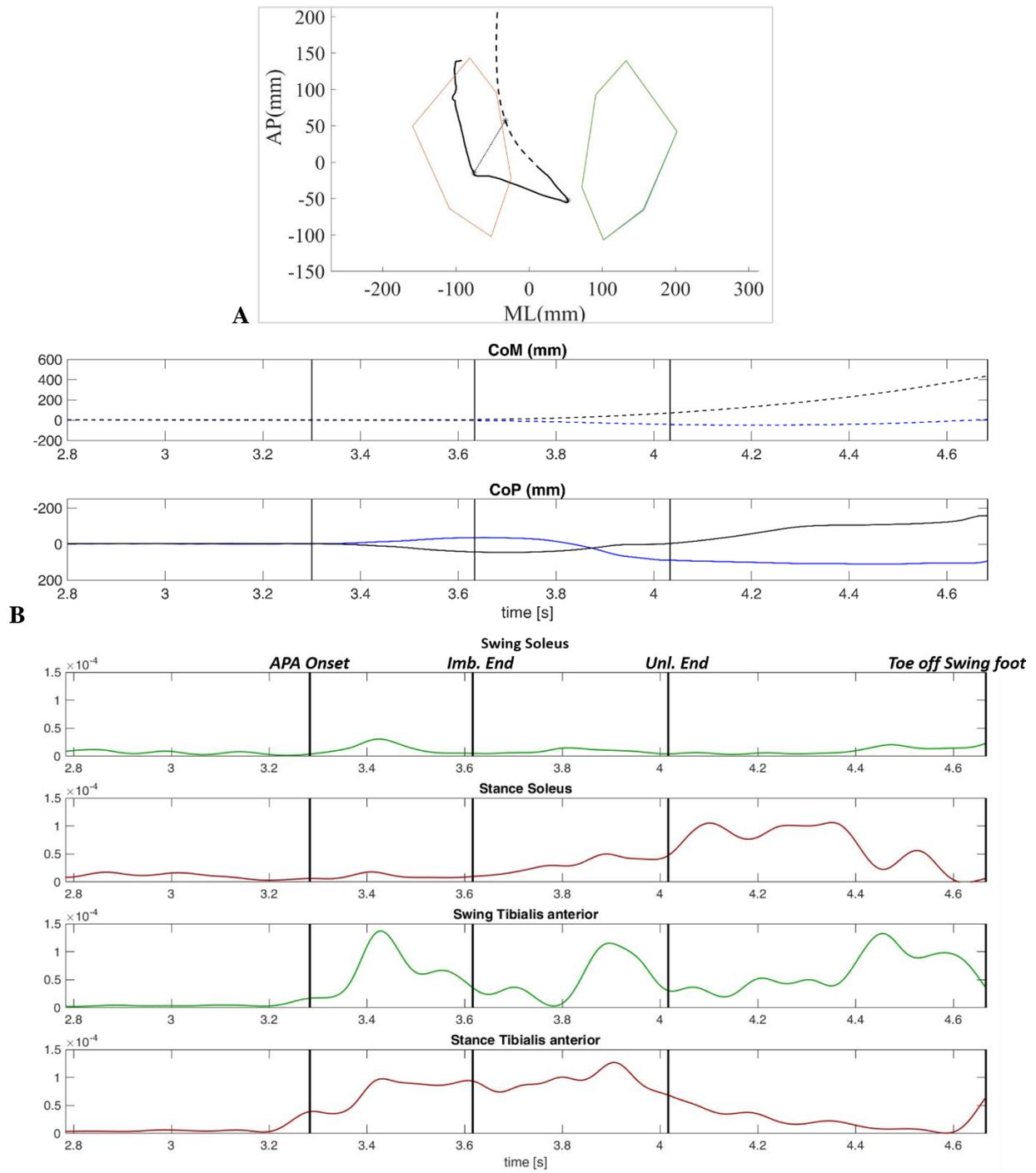
Figure 6. A: CoP and CoM displacements in the transverse plane in one representative HC subject. Plain line was for CoP and dotted line for CoM. B: CoP and CoM displacements in time. Black line was for AP displacement and blue line for ML displacement. C: the related EMG activity during the APAs of gait initiation. Unit of the EMG traces was V.
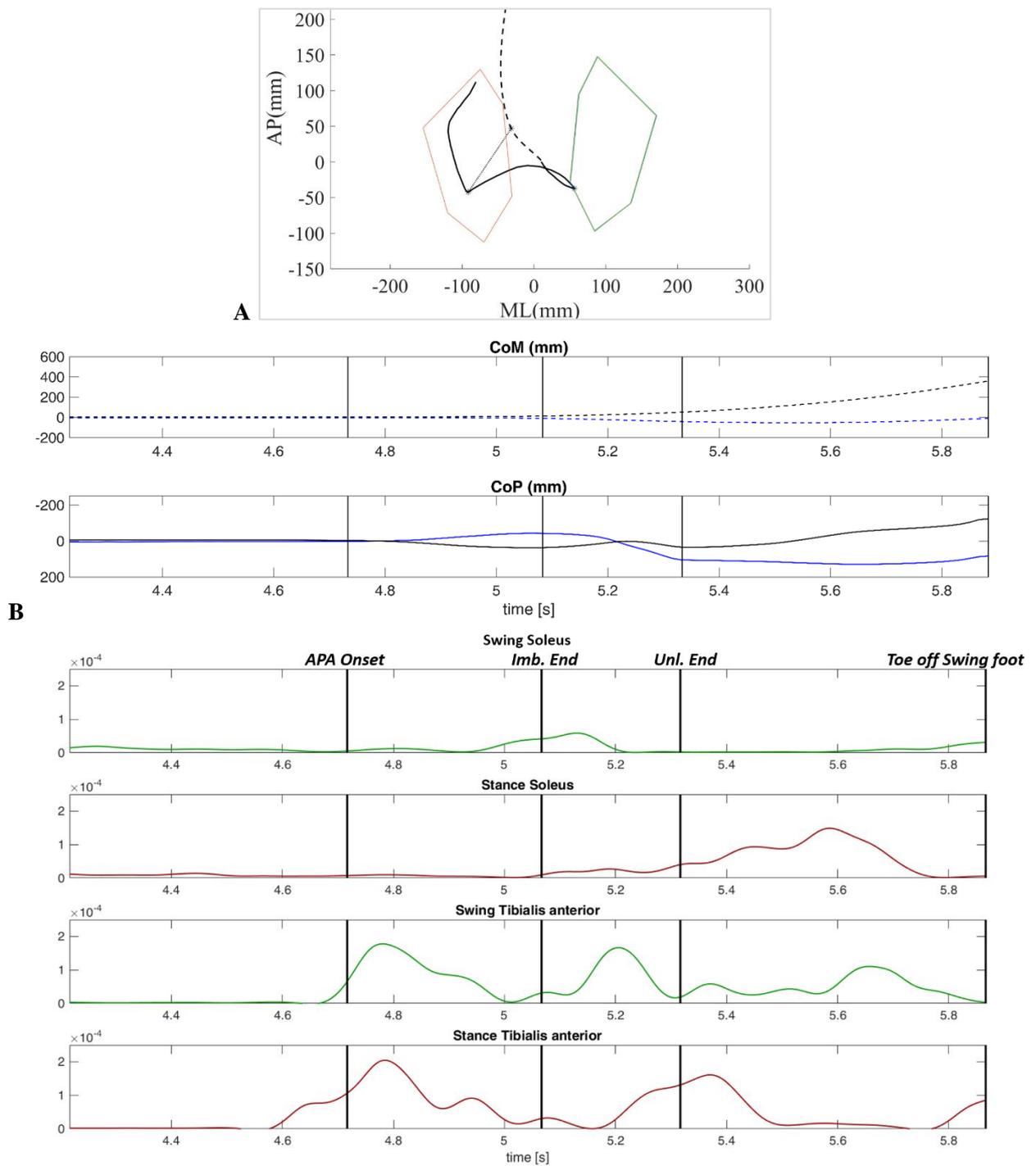
Figure 7. A: *CoP and CoM displacements in the transverse plane in one representative PD_M subject. Plain line was for CoP and dotted line for CoM.* **B:** *CoP and CoM displacements in time. Black line was for AP displacement and blue line for ML displacement.* **C:** *the related EMG activity during the APAs of gait initiation. Unit of the EMG traces was V.*

Patients with Parkinson's disease at an advanced stage

Demographic and clinical data are listed in **Errore. L'autoriferimento non è valido per un segnalibro.**.

Along with disease progression, we were able to describe several abnormalities in APAs production at gait initiation.

The position of the CoP (AP coordinate) at the end of the unloading phase was still more posterior in PD_S than HC, as for PD_M, but in this case it did not reached a statistical significance (Table 10). Both AP and ML displacements and velocities during the imbalance and unloading phases were greatly reduced in PD_S (Table 11).

Moreover, at the end of the unloading phase the CoP positioned more backward (negative AP CoP displacement) and lateral (high CoP-CoM angle at Unl. end). Concerning the CoP-CoM vector, it is worth noticing that the magnitude at the imbalance end was reduced in PD_S, thus suggesting ineffective APAs. These findings were also corroborated by the reduced AP velocity of CoM both at ST_{to} and SW_{to}. Accordingly, the first step was shorter and slower in PD_S than HC (Table 12).

Muscular synergies of TA and SOL in PD_S are reduced, delayed and disaggregated. In particular, the silencing/reactivation bursting of the SOL was greatly diminished and the CoP displacement was mainly modulated by a activation/deactivation of the TA (Figure 8).

Table 9. Demographic and clinical data.
LEDD = L-Dopa Equivalent Daily Dose; UPDRS-III = Unified Parkinson's Disease Rating Scale motor part (III) in meds-off state; BMI = Body mass index. Disease duration was from motor symptoms onset. Values are means and standard deviation.

	HC	PD_S (HY: III-IV)
N. (male/female)	11 (10/1)	7 (4/3)
N. of trials	49	19
Age (years)	62 ± 4	65 ± 8
Weight (kg)	80.1 ± 4.8	71.4 ± 12.7
Height (m)	1.7 ± 0.05	1.7 ± 0.1
BMI	26.3 ± 2	26.1 ± 5.3
Disease duration (years)		12 ± 3
UPDRS-III		28.4 ± 9.2
L-Dopa daily dose		557.1 ± 225.0
LEDD		690.4 ± 205.6

Table 10. Inter-foot distance and CoP-heels distance in during standing in PD_S and HC

	HC			PD_S		
	10th	**Median**	90th	10th	**Median**	90th
IFD% (%)	46.38	**54.38**	64.62	39.66	**53.04**	71.02
CoP-heel distance (%FL)	38.1	**44.11**	52.18	35.84	**39.66**	50.83

Table 11. Spatio-temporal parameters related to imbalance phase in PD_S and HC with comparable IFD%.
Superscript asterisk indicate statistically significant differences (p<0.01) between HC and PD_S. See text for statistical analysis. Abbreviations: FL: foot length; AP: anterior-posterior; ML: medio-lateral.

	HC			PD_S		
	10th	**Median**	90th	10th	**Median**	90th
Imbalance Parameters						
Duration (s)	0.25	**0.28**	0.4	0.212	**0.28**	0.464
AP avg. CoP displacement (%FL)	-16.51	**-7.9 ***	-2.42	-11.54	**-2.23 ***	1.57
ML avg. CoP displacement (%FL)	5.59	**14.13 ***	23.67	1.74	**6.26 ***	16.26
AP avg. CoP velocity (%FL/s)	8.54	**27.63 ***	58.15	0.33	**11.17 ***	48.37
ML avg. CoP velocity (%FL/s)	16.91	**43.51 ***	83.63	5.91	**19.25 ***	60.41
Unloading Parameters						
Duration (s)	0.27	**0.38**	0.58	0.23	**0.35**	1.35
AP avg. CoP displacement (%FL)	-7.8	**3.47 ***	15.06	-13.3	**-8.17 ***	0.87
ML avg. CoP displacement (%FL)	30.97	**50.52**	67.97	34.93	**44.35**	57.47
AP avg. CoP velocity (%FL/s)	1.52	**7.07**	30.38	1.85	**16.67**	49.86
ML avg. CoP velocity (%FL/s)	66.85	**129.87**	240.3	33.77	**110.53**	190.1

Table 12. Parameters related to the APAs end and first step in PD_S and HC with comparable IFD%.
Superscript asterisk indicate statistically significant differences (p<0.01) between HC and PD_S. See text for statistical analysis. Abbreviations: BH: body height; AP: anterior-posterior; ML: medio-lateral; Imb.: Imbalance; Unl.: unloading. Angles were positive if opened toward swing foot and negative if opened toward the stance foot, so that they were positive at the end of unloading phase and negative at the end of imbalance phase.

	HC			PD_S		
	10th	**Median**	90th	10th	**Median**	90th
CoP-CoM vector						
Magnitude at Imb. end (%BH)	1.53	**3.35 ***	4.97	0.44	**2.1 ***	3.22
Orientation at Imb. end (°)	-37.04	**-55.13**	-72.75	-34.83	**-60.61**	-80.78
Magnitude at Unl. end (%BH)	2.28	**4.76**	6.28	3.42	**4.47**	6.96
Orientation at Unl. end (°)	9.95	**29.73 ***	59.59	29.43	**40.62 ***	63.12
CoM parameters						
AP velocity at ST_{to} (%BH/s)	29.31	**42.82 ***	56.32	10.3	**31.21 ***	36.6
AP velocity at Unl. end (%BH/s)	8.16	**13.4 ***	17.3	5.11	**8.28 ***	13.71
AP acceleleration at Unl. end (%BH/s^2)	17.14	**42.82**	56.73	26.3	**35.9**	61.87
First step						
Swing duration (s)	0.55	**0.67**	0.97	0.47	**0.62**	0.75
Length (%BH)	25.03	**29.97 ***	35.44	10.44	**19.87 ***	24.65
Peak velocity (%BH/s)	69.23	**91.2 ***	111.2	50.6	**70.83 ***	95.37
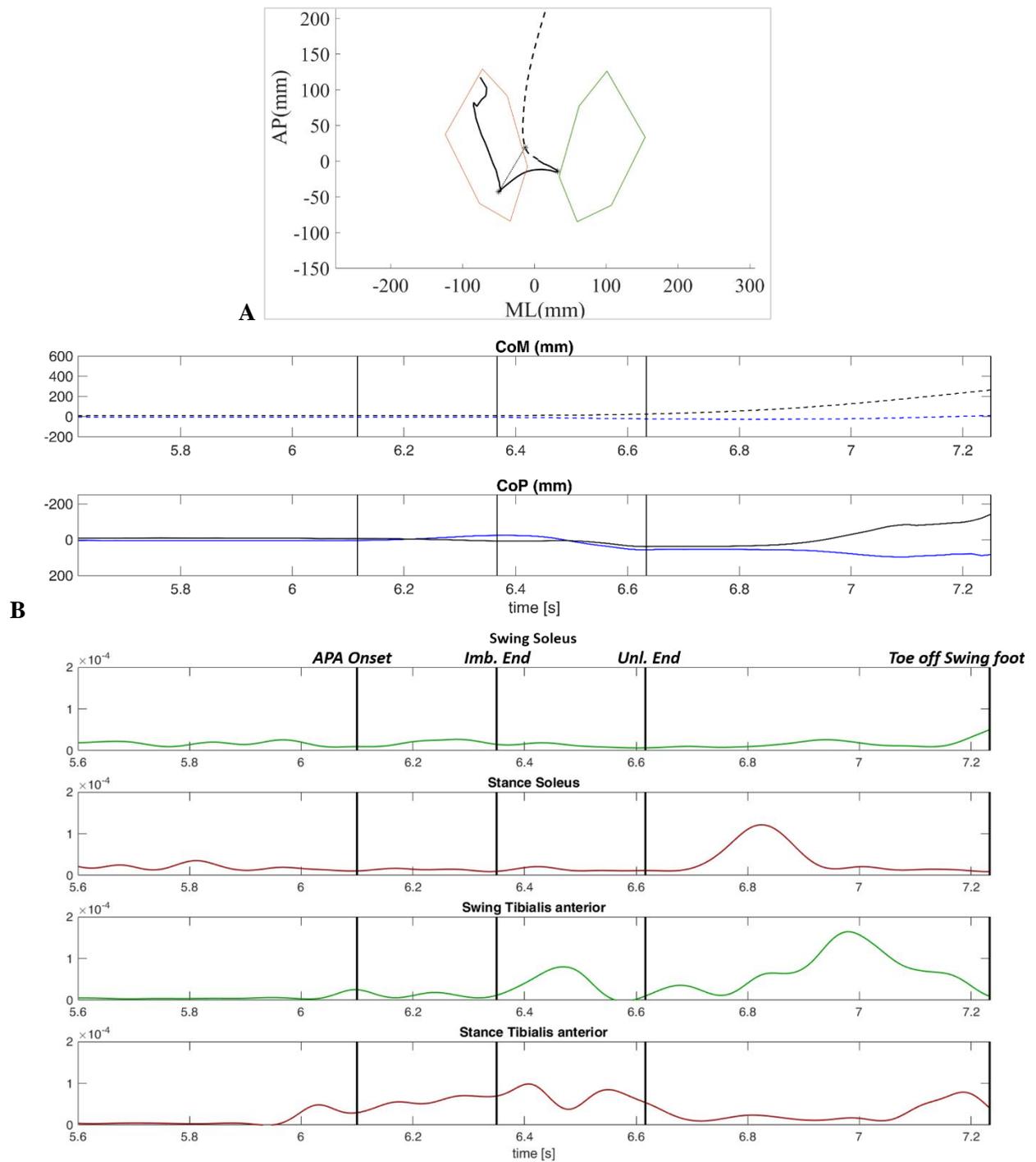
23

Patients with Progressive Supranuclear Palsy

Demographic and clinical data are listed in Table 13.

At the end of the unloading phase, the CoP (AP coordinate) positioned more posterior (closer to the line connecting the heels) in PSP than HC (Table 14). All parameters of the imbalance and unloading phases were significantly reduced in PSP, with the only exception of the ML displacement of CoP during the unloading phase, possibly due to the IFD% matching with HC, and the AP mean velocity of the CoP in the unloading phase, which was still reduced in PSP, but did not reached a statistical significance (Table 15).

Based on the displacement of the CoP during the imbalance phase, we were able to recognize three different gait initiation patters in PSP patients. The first patter (27/35 trials) was defined by a normal displacement of the CoP, but a reduced velocity (loss of temporal scaling) (Figure 9). The second (3/35 trials) and third patters (5/35 trials) showed both an abnormal temporal and spatial scaling as seen by the reduced velocity and the absence (second pattern) or "reversed" (third pattern) displacement of the CoP (Figure 10).

In almost all trials, PSP patients had an increased and tonic activity of the TA bilaterally. In the first patter, the synergic activity of TA and SOL was grossly preserved but delayed, possibly due to a fragmented and scaled activity of the TA. In the second pattern, the displacement of the CoP was accomplished almost exclusively by modulating (silencing) the TA activity. In the third patter, TA and SOL synergic activity was loss and the patient was able to start walking possibly by other compensatory mechanisms (e.g. trunk movements).

These abnormalities in APAs production and execution were clearly reflected in the alterations of functional measurements, such as the CoP-CoM vector magnitude and orientation as well as CoM and first step measurements (Table 16).

Table 13. Demographic and clinical data.
BMI = Body mass index. Disease duration was from motor symptoms onset. Values are means and standard deviation.

	HC	PSP
N. (male/female)	(10/3)	(6/9)
N. of trials		2-5
Age (years)	62 ± 4	65 ± 4
Weight (kg)	78.2 ± 10.8	72.9 ± 9.6
Height (m)	1.7 ± 0.1	1.6 ± 0.1
BMI	26.3 ± 3.1	27.5 ± 5.1
Disease duration (years)		6.5 ± 2.5
PSPRS		35.8±12.2

Table 14. Inter-foot distance and CoP-heels distance in during standing in PSP and HC.

	HC			PSP		
	10th	Median	90th	10th	Median	90th
IFD% (%)	61.83	**69.98**	75.27	55.18	**70.73**	77.93
CoP-heel distance (%FL)	37.83	**45.15***	51.85	34.83	**39.99***	48.33

Table 15. Spatio-temporal parameters related to the APAs phases in HC and PSP.
*Superscript asterisk indicate statistically significant differences (p<0.01) between HC and PSP. See text for statistical analysis. CoM lateral displacement was positive if directed to the swing foot and negative if oriented to the stance foot.*

Parameters	HC			PSP		
	10th	Median	90th	10th	Median	90th
Imbalance phase						
Duration (s)	0.23	**0.32**	0.43	0.26	**0.35**	0.89
AP displacement (%FL)	-26.64	**-12.8***	-2.65	-5.9	**-2.93***	8.11
ML displacement (%FL)	4.36	**13.95***	29.55	0.85	**7.10***	15.36
AP mean velocity (%FL/s)	10.74	**39.96***	95.97	3.34	**9.72***	19.14
ML mean velocity (%FL/s)	17	**43.62***	106.66	1.34	**16.49***	49.9
Unloading phase						
Duration (s)	0.26	**0.35***	0.56	0.33	**0.62***	1.37
AP displacement (%FL)	-3.21	**5.84***	23.48	-14.52	**0.31***	17.83
ML displacement (%FL)	42.17	**-55.8**	83.29	39.18	**-56.47**	70.88
AP mean velocity (%FL/s)	3.45	**14.54**	64.94	1.55	**11.28**	44.32
ML mean velocity (%FL/s)	98.37	**151.57***	301.8	45.6	**95.23***	160.1

Table 16. Parameters related to the APAs end and first step in HC and PSP.
Superscript asterisk indicate statistically significant differences (p<0.01) between HC and PSP. See text for statistical analysis.

Parameters	HC			PSP		
	10th	Median	90th	10th	Median	90th
CoP-CoM vector						
Magnitude at Imb. end (%BH)	1.8	**3.88***	6.44	0.6	**1.6***	2.95
Orientation at Imb. end (°)	-26	**-49.71***	-68.2	-41	**-70.29***	-86.3
Magnitude at Unl. end (%BH)	3.5	**5.4***	8.38	2.4	**3.72***	5.6
Orientation at Unl. end (°)	1	**35.91***	66.7	17	**55.43***	73.5
CoM parameters						
AP velocity at ST_{to} (%BH/s)	25	**46.77***	65.2	4.7	**17.4***	31.4
AP velocity at Unl. end (%BH/s)	9.3	**13.51***	21.8	1.5	**6.51***	11.5
AP acceleleration at Unl. end (%BH/s^2)	25	**43.72***	80.1	3.2	**23.36***	49.3
First step						
Swing Duration (s)	0.3	**0.62***	0.77	0.7	**0.82***	1.34
Length (%BH)	17	**31.78***	38.5	3.2	**18.07***	28.7
Peak velocity (%BH/s)	56	**91.93***	146	20	**50.94***	82.9

A

B
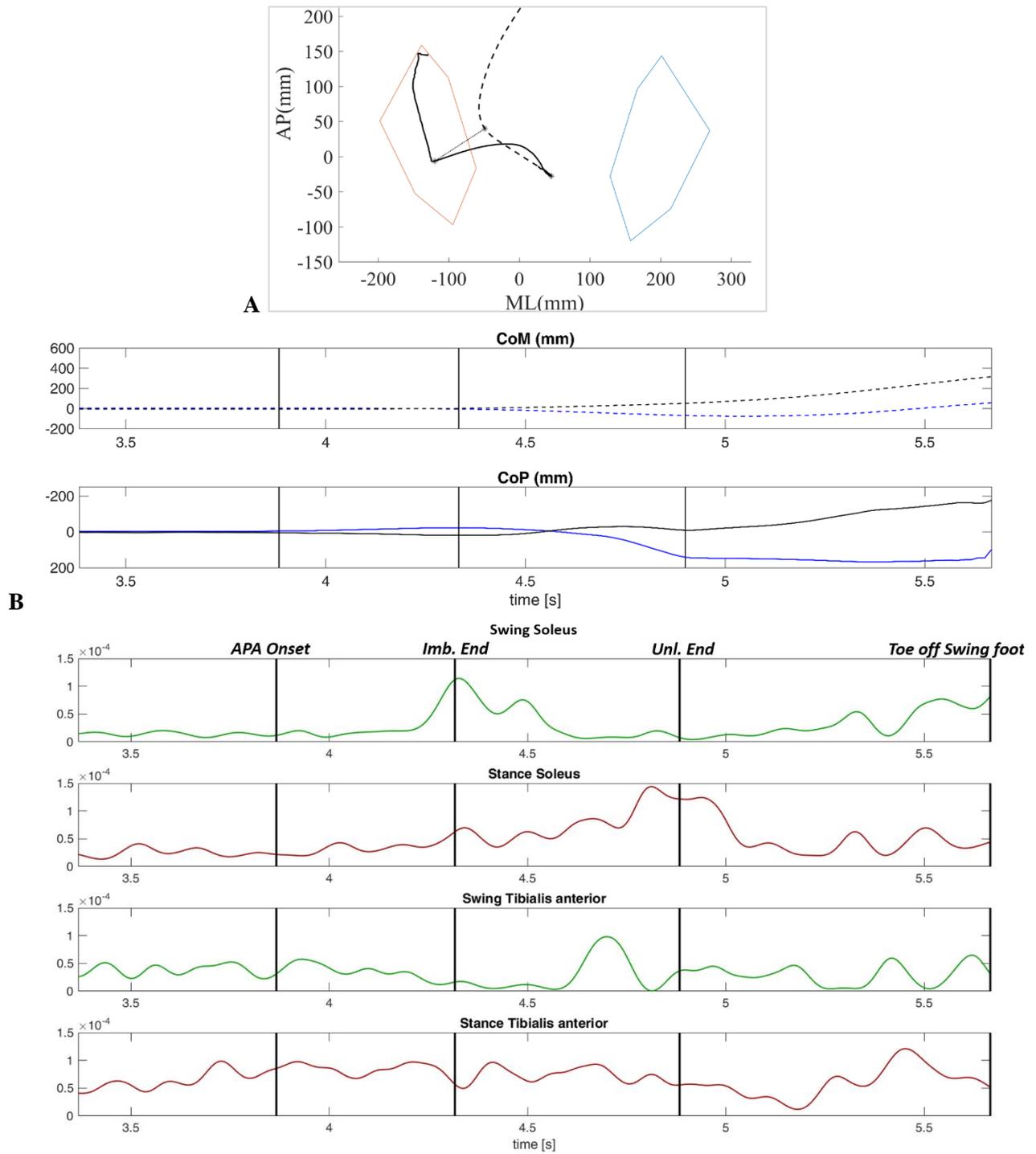
C

Figure 9. A: *CoP and CoM displacements in the transverse plane in one representative PSP subject. Plain line was for CoP and dotted line for CoM.* ***B****: CoP and CoM displacements in time. Black line was for AP displacement and blue line for ML displacement.* ***C****: the related EMG activity during the APAs of gait initiation. Unit of the EMG traces was V.*

26
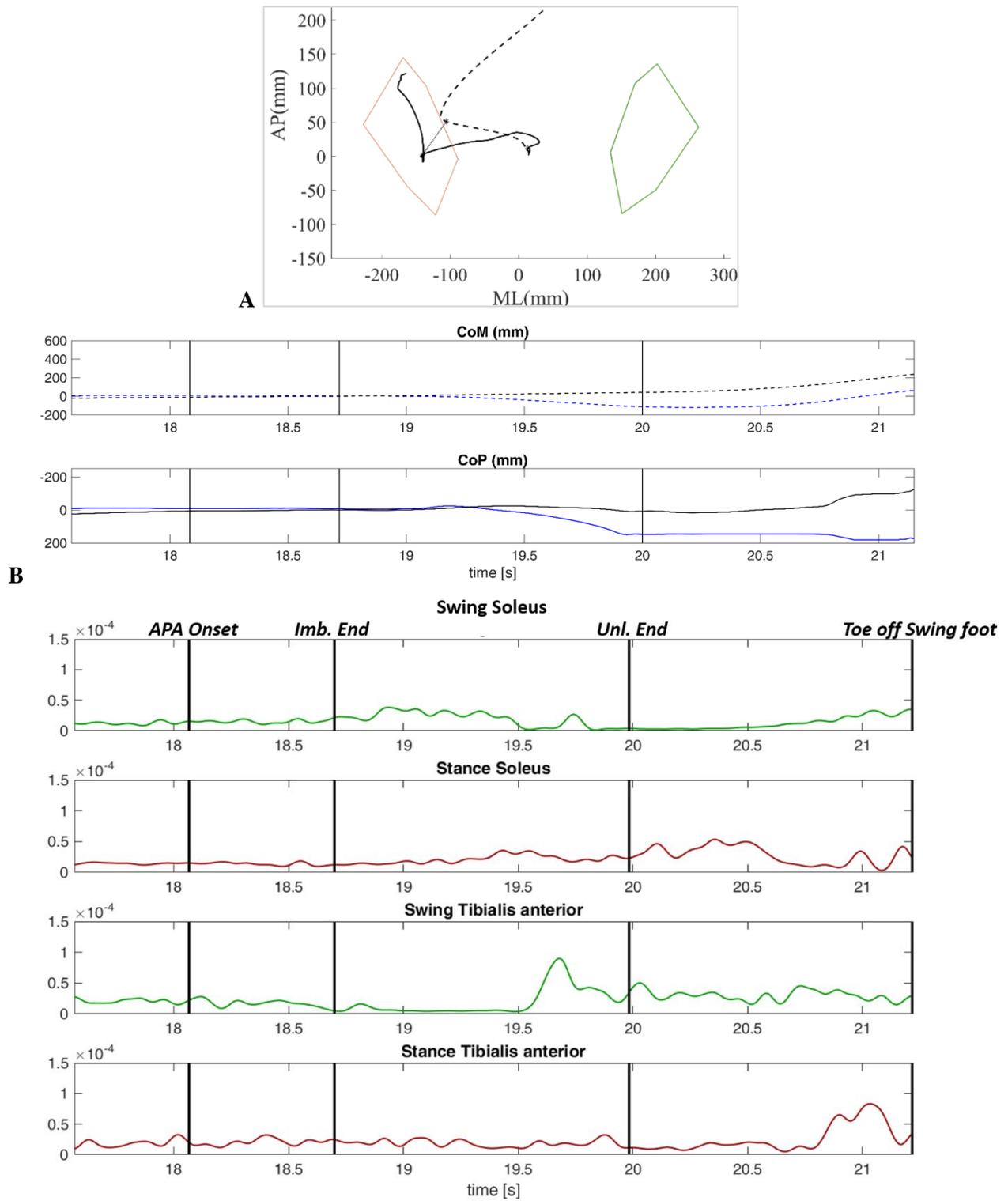
Figure 10. A: *CoP and CoM displacements in the transverse plane in one representative PSP subject with anterior imbalance. Plain line was for CoP and dotted line for CoM.* **B:** *CoP and CoM displacements in time. Black line was for AP displacement and blue line for ML displacement.* **C:** *the related EMG activity during the APAs of gait initiation. Unit of the EMG traces was V.*

Discussion

In this study, we showed relatively preserved APAs at gait initiation in patients with PD at an early stage. Carpinella and coll. found similar results, although they reported a significant reduction of backward CoP displacement during the imbalance and, for the execution of the first step, a significant increase in the duration of the swing phase and a reduction of walking velocity (Carpinella et al., 2010). In our opinion, these discrepancies are mainly related to the selected set of trials of HC used for comparisons. Indeed, as showed in Chapter II, the distance between the feet can greatly influence quantitative measurements of APAs at gait initiation. Another relevant difference between the study of Carpinella and coll. and this study was the medical conditions in which the patients were investigated. Carpinella and coll. tested the patients while on their routine therapy; here all patients were investigated after overnight suspension of all dopaminergic drugs, thus avoiding a bias related to the effect of a dopaminergic replacement therapy. Anyhow, in line Carpinella and coll. the evaluation of EMG profiles failed to disclose any significant alterations of the muscular synergy further supporting an overall preserved production and execution of APAs at gait initiation in early-stage PD patients. Of relevance to our study, at the end of the unloading phase, in both PD_M and PD_S, the CoP placed backwards (closer to the line connecting the heels) from its original position at the beginning of this phase, whereas in HC the CoP always positioned forward (Table 7, Figure 7, summarized in Table 17).

Table 17. Comparison about the absolute values of CoP displacements in AP and ML directions during imbalance and unloading phases.
* Difference greater than 5%FL but not statistically significant.

	PD_M vs. HC	PD_S vs. HC	PD_S vs. PD_M
AP avg. CoP displacement (%FL) at Imb. end	=	<	<
ML avg. CoP displacement (%FL) at Imb. end	=	<	<
AP avg. CoP displacement (%FL) at Unl. end	post. vs. ant.	post. vs. ant.	=
ML avg. CoP displacement (%FL) at Unl. end	=	<*	<

Such a CoP displacement might suggest that PD_M mostly rely on the ankle plantarflexion/dorsiflexion muscles at gait initiation (i.e. ankle strategy). This hypothesis is also supported by a different activity of the TA, which is continuative active throughout the APAs in HC, while in PD_M subjects it is silenced at the end of the imbalance phase and re-activated during the unloading phase.

With regards to PD_S, it is worth noticing at first that these patients showed comparable IFD% with PD_M, thus allowing a direct comparison between the two groups (Table 3, Chapter I). Along with PD progression, the pathogenic process variably involves at a functional level the mesencephalic locomotor region (MLR), thus directly impairs the execution of APAs, with a consequent reduction in forward propulsion of the CoM. Indeed, PD_S could not rely on TA and SOL synergic activity to start walking and showed altered biomechanical parameters, in particular in the imbalance phase (Table 11; Table 3 of Chapter I). In PD_S, the CoP displacement was very limited in lateral direction during all APAs phases, thus suggesting an impairment of the hip in the frontal plan. This finding, combined with the backward positioning of the CoP (from its original position at the beginning of this phase) also suggests a desynchronization of the ankle and hip strategy.

We advance the hypothesis that these APAs abnormalities in PD can be related to a different distribution of the *rigidity* between trunk and limbs. Early-stage PD patients usually experience a predominant appendicular rigidity (often asymmetric), but some patients additionally show moderate axial symptoms, which are definitely more pronounced at advance stages of PD. Accordingly, two main postural profiles, in which the forward inclination of the trunk was greater (type I) or lower (type II) as compared with the inclination of the thigh and shank, have been described in PD (Crenna et al., 2006). A different distribution of axial and appendicular *rigidity* could favor a hip or ankle strategy for the execution of APAs at gait initiation (Kuo, Speers, Peterka, & Horak, 1998). Despite its relevance (Crenna & Frigo, 1991), the influence of the different distribution of akinetic-rigid symptoms as well the relative contribution of the trunk, hip and ankle at gait initiation has not been investigated in PD patients and it will be addressed in future studies.

With regards to PSP patients, despite we enrolled only patients able to stand and start walking unassisted, the neurodegenerative process involved already several cortical and subcortical (also including the MLR) brain areas. Therefore, not only the execution of a coherent set of motor commands (i.e. APAs), but necessarily also the production (*feedforward* organization) of such commands is abnormal. The complete deterioration of APAs at gait initiation showed in our study supports this hypothesis.

It was decided to investigate these patients as a paradigmatic example of a neurological disorder primarily (but not exclusively) defined, at least at an early stage, by an impairment of balance. More importantly, PSP is a devastating neurodegenerative disease with no cure available. A better understanding of the pathophysiological mechanism of this disease could provide useful information for a better differential diagnosis and, hopefully, to test new treatments (Appendix C).

Canesi M, Giordano R, Lazzari L, Isalberti M, Isaias IU, Benti R, Rampini P, Marotta G, Colombo A, Cereda E, Dipaola M, et al. (2016)
Finding a new therapeutic approach for no-option Parkinsonisms: mesenchymal stromal cells for progressive supranuclear palsy.
J Transl Med. 2016;14(1):127. doi: 10.1186/s12967-016-0880-2.

Abstract – Background: The trophic, anti-apoptotic and regenerative effects of bone marrow mesenchymal stromal cells (MSC) may reduce neuronal cell loss in neurodegenerative disorders.
Methods: We used MSC as a novel candidate therapeutic tool in a pilot phase-I study for patients affected by progressive supranuclear palsy (PSP), a rare, severe and no-option form of Parkinsonism. Five patients received the cells by infusion into the cerebral arteries. Effects were assessed using the best available motor function rating scales (UPDRS, Hoehn and Yahr, PSP rating scale), as well as neuropsychological assessments, gait analysis and brain imaging before and after cell administration.
Results: One year after cell infusion, all treated patients were alive, except one, who died 9 months after the infusion for reasons not related to cell administration or to disease progression (accidental fall). In all treated patients motor function rating scales remained stable for at least six-months during the one-year follow-up.
Conclusions: We have demonstrated for the first time that MSC administration is feasible in subjects with PSP. In these patients, in whom deterioration of motor function is invariably rapid, we recorded clinical stabilization for at least 6 months. These encouraging results pave the way to the next randomized, placebo-controlled phase-II study that will definitively provide information on the efficacy of this innovative approach. Trial registration ClinicalTrials.gov NCT01824121

One study only investigated gait initiation failure in PSP patients (Amano et al., 2015). The authors described a unique and inefficient gait initiation strategy in PSP patients, who shifted their CoP anteriorly and toward the stance limb prior to stepping. In our study, this strategy was found only in a subgroup of trials (5/35). On the contrary, we mostly identified a CoP displacement during gait initiation similar to HC. Still, such a pattern did not follow a proper synergic activity of TA and SOL, which was delayed and disaggregated. Our results suggest a more complex scenario than what proposed by Amano and coll., possibly resembling different compensatory strategies put in action by PSP patients to initiate walking. It is worth mentioning that the diagnosis of PSP is usually delayed in time and confirmed, at clinical level, only when symptoms are fully manifest and severely impair the patient's mobility. In particular, the loss of postural reflexes combined with a severe axial rigidity, lead to a "stopped posture" which is maintained by reducing the swinging of the CoP during stance and by a tonic activation of the TA, bilaterally. These patients presented great difficulties in mastering both the hip and even more the ankle strategy, as seen also by an impaired (sometimes even reversed) displacement of CoP during the imbalance phase. We can further speculate that, to start walking, PSP patients combine a silencing of the tonically activated TA with trunk movements to produce a forward acceleration of

29

the CoM. Indeed, PSP relied mostly on the unloading phase, rather than the imbalance phase, to produce a sufficient forward acceleration of CoM. The very large angle of CoP-CoM vector at the end of imbalance phase would indicate that the imbalance in PSP had the only effect to displace CoM toward the stance foot, rather than projecting it forward. In our opinion, the patter 2 and 3 should be considered as a continuum of compensatory strategies that would allow PSP patients to efficiently start walking in the absence (impaired production and execution) of APAs. The pattern 1, despite showing a CoP displacement similar to HC, would instead be disadvantageous for the patients as not supported by a correct APAs execution, in particular the synergic activity of the TA and SOL. Indeed, 4 of 5 falls at the end of the first step occurred in the case of a patter 1, and only one with a pattern 2.

PSP is a rare disease and such gait analyses are of great discomfort for the patients. To further understand and explore possible compensatory strategies we decided to simulate gait initiation patterns with a model of the human body.

CHAPTER IV

A MUSCULOSKELETAL MODEL FOR APAS OF GAIT INITIATION

Introduction

The APAs of gait initiation were deeply explored through the multi-body simulation software SimWise 4D by Design Simulation Technologies (DST). This software was used to build a model of the human body and to simulate the dynamic effect of activation or inhibition of relevant muscles, the ones that are mostly involved in the preparation of gait initiation. In this way it was possible to study the effects of muscles synergies on the whole body, and to explore the influence of different geometrical initial condition on the effects produced by muscles activity.

In this chapter, some models of the human body were described. Moreover, some software used in literature to implement the musculoskeletal models of the human system were listed and briefly described. These software were divided on the basis of the type of dynamic model implemented: forward and inverse dynamic models.

Then the simulation software SimWise 4D will be introduce and the musculoskeletal model for the simulation of anticipatory postural adjustment will be presented.

The human body modeling

The study of human body movement and the acquisition of quantitative information about a motor task requires the development of a model of the human system. This means to define the anatomical segments with their geometrical, structural and inertial properties, the joints that link one segment to another with their kinematical properties, and the type of interaction between the anatomical segments.

Typically, each anatomical segment is assumed to have the characteristics of a rigid-body and the whole musculoskeletal system is assumed to be a connection of them, so that the standard methods of multibody dynamics can be applied.

In biomechanical literature, different approaches were used to model the human body. One was to use mathematical models of the body segments and calculate anthropometric measurements to determine the dimensions of the body segments that were identified. This type of methods requires to collect a number of anthropometric measurements from the participants and is limited by the accuracy of the mathematical model of the body segments. The first mathematical model of this type was suggested by Hanavan in 1964 and was represented by 15 body segments, as cylinders and spheres, and required 25 anthropometric measurements (Hanavan, 1964). More detailed models were presented by Hatze that required 95 measurements. This huge quantity of measurements made these methods inefficient for studies with a large number of participants because of the time and discomfort for them (Hatze, 1980).

The photogrammetry approach lets to gain surface data. In 1978, Jensen proposed the use of stereophotogrammetry to estimate body segment parameters (Jensen, 1978).

Another approach relies on X-ray or MRI based tomography to extract subject-specific body segment parameters from participants. Unlike other methods, CT or MRI scans provide also information about internal structures such as tissue composition, which should improve the reconstruction accuracy (Martin et al., 1989; Mungiole & Martin, 1990; Pearsall, Reid & Livingston, 1996; Bauer et al., 2007).

An approximation of inertial body segment parameters was also possible by adjusting previously reported average values from cadavers or using regression models. This last method requires only a very few subject-specific measurements (commonly subject height and weight), derived from participants in a number of famous studies (Dempster, 1955; Clauser, McConville & Young, 1969; McConville, Clauser & Churchill, 1980; Zatsiorsky and Seluyanov 1983; Leva, 1996). The reliability of such regression models is, however, rather low and the models are only applicable to a population similar to the one used to derive the regression equations.

Other methods were used to obtain volumetric data of body segments that, combined with body density assumptions, can provide subject-specific inertial body segment parameters (Sheets, Corazza & Andriacchi, 2010).

These models allow to calculate the inertial properties of the anatomical segments and of the whole body, and can be useful to simulate the human movement.

Recently, the Kinect sensor was used to estimate body segment lengths but not their volumetric data that are required to estimate inertial properties (Bonnechère et al., 2014).

The most widespread current approach is patch-based multi-view stereo reconstruction (Furukawa & Ponce, 2010). This photogrammetric approach, currently used and accepted for producing 3D models in areas such as archaeology (McCarthy, 2014) and paleontology (Falkingham, 2012), is even used for markerless motion capture (Sellers & Hirasaki, 2014).

The modeling of the human posture

The common denominator in the assessment of human balance and posture is the inverted pendulum model (D. A. Winter, 1995). In fact, the human body system during orthostatic upright standing could be modeled in the sagittal plane as a mass sustained by a beam hinged at the ground (Figure 11), under the following assumptions:

1. all the mass of the subject is concentrated in his center of gravity, and this coincide with the center of gravity of the mass of the pendulum;
2. the beam is without mass and is bind to the ground though an ideal hinge. The hinge represent the ankle joint;
3. the actuator coaxial with the hinge represents the action of the plantar-flexor muscle; the torque produced by the actuator is equal to the torque of the ground reaction force Rd (R is the ground reaction force and d is the distance between R and the center P of the hinge joint). According to the third dynamic law (action-reaction principle), the torque applied at the pendulum beam is $-Rd$.

Assuming that the mass m has an angular acceleration $\ddot{\theta}$, the equilibrium equation is:

$$-Rd + m(g + \ddot{y})L\sin\theta - m\ddot{x}L\cos\theta = 0 \qquad (1)$$

where m is the mass, g is the gravity acceleration, L is the distance between the center of gravity of m and P, θ is the angle between the beam and the vertical axis. Assuming that:

$$y = L\cos\theta \qquad \dot{y} = -L\dot{\theta}\sin\theta \qquad \ddot{y} = -L\ddot{\theta}\sin\theta - L\dot{\theta}^2\cos\theta$$
$$x = L\sin\theta \qquad \dot{x} = L\dot{\theta}\cos\theta \qquad \ddot{x} = L\ddot{\theta}\cos\theta - L\dot{\theta}^2\sin\theta$$

and

$$mgb - Rd = mL^2\ddot{\theta}$$

we set $b = L\sin\theta$ the distance between the center of gravity and P, and $J_m = mL^2$ the moment of inertia of the mass m respect to P. The equation (1) becomes:

$$-Rd + mgb = J_m\ddot{\theta} \qquad (2)$$

The inverted pendulum model relates the controlled variable (CoM) with the controlling variable (CoP). Such a model provides an analytic relationship between these two commonly measured variables and the horizontal acceleration of the CoM (David A. Winter et al., 1998). The CoP-CoM distance is indeed proportional to the horizontal acceleration of the CoM in both the sagittal (anterior/posterior direction, A/P) and frontal (medial/ lateral direction, M/L) planes (David A. Winter et al., 1998).
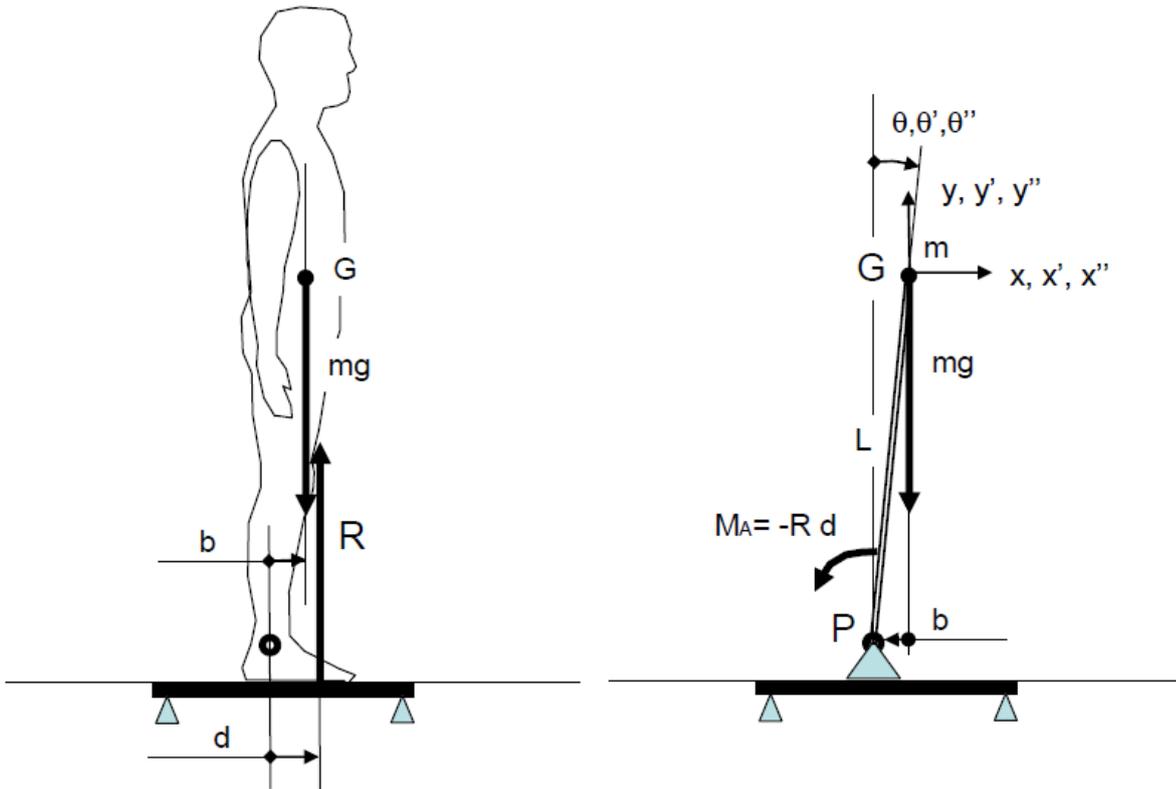
Figure 11. *The inverted pendulum model.*

In particular in the sagittal plane, if $mgb > \mathrm{Rd}$, the body experiences a clockwise angular acceleration. In order to correct this forward sway, the subject has to increase the plantar-flexion action so that $\mathrm{Rd} > mgb$. Now the angular acceleration is inverted and the angular velocity starts to decrease until inverts the sign when the integral of negative angular acceleration reaches the value of the previous positive acceleration. At this point, both angular acceleration and angular velocity are negative (counterclockwise) and the body will start to sway backward.

In the human body, when the central nervous system senses that the center of mass (CoM) of the body is shifting backward it controls the position of the center of pressure (CoP) decreasing the plantar flexion action until the CoP is positioned behind the CoM. The angular acceleration will reverse to be negative again, the angular velocity will decrease until invert the sign and the CoM will reverse to displace forward.
From this sequence of the displacement of the CoP and CoM relative one to each other, Winter highlights that is possible to observe that the plantar-flexion and the dorsi-flexion actions that controls the ankle movement can regulate the position of the CoM of the body. Moreover, the CoP displacement has to be wider respect to the CoM one.

Stiffness control model
Winter et al. hypothesized a simple stiffness model that generates the appropriate moment at the ankle joint and suggested that the role of the central nervous system would be to set the muscle tone at specific balance control sites, changing the stiffness constant to balance the pendulum system (David A. Winter et al., 1998). The stiffness control model purposed is an inverted pendulum system with a rotational spring that produces a moment at the base of pendulum (the ankle joint). In static condition, the moment due to the spring, $K\theta$, balances the moment about the ankle joint, $mgL \sin\theta \approx mgL\theta$, where K is the rotational spring stiffness in Nm/rad and θ is the angle of the pendulum from vertical. Thus:

$$K\theta - mgL\theta = -J_m \ddot{\theta}$$

For small angles of sway:

$$\theta \approx b/L$$

$$\frac{Kb}{mgL} - b = -\frac{J_m \ddot{x}}{mgL} \qquad (3)$$

The first term of the equation represents the position of the center of pressure (d) and it is proportional to the CoM position with respect to the ankle joint in the A/P direction, b, and in phase with b. If the stiffness K is greater than mgL, the system will oscillate and the CoP trajectory will be larger than the CoM trajectory. The frequency of the oscillation is the undamped natural frequency, ω_n, which is a function of the stiffness and the inertia:

$$\omega_n = \sqrt{\frac{K_e}{J_m}} \qquad (4)$$

where K_e is the effective stiffness of the inverted pendulum, which is $< K$ because the gravitational spring, mgL, acts on the system and reduce the stiffness K, thus $K_e = K - mgL$.

The simplified stiffness model will oscillate at ω_n: any small damping present will result in the CoM oscillations getting closer to zero. During quiet standing the CoP and CoM excursions do not oscillate at a single frequency and these oscillations continue, thus the energy is continuously being generated into the mass, spring, and damper system, creating a tuned mechanical circuit. The stiffness K_e could be estimated analyzing the amplitude spectrum of the CoP-CoM signal, indeed K_e determines the acceleration of the CoM, and the CoP-CoM is proportional to the acceleration of the CoM, as we see from from equation (3). This spectrum represents the response of a tuned mechanical circuit and the equation of the amplitude spectrum of is described by

$$A(\omega) = \frac{C}{\sqrt{1 + \left[\frac{I\omega}{B} - \frac{K_e}{\omega B}\right]^2}}$$

where I, K_e and B are the inertial, spring and damping constants and C is a constant. I is determined by anthropometric measures (Winter 1990). This response reaches a maximum when $(I\omega/B - K_e/\omega B) = 0$ or when $\omega_n = \sqrt{K_e/I}$.

A curve fit of this tuned mechanical system response yields ω_n. The optimization program varies C, K_e and B to achieve this fit, setting I as the subject's I. K_e and B can be determined in two ways. K_e and B can be yielded by the optimization program. Alternately, K_e can be calculated from equation (4) and B can be calculated from $B = BW \times I$, where BW is the bandwidth of the tuned mechanical system. Thus we have an analytic way for the stiffness and damping estimation, and setting these parameters it is possible to control upright balance.

The authors showed that the simplified (undamped) stiffness control model of the inverted pendulum can predict the magnitude of sway, $b(t)$:

$$b(t) = \sqrt{\frac{b_0^2 \omega_n^2 + V_0^2}{\omega_n^2}} \sin(\omega t + \varphi)$$

where V_0 is the horizontal velocity of the CoM when it is at ''top dead center'', and b_0 is the horizontal displacement of the CoM at t=0.

Thus, if we start the pendulum oscillating at $b_0 = 0$ at t=0 the amplitude of the oscillation is:

$$X = \sqrt{\frac{V_0^2}{\omega_n^2}} = \frac{V_0}{\sqrt{K_e/J_m}} = \frac{V_0 \sqrt{J_m}}{\sqrt{K_e}}$$

As shown, the displacement of CoM is proportional to $\sqrt{K_e}$. This means that, although CoM displacement is affected by the magnitude of initial velocity, the curve relating CoM displacement and K_e have the same shape. The authors sentenced three predictions in support of the validity of the stiffness control model of the inverted pendulum.

The first prediction states that CoP should oscillate effectively in phase with CoM: the CoP moves and tracks the CoM with no time lag, as predicted by "springs" at the ankle joint.

The second prediction states that the sway would be proportional to $\sqrt{K_e}$, thus the spring-like nature of the plantar-flexors in A/P direction represents a simple 0th order feedback control. The role of the central nervous system in this balance control appears to be to set the muscle tone such that the spring constant, K, is sufficiently large to overcome the gravitational load (mgL) and to cause CoP to move more than CoM.

The third prediction demonstrates the variability of stiffness, K_e, over the 2-min standing period. In particular, the authors revealed that, when the control nervous system controls the muscle tone (stiffness) at the wide stance width, it can afford to be quite approxymate, whereas at the narrow stance width it must be more rigidly controlled. Thus, wide stance widths would be recommended for balance challenged patients.

Finally, they speculated that there was no evidence of reactive control. Indeed, the visual system does not seem to contribute because it does not result any difference between eyes close and eyes open. Moreover, the joint receptors have the potential to feed information to a CoM estimator, because AP and ML accelerations are less than the threshold of otolith sensation in humans (Benson et al. 1986). Thus, based on the borderline sensory thresholds and afferent and efferent delay estimates, a reactive control would not be predicted in quiet standing.

A challenge to stiffness control hypothesis

The theoretical consideration proposed by Winter and coll. in 1998 was that the phase lock between CoM and CoP is incompatible with the afferent and efferent delays associated with active control.

This hypothesis was challenged by Morasso and Schieppati (Morasso & Schieppati, 1999). With a biomechanical analysis of the human inverted pendulum, the authors demonstrated that the phase relation is a consequence of the dynamics of the plant and is independent of the mechanism of stabilization; therefore, it cannot be used as a valid argument for deciding whether the stabilization mechanism of the system is predominantly due to stiffness or to active control.

As seen in the previous section, Winter et al. (1998) pointed out that there is a critical value of stiffness for the stabilization of the ankle $K_c = mgL$. Morasso and Sanguineti reported that, in literature, results were quoted that show a range of values of ankle stiffness that are significantly lower than the critical level (Morasso & Sanguineti, 2002). Then, Winter and coll. proposed a new method for estimating the ankle joint stiffness that yielded a value 8.8% greater, on average, than the critical level (Winter, Patla, Rietdyk, & Ishac, 2001), suggesting that this result might be related to the high nonlinear stiffness of the series elastic element of the muscles of the ankle.

Morasso and Sanguineti demonstrated that the lines of defense of the stiffness control purposed by Winter and coll. model were incorrect. First, they sentenced that the method of stiffness estimation they implemented cannot distinguish the effects of stiffness compensation from the active control. For this reason, they overestimated the real level of stiffness. Second, the series elastic element of ankle muscles could not provide enough stiffness to stabilize the body during quiet standing.

They supported their thesis with a methodological analysis of the experimental approach and with a new simulation study with a realistic model of ankle muscles that shows the mechanical instability of the system without an anticipatory control input. Particularly, they demonstrated that the ankle stiffness can only account for about 60% of stabilization forces.

Morasso and Sanguineti referred to a set of experiments (Hunter & Kearney, 1982; Weiss, Hunter, & Kearney, 1988) that cover the whole range of muscle activation up to maximum voluntary contraction for both plantarflexion and dorsiflexion. The authors of these studies used an actuator to generate pseudo-random joint perturbations, applied on a sustained bias torque from which it was possible to evaluate the dependence on this torque of the viscous and elastic components of the joint mechanical impedance.

The studies revealed that:
1) the ankle joint stiffness was linearly dependent on the level of bias torque for both dorsiflexion and plantarflexion,
2) the joint viscosity grows less linearly in such a way as to keep the damping parameter of the ankle joint fixed at a value of about 0.25.

In their study, Morasso and Sanguineti used an inverted pendulum model based on equation (2), without the small-angle approximation. They assumed that the ankle is command by a single dorsi-flexor (tibialis anterior) and a single plantar-flexor (soleus and gastrocnemius). Moment arms and physiological cross-section areas were determined from the literature (Dariush, Parnianpour, & Hemami, 1998; David A. Winter, 1990).

Through this model, the authors demonstrated that the ideal standing posture is not a point attractor but an unstable saddle point, and argued that the nonlinear dynamics and the stiff series element are not valid substitutes for the insufficient static stiffness.

The simulations also suggest that in normal subjects the two stabilizing mechanisms, active control and stiffness, contribute about equal amounts of the restoring forces necessary to prevent falling.

Theoretical framework for dynamic simulation

The understanding of movement dynamics fascinated many researchers who have performed an extensive range of studies to describe the elements of the human neuromusculoskeletal system. However, the studies that use only experiments to approach this topic have tow fundamental limitations. The first is that important variables, including the forces generated by muscles, are not generally measurable in experiments. Second, it is difficult to establish cause-effect relationships in complex dynamic systems from experimental data alone. For these reasons, the implement of theoretical frameworks and the use of dynamic simulations combined with experiments has been introduced in literature.

Forward and inverse dynamics models

Human movement is the result of the coordinated activity of many muscles that actuate multiple joints simultaneously and create interaction forces with the environment. Motion analysis allows recording human movement at different levels including electromyography, foot-ground reaction forces and body kinematics. However, the sole observation and analysis of this information provide a limited view of movement and does not allow establishing direct cause-effect relationships between the underlying neuromuscular mechanisms and the final observed motion.

Computer simulation and computational modeling have emerged as powerful tools to understand the dynamics underlying human movement.

The musculoskeletal models can be divided into two groups on the basis of the type of problem resolved through the model: forward and inverse dynamic models.

As is known, kinematic variables are strictly related to the internal and external forces and the torques applied to a structure. The link between kinematic variables and forces is define by the equations for the dynamic equilibrium (second dynamic law):

$$\frac{d\Gamma}{dt} = \sum M \qquad \frac{dQ}{dt} = \sum F$$

where $d\Gamma/dt$ is the derivative of the angular momentum of whole system respect to a point ($\Gamma = \sum \Gamma_j$) and $\sum M$ is the summation (the resultant) of all the moments, internal and external applied to the system. dQ/dt is the derivative of the momentum of the system ($Q = \sum Q_j$) and $\sum F$ is the summation (the resultant) of all the forces, internal and external applied to the system.

All kinematic variables and inertial parameters are collected in the terms $d\Gamma/dt$ and dQ/dt, in fact, for a single rigid body:

$$\vec{Q} = m\overrightarrow{V_{CoG}} \text{ and } \vec{\Gamma_0} = (\overrightarrow{CoG} - O)\wedge\vec{Q} + I_{mx}\omega_x\vec{\imath} + I_{my}\omega_y\vec{\jmath} + I_{mk}\omega_k\vec{k}$$

where V_{CoG} is the velocity of center of gravity (CoG), m is the body mass, I_{mx}, I_{my}, I_{mk} are the principal inertial moments, ω_x, ω_y, ω_k are the components of angular velocity respect to the local coordinate system of the moving body, i, j, k are the versors of the axis in movement.

A forward dynamic model computes the motion based on a predicted muscular activation. In particular, if the forces and the moments are known, and the inertial properties of the bodies that make up the system are also known, it is possible to calculate the kinematic variables and determine the motion of the system. This kind of model is usually a detailed attractive model, because it is able to describe various physical phenomena. On the other hand, it is a very computationally demanding and time-consuming problem because has to solve non linear differential equations. Furthermore, the estimation of muscle forces requires a costly optimization

approach to ensure that the model performs a specific task. An inverse dynamics model computes the muscle activation of a known motion, on the basis of the measurement of kinematic and kinetic quantities. This method introduce many restrictions in the model, but it is computationally much more convenient.

The modeling systems that allows forward dynamics analysis help in discovering the principles that govern the coordination of muscles during normal movement. Those instruments could be also used to determine how neuromuscular impairments contribute to an abnormal movement (movements in individuals with cerebral palsy, stroke, osteoarthritis, Parkinson's disease, etc), and to predict the functional consequences of a hypothetical treatments. To achieve these goals, the theoretical framework must reveal the cause-effect relationships between neuromuscular excitation patterns, muscle forces, and motions of the body.

Simulations also enable cause-effect relationships to be identified and allow the perform "what if?" studies in which, for example, the excitation pattern of a muscle can be changed and the resulting motion can be observed (Delp et al., 2007).

An example of forward dynamics model is OpenSim, an open-source program that aims to provide researches with a simulation platform for neuromuscular systems and rigid-body dynamics (http://opensim.stanford.edu/). This tool allows to create subject-specific musculoskeletal models and to perform inverse kinematics and inverse dynamics simulations of movement, and lets the user to derive the underlying muscle dynamics.

SimTrack, in particular, is a tool of OpenSim capable of generating muscle-actuated simulations of subject-specific motion (Figure 12 from (Delp et al., 2007).
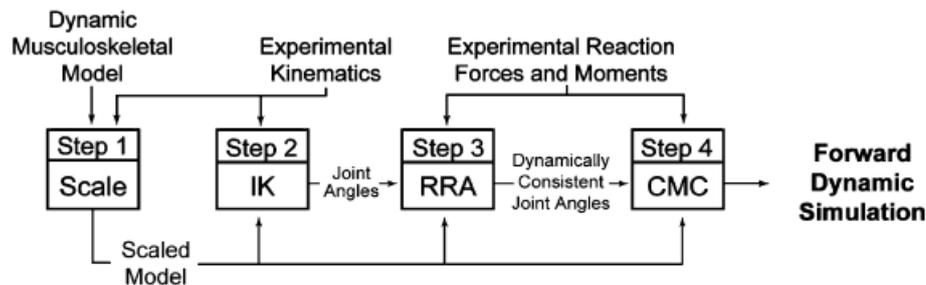
Figure 12. *Steps for generating a muscle-driven simulation of a subject's motion with SimTrack. The inputs are a dynamic musculoskeletal model, experimental kinematics (i.e., x-y-z trajectories of marker data, joint centers, and joint angles), and experimental reaction forces and moments obtained from a subject. In Step 1, the experimental kinematics are used to scale the musculoskeletal model to match the dimensions of the subject. In Step 2, an inverse kinematics (IK) problem is solved to find the model joint angles that best reproduce the experimental kinematics. In Step 3, a residual reduction algorithm (RRA) is used to refine the model kinematics so that they are more dynamically consistent with the experimental reaction forces and moments. In Step 4, a computed muscle control (CMC) algorithm is used to find a set of muscle excitations that will generate a forward dynamic simulation that closely tracks the motion of the subject (Delp et al., 2007).*

The accuracy of a simulation depends on the fidelity of the underlying mathematical model of the neuromusculoskeletal system. Many assumptions are made in the development of musculoskeletal models, and some of these assumptions are based on limited experimental evidence. It is critically important to test each simulation to establish its limitations. As more investigators use simulations of musculoskeletal dynamics, it is essential that each scientist tests the accuracy of their simulations in the context of their specific scientific study.

Another tool that allows forward dynamics analysis is multi-body simulation software SimWise 4D by Design Simulation Technologies (DST). In this case, the user choses to simulate the human body with a different number of geometrical solids. Each solid represents the main anatomical segments of the human body that the user needs to simulate a specific movement. The mass density of the solids is uniform.

The solid segments should be connected by means of different type of constraints (e.g. spherical hinges, cylindrical hinges, spring/damper elements).

The movement of one segment relative to another could be controlled through a revolute motor or with linear actuators or spring/damper elements that represent the muscles. The activation of the muscles could be simulated by the changing of elastic constant value of the spring or shortening the natural length of the spring.

This force perturbation determines accelerations in all segments of the model because of their dynamic coupling.

After determining the time interval between animation frames, the calculator uses an integrator to compute simulation results. SimWise provides two types of integrators: Euler mode and Kutta-Merson mode. The first one is approximate and fast, and employs a simple integration method that optimizes the simulation for speed. This mode is appropriate to a rough prototype of the model. Kutta-Merson mode is more accurate and employs a more sophisticated integration method. In this case, the calculator requires more time to compute simulation results, but they are much more accurate than those computed in Euler mode.

By default, a gravitational force equal to the earth's gravity acts upon the bodies of the model. It is possible to adjust the direction and magnitude of the gravitational force to model other environments or disable it completely.

An example of inverse dynamics modeling system is AnyBody, designed to be a tool that allows to construct models from scratch or use or modify an existing models to suit different purposes. This system is thought to facilitate model exchange and cooperation on model development. When it has sufficient numerical efficiency, it allows ergonomic design optimization on inexpensive computers. Finally, this system make possible to handle body models with a realistic level of complexity.

It offers the opportunity to analyze muscle recruitment together with general model building facilities.

Naturally, muscle activation and in particular muscle forces cannot be measured accurately and the nature of the system makes it impossible to measure all muscles. This is a problem when you want to validate computational models, but it also gives the models a special importance, since they are, in many cases, the only way to estimate certain valuable information such as the internal forces in the body.

Description of the model for APAs of gait initiation

The model here implemented was designed to be an instrument for studying the anticipatory postural adjustment of gait initiation in human subjects. The model was composed of 13 geometrical solids representing the main anatomical segments of the human body (Table 18). The human subject simulated was 165 cm tall and has 60 kg of body mass. Size and mass of anatomical segments were defined according to the literature (Zatsiorsky & Seluyanov, 1983).

Table 18. Anthropometric parameters of the human body model.
Mass ratio: percentage of segment mass in relation to body mass; h, height; r, radius; l, length; w, width.

	Mass ratio (%)	Mass (kg)	Size (m)		
Whole body	100	60	h =1.65		
Head	7.83	4.7	r =0.1		
Trunk and pelvis	43.17	25.9			
Trunk	32.33	19.4	l =0.18	w =0.28	h =0.35
Pelvis	10.83	6.5	l =0.14	w =0.24	h =0.16
Upper limb	4.83	2.9			
Upper arm	2.17	1.3	r =0.04	l =0.28	
Forearm and hand	2.67	1.6	r =0.035	l =0.25	
Lower limb	19.4	11.64			
Thigh	14	8.4	r =0.06	l =0.36	
Shank	4	2.4	r =0.045	l =0.36	
Foot	1.4	0.84	l =0.24	w =0.08	h =0.06

The mass density of the bodies was uniform, so that centre of mass and central moments of inertia could be defined by simple geometrical calculations.

The simulation software Simwise 4D was used to implement the model and to calculate the forward dynamics (Simwise 4D, Design Simulation Technologies, DST) (Figure 13).
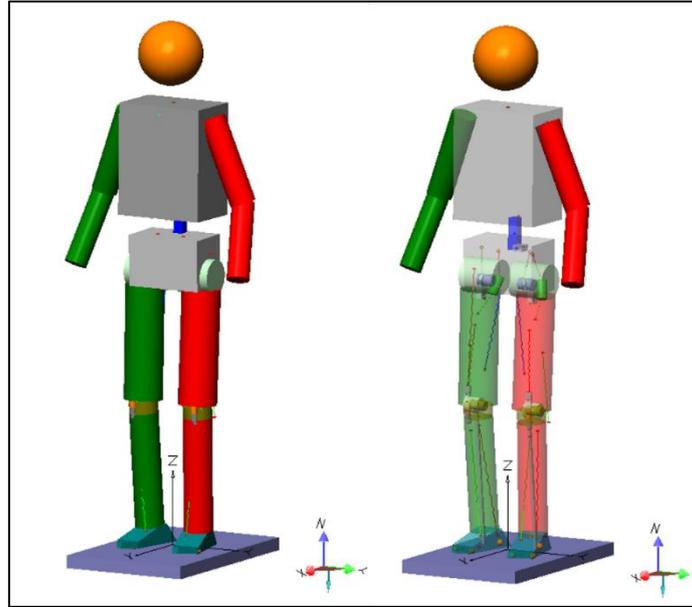
Figure 13. *The model of the human body was implemented in Simwise 4D, (Design Simulation Technologies, DST). A. the major segments were represented B. the internal structure of the legs and hips of the model were shown.*

The solid segments were connected by rigid constraints, with the exception of the joint that represents the hip, knee and ankle joints of the model, for which rotational constraints were used.

A cylindrical hinge was used to simulate each degree of freedom at the hips, knees and ankles (revolute joints, 1 degree of freedom). In particular, the following degrees of freedom were simulated: abduction-adduction, internal-external rotation, and flexion-extension at the hip, flexion-extension and internal-external rotation at the knee, plantar-flexion and dorsi-flexion at the ankle.

The axes of flexion-extension were oriented horizontally and parallel to the frontal plane for all the three joints. The axes of ab-adduction movement of the hips were oriented horizontally and parallel to the sagittal plane.

Six monoarticular muscles per leg were modeled in the simulations: they were the muscles that by their tone resist the force of gravity in the maintenance of normal standing posture (gluteus maximus, rectus femoris and soleus) and their antagonists (iliacus, biceps femoris capo brevis and tibialis anterior).

The muscles were represented by mechanical spring/damper elements (Figure 14).

In order to consider future evolution of the model and get it ready for the simulation of more complex movements, the transmission of the force of the rectu femoris, iliacus and gluteus maximus muscles was realized including rods, that simulated the tendon elements, and wrap surfaces on which muscle-tendon structures wraps up (Figure 15).

All the body and its left and right segments were symmetrical. The origin and insertion of all the muscles were also symmetrical in the two legs. In Table 19 joints, muscles and their action on the joint were collected. The distance from the origin point and from the insertion point of each muscle from the related joint is expressed respect to the coordinate system integral with the segment in which the points are placed.

For all the spring/damper elements, the adopted force generation law was: $F = K\Delta L^2 + c\dot{\Delta L}$ (where K was the stiffness coefficient, c was the damper coefficient and ΔL was the change between the postural equilibrium length of the spring, L_E, and the rest length, L_R^0).

At $t = 0$, L_R^0 was inferior to L_E to guarantee the minimum force to the muscle and maintain the model in standing position. The activation of a muscle was simulated by shortening natural length of the spring ($L_R^1 < L_R^0$), so that the muscle was lengthened. In this way, the initial force abruptly rose by $\Delta F = K((L_E - L_R^1)^2 - (L_E - L_R^0)^2)$.

A threshold was set to simulate the contraction of the muscle: the spring/damper elements were active only when the current length value was superior respect to the natural length value. In this way, the element exerted a force only when its length was longer but not when it was compressed, as the muscle.

The force perturbation produced by a spring damper element, induced accelerations in all segments of the model because of their dynamic coupling.

The displacement of the segments was computed by double integration (Kutta–Merson numerical method) starting from the initial kinematic condition and taking into account the ground reaction forces as an external constraint.

The floor was simulated with two rectangular plats positioned side by side, one under each foot. Each one was large 0.2 m, long 0.6 m, thick 0.04 m and weight 10 kg, and was constrained to the Ground of the Simwise 4D software with a rigid constraint positioned in the center of the superior surface of the platform. This expedient let us to measure the forces that reacts to the forces acting on the platform, as the gravity force and the contact forces with the human model.

The contact between the feet and the platforms was simulated with three little spherical bodies (diameter 0.02 m) with negligible mass linked under each foot with rigid constraints. The ground reaction forces resulted from a "non-penetration" constraint between these spherical bodies and the ground.

To compute collision response forces between each little sphere and platforms the Impulse/Momentum contact option was chosen, setting coefficients of restitution at zero and friction coefficient at 0.5.

As a consequence of the movement, the spring representing the activated muscle shortened (the current length of the spring decreased, $L_E^1 < L_E$) and the force vanished to zero.

The viscous damping coefficient of all the spring/damper elements was set to 1 Ns/m to smooth out the movement and to achieve a new steady state without oscillations.
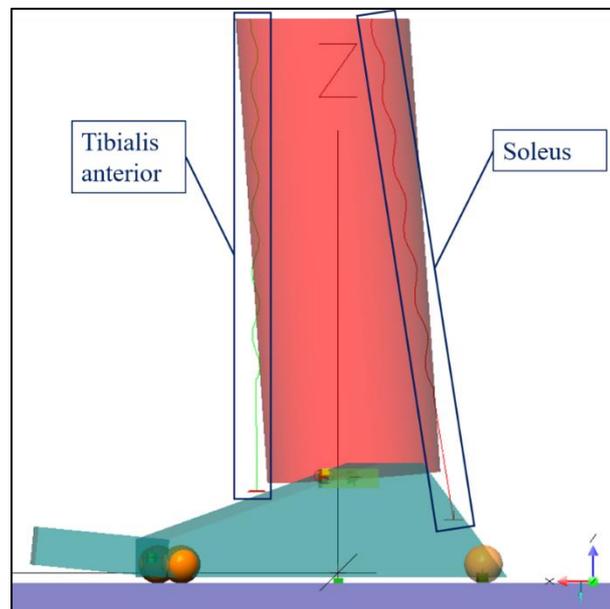
Figure 14. Sagittal view of the left ankle joint. Soleus (red spring-damper element) and tibialis anterior (green spring-damper element) muscles were evidenced.
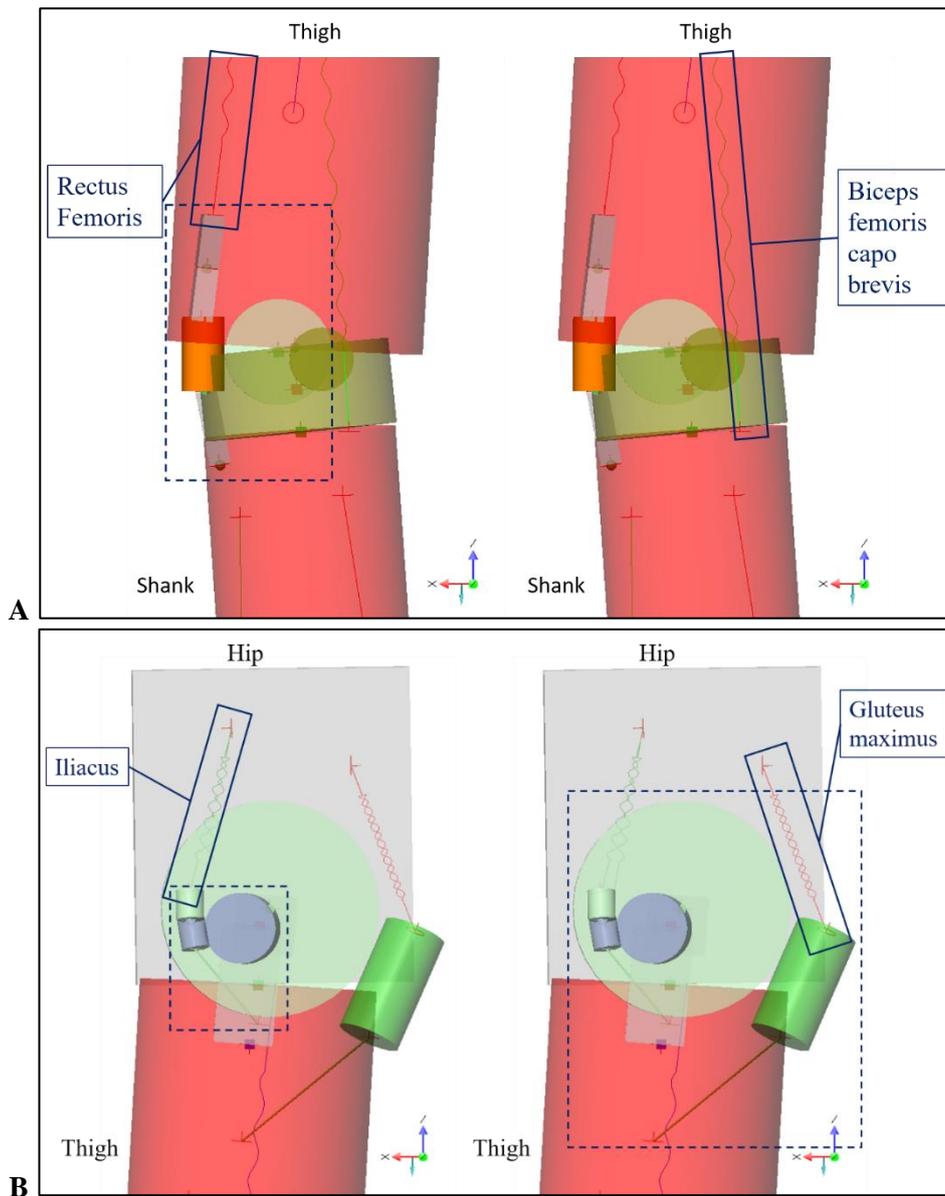
Figure 15. *Sagittal view of the knee (**A**) and hip (**B**) joints. Antagonist muscles were evidenced separately: anterior monoarticular muscles were shown on the left and posterior monoarticular muscles were shown on the right. In figures were separately evidenced antigravity muscles (red spring-damper elements) and their antagonist monoarticular muscles (green spring-damper elements). Dashed square evidenced the transmission system of force for rectu femoris, iliacus and gluteus maximus muscles.*

Table 19. Distances of the origin and the insertion points of the muscle.
For rectu femoris, iliacus and gluteus maximus muscles the insertion point was that of the rod.

Joint	Muscle	Direction of distance	Origin–Joint (mm)	Insertion–Joint (mm)	Wrap surface radius (mm)
	Pelvis	**Thigh**			
Hip	Flexor: **Iliacus**	**Δx** Anterior (+) / Posterior (-)	20	4	25
		Δy External (+) / Internal (-)	85	2.7	
		Δz Proximal (+) / Distal (-)	50	100	
	Extensor: **Gluteus Maximum**	**Δx** Anterior (+) / Posterior (-)	-40	-1.8	71
		Δy External (+) / Internal (-)	60	-10	
		Δz Proximal (+) / Distal (-)	30	160	
	Thigh	**Shank**			
Knee	Flexor: **Biceps femoris capo brevis**	**Δx** Anterior (+) / Posterior (-)	0.9	-25.6	
		Δy External (+) / Internal (-)	31	45	
		Δz Proximal (+) / Distal (-)	-0.7	179.6	
	Extensor: **Vasto intermedius**	**Δx** Anterior (+) / Posterior (-)	29	37	35
		Δy External (+) / Internal (-)	-3.5	16	
		Δz Proximal (+) / Distal (-)	68.8	167	
	Shank	**Foot**			
Ankle	Flexor: **Tibialis Anterior**	**Δx** Anterior (+) / Posterior (-)	29.7	43	
		Δy External (+) / Internal (-)	13	-20	
		Δz Proximal (+) / Distal (-)	142	45	
	Extensor: **Soleus**	**Δx** Anterior (+) / Posterior (-)	-18.7	-59	
		Δy External (+) / Internal (-)	9	0	
		Δz Proximal (+) / Distal (-)	149	30	

Simulation conditions

Gravity was included in the computation, so that internal muscle forces were required to keep the system in its static equilibrium. To simplify the analysis of the perturbation introduced with the variation of spring/damper elements natural length, the perfect symmetry of all the elements between left and right sides was verified. Furthermore, we neglected the internal-external rotation of hip and knee joints.

All initial velocities and accelerations were set to zero. Then, spring stiffness coefficient and natural length were set so that their action compensate the effect of gravity maintaining the model in up standing position (Table 20).

The initial configuration of the model was defined to correspond with standing up-right posture, and to the conventional descriptors of stance phase (Perry, 1992). The minimum and maximum values of the range of motion of the joints in the sagittal plane were set according to Roaas 1982.

The two muscles mostly involved in the anticipatory postural adjustments of gait initiation are the tibialis anterior, monoarticular muscles of ankle plantarflexion, and the soleus muscles which is the monoarticular muscles of ankle dorsiflexion. In this work, the combined action of these two muscles was investigated, altering the torque necessary to maintaining the postural equilibrium of the model. To better govern the torque applied at the ankle joints, a revolute motor constraint was added at each ankle joint coaxial to the revolute joint.

This kind of constraint exerts as much torque as necessary to maintain the given condition specified in terms of orientation, angular velocity, angular acceleration or torque.

Table 20. Natural length, current length and stiffness and dumper coefficients of the spring dumper elements that simulated muscles of the model.

Muscle	Rest Length L_R^0 (mm)	Postural Equilibrium Length L_E (mm)	Stiffness coefficient K (N/mm^2)	Damper coefficient c (N*s/mm)
Gluteus maximus	90.0	90.65	40	0.1
Iliacus	86.33	86.33	70	0.1
Biceps femoris capo brevis	219.76	219.43	10	0.1
Vasto intermedius	188.18	188.80	160	0.1
Soleus	356.5	357.20	40	0.1
Tibialis anterior	327.0	328.36	60	0.1

The orientation of the motors was controlled, to calculate the torque applied to the ankle joints as a result of the action of the spring-damper elements simulating soleus and tibialis. Particularly, the orientation of each motor was set to zero and the activity of calf muscles were turned off. The torque meter insert at each ankle joint measured the total torque that was applied to the ankle by the springs to maintain the standing position. The value of the torque measured at each joint was 3.486,72 Nmm.

The force exerted by the body mass, recorded from the meters at both platforms, was 590,595 N, while the position of the CoM in the anterior posterior direction was 3.9 mm. The perfect symmetry of the system was assumed, and the measure of the torque at each ankle was calculated knowing the force and its distance from the ankle joint:

$$T_{ankle} = -\frac{(b \cdot F_{BM})}{2}$$

where b was the sum of the position of the CoM in anterior posterior direction ($CoMx$) and the position of the ankle joint in the reference system (d), while F_{BM} was the force exerted by the body mass. The minus sign in the equation stands for a plantarflexion torque. Substituting the known value in the steady state position of our model, we obtain:

$$T_{ankle} = -\frac{b \cdot F_{BM}}{2} = -\frac{(d + CoMx) \cdot F_{BM}}{2} = -\frac{(7.88 + 3.9)\ mm \cdot 590.595\ N}{2} = -3.478,6\ Nmm$$

This value was very close to the value measured by the torque meter at the revolute motor constraint.

Thus, the torque exerted at the ankle by the muscles of each leg during the bipodalic standing position of the human body is T_{ankle}.

The following conditions were simulated using the musculoskeletal model here implemented:
1. the monolateral inhibition of soleus muscle,
2. the bilateral inhibition of both soleus,
3. the combined action of soleus inhibition and tibialis anterior activation on one leg,
4. the synergic action of soleus and tibialis anterior in both legs,
5. the influence of the delay in the action of the couple of muscles between legs,
6. the influence of the amplitude of the stimulation,
7. the influence of the delay between the inhibition of soleus and the activation of tibialis anterior,

and two pathological pattern of muscular activity:

8. reduced velocity of dorsiflexion action in the stance ankle respect to the swing one, as seen in subjects with Parkinson disease at mild stage of the disease (Figure 7),
9. delayed and reduced dorsiflexion torque of the swing ankle respect to the stance ankle, as seen in subjects with severe Parkinson disease (Figure 8).

Particularly, the inhibition and the activation of muscles on the shank were obtained by controlling the motors at the ankle joints with the torque control. In this way, it was possible to control directly the total torque applied to the ankle joints as a result of the TA and SOL muscles action.

In particular, the inhibition of the SOL was simulated by means of the command if, whose syntax was:

$$if(a, b, c)$$

that takes a statement a and two numbers, b and c. If a is true, then returns b. Otherwise, returns c.

In the case of those simulations, the a condition was based on the time in which the perturbation is wanted, b and c were the statement of the torque.

The action of the TA was simulated with the $step$ command, whose syntax was:

$$step(y0, t0, yf, tf)$$

This syntax creates a function whose value is $y0$ from $t = 0$ to $t = t0$ and whose value increases (or decreases) to yf at tf and then stays constant thereafter. Step is continuous in value and all its derivatives at both $t0$ and tf.

The choice of the value of the torque variation to apply at the ankles was done on the basis of the estimation of the plantarflexion produced by the synergic action of SOL and TA during the anticipatory postural adjustments of gait initiation.

For this estimation, we considered a mean male subject whose weight force is $F_{BM} = 780N$ and whose foot is $260\ mm$ length (FL).

From the experimental results obtained on healthy control subjects and described in the previous section (Chapter I and Chapter II), we know that the position of the CoP in the sagittal plane during standing, expressed in percentage of foot length, is $x_{CoP} = 45\ \%FL$ while his ankles at $x_{ankle} = 20\ \%FL$ from the heels. When the SOL muscles were inhibited and the TA were activated a dorsiflexion was produced at both ankles and the CoP displaced posteriorly $\Delta CoP_{AP} = 13\%FL$. The torque variation necessary to produce this displacement was:

$$\Delta T_{ankle} = \frac{\Delta CoP_{AP} \cdot F_{BM}}{2} = \frac{33.8\ mm \cdot 780\ N}{2} = 13.182\ Nmm$$

Thus, the torque that we will applied in the model to simulate the ankle dorsiflexion was 13.478,6 Nmm, that represented the synergic action of SOL inhibition (3.478,6 Nmm) and TA activation (10.000 Nmm).

Results from modeling

In this chapter, the results obtained through the model are shown. Firstly, the effect of the inhibition of SOL was investigated. The inhibition of SOL was obtained switching off the plantarflexion torque acting at the ankles to maintain the CoP anteriorly respect to the ankles, and the body in upright standing position. Then, the effect of the synergic action of SOL inhibition and TA activation was explored. This synergy was obtained with the variation of the torque until obtain a net dorsiflexion of the ankles. The effects of the torque variation on forces and displacement of CoP and CoM were described. Moreover, two pathological patterns of muscular activity were simulated. In particular, those patterns observed in the APAs of patients with PD at mild and severe stages of disease were reproduced.

Effects of dorsiflexion on CoP and CoM displacements

In this section, the results related to the inhibition of the SOL will be shown. In particular, the inhibition of one single SOL and the bilateral inhibition of both muscles were compared.

Inhibition of soleus muscles

The inhibition of just one SOL was simulated reducing the plantarflexion moment applied to the ankle joint until it was set to zero. The following results will show the displacement of the CoP, CoM and forces under each foot caused by a complete inhibition of the soleus muscle, for one or both legs. The torque at left ankle was set to zero at time 0.02 s using the if command (Figure 16. A). The effect of this little perturbation, as expected, was a decrease of force under the left foot and a correspondent increase of the force under the right foot (Figure 16. B).

Before the perturbation, the CoP was anterior respect to the ankle joints position about 12.5 mm. Because of the perturbation on the left ankle, the CoP displaced posteriorly about 6 mm and toward the right foot about 12 mm (Figure 17). The displacement of the CoP was suddenly followed by a slight displacement of the CoM forward and toward the left foot within 80 ms after the perturbation. This restrained displacement of the CoM was probably due to the rapidity of the stimulus, which was also reduced in amplitude, and to the rigidity of the feet simulated as rigid bodies.

When both the SOL were inhibited, setting to zero the torque at both ankles at time 0.02 s using the if command, the forces under both feet decreased as shown in Figure 18.

The CoP suddenly moved posteriorly reaching the position of the ankle joints as shown in Figure 19. Regarding the lateral direction, CoP displaced also slightly toward the right foot (less than 2 mm). This measurement was considered negligible because presumably due to a not complet symmetry in the model. The entities of the CoP displacement was significantly increased respect those produced by the inhibition of one single SOL.

Thus, if the torque applied at each ankle joint was set to zero, the CoP displaced back toward the position of the ankle joints in the reference system. This result was expected, because during standing position the soleus muscles were active to keep the CoP position anteriorly respect to the ankles.
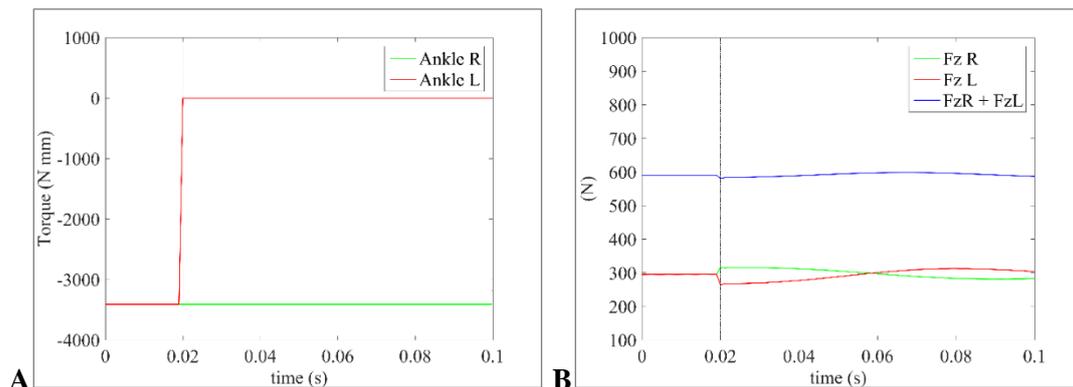

*Figure 16. **A.** Torque at left ankle joint. The negative sign of the torque represent a plantarflexion the positive sign represents a dorsiflexion. **B.** Vertical force under right and left foot and the total vertical force under the base of support. Dotted vertical black line indicates the time of the perturbation.*
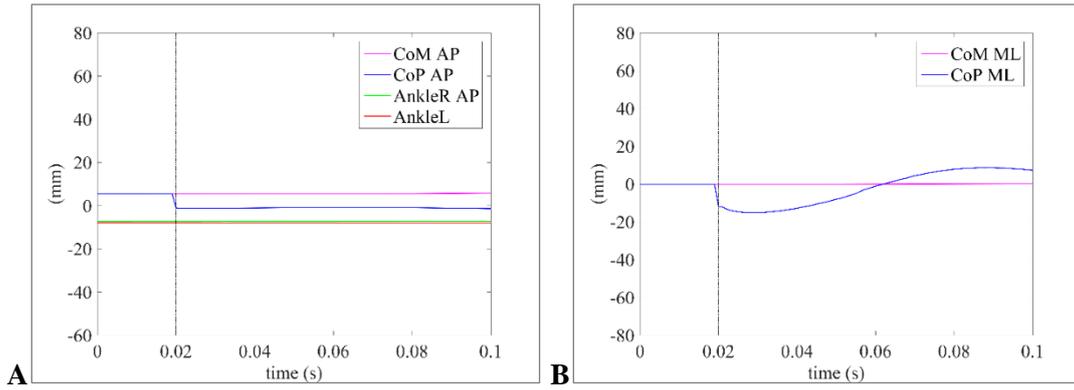
Figure 17. A. *The anterior posterior displacement of the CoP respect to the position of the CoM and the ankles position.* ***B.*** *The lateral displacement of the CoP respect to the CoM. The displacement was considered negative if posterior and toward the right foot.*
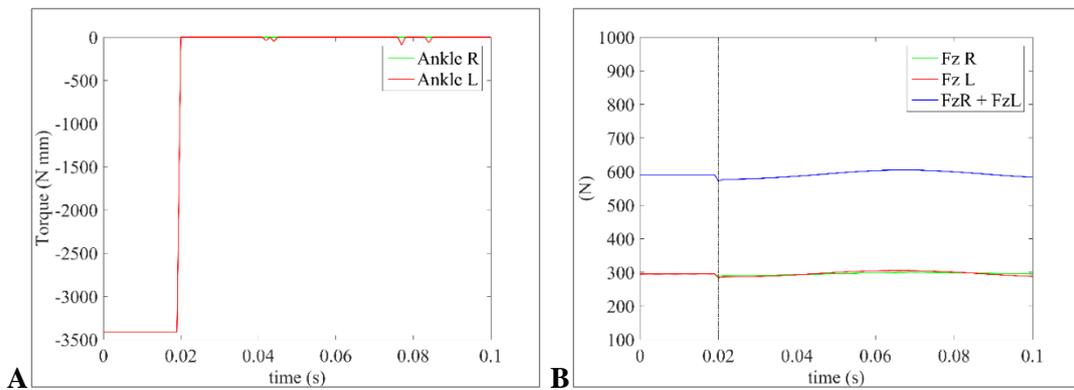
Figure 18. A. *Torque at both ankle joints. The negative sign of the torque represent a plantarflexion.* ***B.*** *Vertical force under right and left foot and the total vertical force under the base of support. Dotted vertical black line indicates the time of the perturbation.*
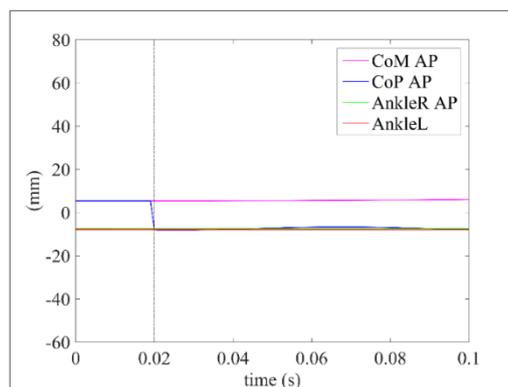

Figure 19. *The anterior posterior displacement of the CoP respect to the position of the CoM and the ankles position.*

Synergic inhibition of soleus and activation of tibialis anterior

The activation of the TA, summed to the inhibition of the SOL, was simulated inducing a dorsiflexion moment at one or both ankles. The effect due to the synergy SOL-TA at one single foot it is shown and then the displacement of the CoP and the force variations obtained after the bilateral perturbation of the four muscles it is represented.

Moreover, the delay between the perturbation given at the two ankles, as the effect produced by the difference in amplitude of the perturbations was investigated to recognize the effects related to each cause. The variation of the torque at the ankles was obtained through the command *step*.

In Figure 20. A, it was shown the action of a dorsiflexion torque of 13.478,6 *Nmm* applied at the left leg while at the right one continued to be applied the plantarflexion torque necessary to maintain the steady standing posture of the model.

This torque variation simulated the SOL inhibition and the TA activation at the right shank. The effect of this perturbation was an increase of the vertical force under the left foot (about 100 N) and a correspondent decrease of the vertical force under the left foot that results in a decrease of the total force under the global base of support (Figure 20. B). As was expected, this reduction is greater than that observed after the inhibition of the SOL.

As a consequence, the CoP displaced posteriorly (about 25 mm) and toward the right foot (about 45 mm) (Figure 21).

In Figure 22, the bilateral and simultaneous dorsiflexion of both ankles was shown. This perturbation caused a comparable reduction of the vertical force under each foot that resulted in the reduction of the total vertical force. The force variation here observed was greater than that produced by the dorsiflexion of just one ankle.

The displacement of the CoP was about 50 mm posteriorly and slightly toward the right foot (about 5 mm), probably due to an asymmetry in the model (Figure 23). Of note, the displacement produced by the bilateral dorsiflexion was significantly greater than that caused by the soleus inhibition, whose primary effect was to displace the CoP back and close to the ankles position.

The effect of a delay between the dorsiflexion of the two ankles was investigated. The left ankle was first dorsiflexed and, after 10 ms, the right one was perturbed with a torque variation of the same intensity (Figure 24. A).

As a result, the CoP suddenly displaced posteriorly (about 25 mm) and toward the right foot (about 45 mm), as was expected from the dorsiflexion of the left foot. After the torque variation of the other ankle, the CoP displaced toward the left foot turning back laterally and posteriorly (Figure 25). Thus, the CoP reached the same final posterior displacement obtained with the simultaneous dorsiflexion of both ankles but switching lateral direction on the basis of the side more perturbed. Thus, with a delay in the activation of one of the ankles it was possible to control the direction of the CoP displacement, and therefore also the CoM displacement in the opposite direction.

When the torque at the ankles was varied simultaneously in both legs but with different amplitudes as shown in Figure 26, the CoP suddenly displaced posteriorly (45 mm) toward the less perturbed foot (Figure 27). In particular, a greater dorsiflexion was imposed at the left ankle, and the CoP displaced backward and toward the right foot but less than what happened when the only left ankle was dorsiflexed (25 mm vs 45 mm).
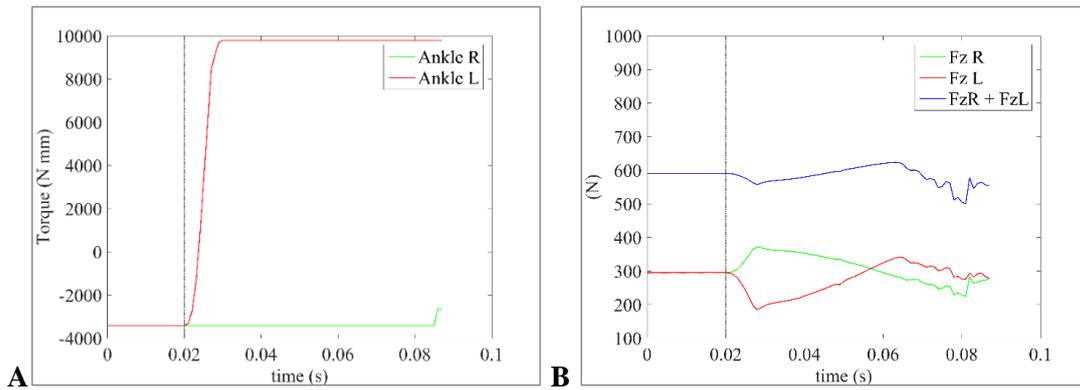
Figure 20. A. Torque at left ankle joint. The negative sign of the torque represent a plantarflexion the positive sign represents a dorsiflexion. B. Vertical force under right and left foot and the total vertical force under the base of support. Dotted vertical black line indicates the time of the perturbation.
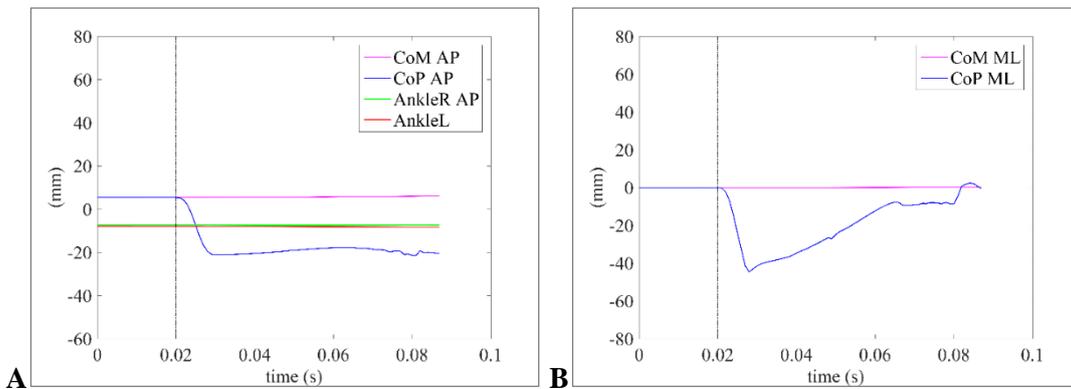

*Figure 21. A. The anterior posterior displacement of the CoP respect to the position of the CoM and the ankles position. B. The lateral displacement of the CoP respect to the CoM. The displacement was considered negative if posterior and toward the right foot.*
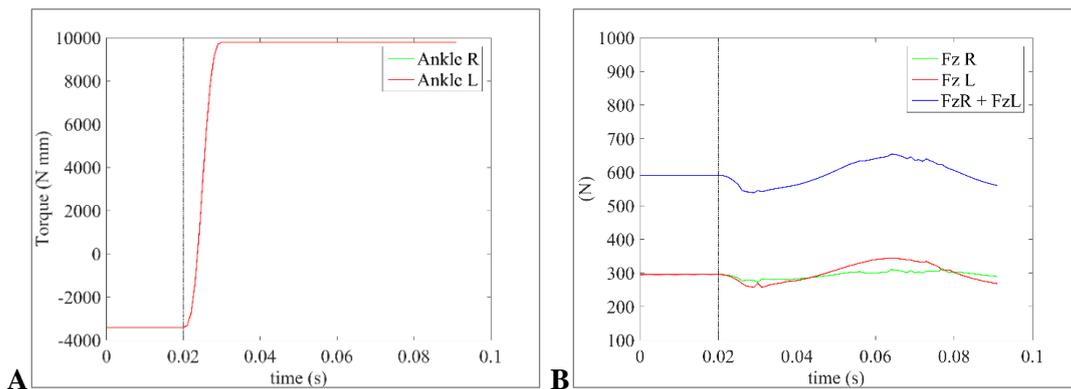

Figure 22. A. Torque at both ankle joints. The negative sign of the torque represent a plantarflexion the positive sign represents a dorsiflexion. B. Vertical force under right and left foot and the total vertical force under the base of support. Dotted vertical black line indicates the time of the perturbation.
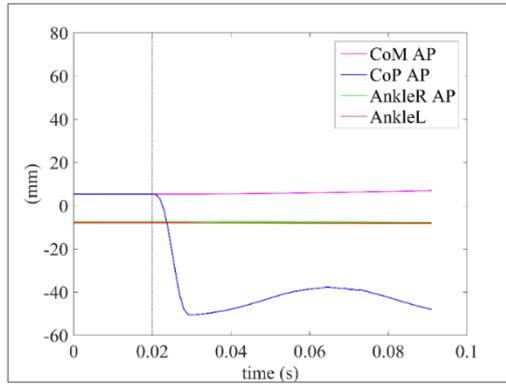
Figure 23. *The anterior posterior displacement of the CoP respect to the position of the CoM and the ankles position.*
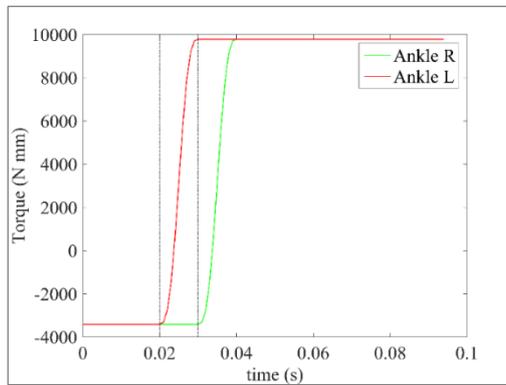
Figure 24. *Torque delayed at the tow ankle joints. The negative sign of the torque represent a plantarflexion, the positive sign represents a dorsiflexion Dotted vertical black line indicates the time of the perturbation.*
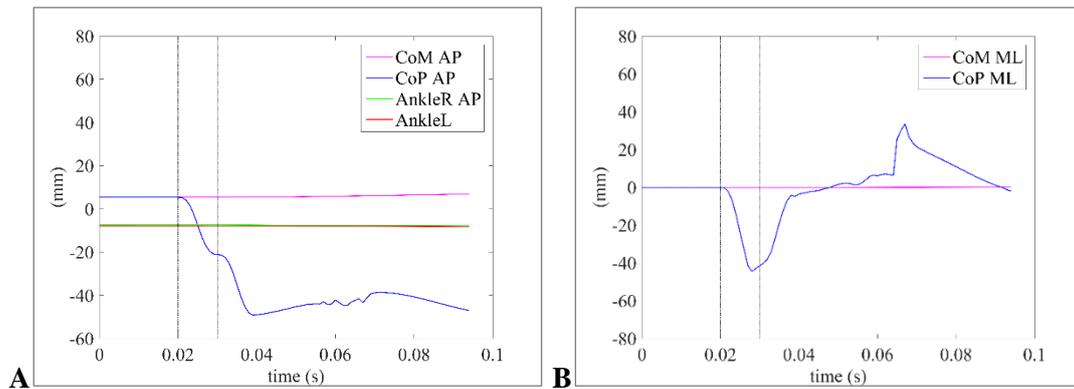
Figure 25. A. *The anterior posterior displacement of the CoP respect to the position of the CoM and the ankles position.* ***B.*** *The lateral displacement of the CoP respect to the CoM. The displacement was considered negative if posterior and toward the right foot.*
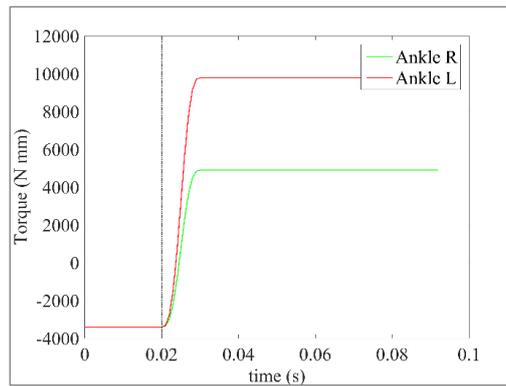
Figure 26. *Different torques at tow ankle joints. The negative sign of the torque represent a plantarflexion the positive sign represents a dorsiflexion. Dotted vertical black line indicates the time of the perturbation.*
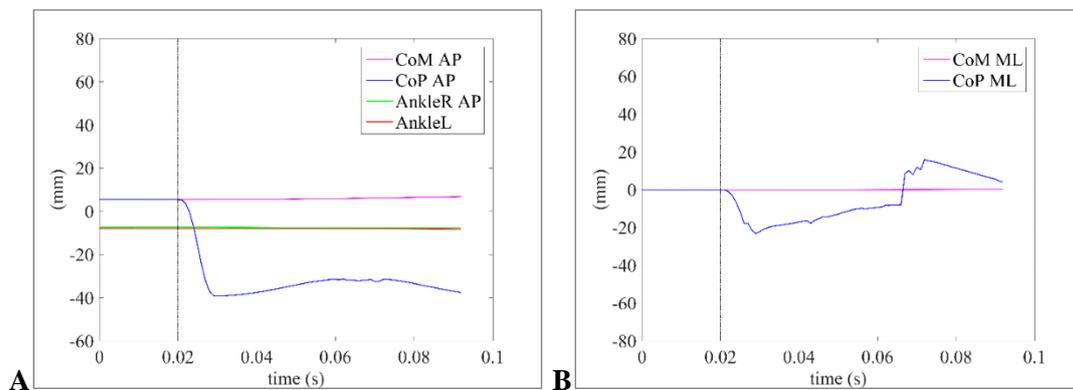
Figure 27. A. *The anterior posterior displacement of the CoP respect to the position of the CoM and the ankles position. **B**. The lateral displacement of the CoP respect to the CoM. The displacement was considered negative if posterior and toward the right foot.*

In Figure 28, the simulation of a delay between the inhibition of SOL and the activation of the TA was shown. Thus, a delay of 10 ms was imposed after setting to zero the plantarflexion torque existing at the ankles, necessary to maintain the equilibrium during the standing position, and before increasing the torque that produced a dorsiflexion of the feet.

Because of the symmetry of the perturbation in the two legs, the lateral displacement of the CoP was negligible, while the amplitude of the posterior displacement was visible and found conserved respect to the bilateral simultaneous dorsiflexion, without any delay between soleus inhibition and TA activation (Figure 29). Of course, the time necessary to reach the maximum posterior displacement was increased.
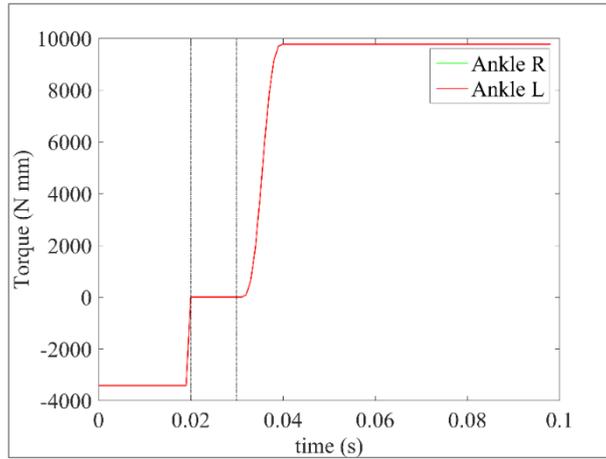
Figure 28. *Torque at both ankle joints. The negative sign of the torque represent a plantarflexion the positive sign represents a dorsiflexion. Dotted vertical black line indicates the time of the perturbation: one at 0.02 s and the other at 0.03 s.*
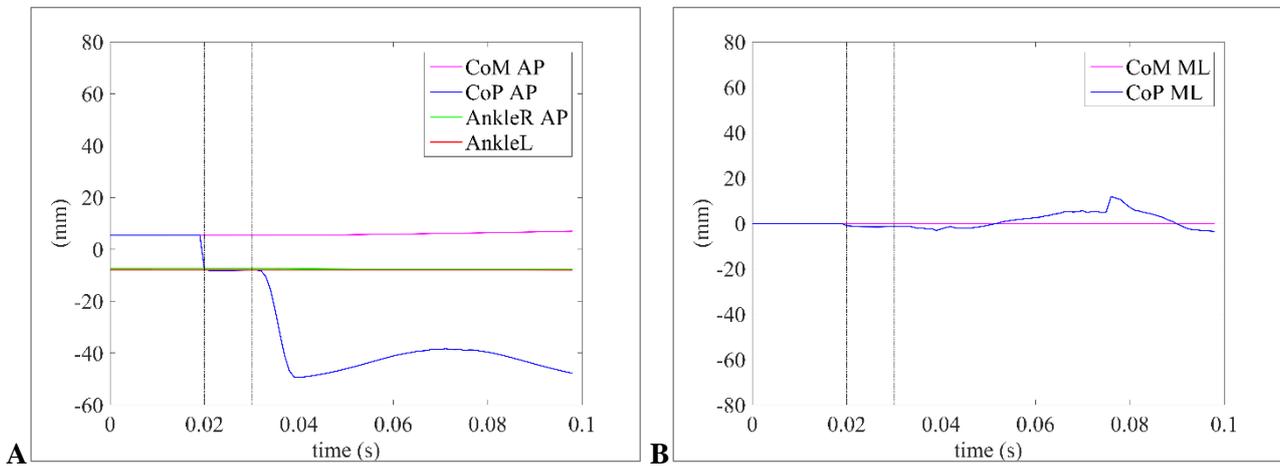
Figure 29. A. *The anterior posterior displacement of the CoP respect to the position of the CoM and the ankles position.* ***B.*** *The lateral displacement of the CoP respect to the CoM. The displacement was considered negative if posterior and toward the right foot.*

Summary of key results

This section has the aim to provide an overview of the results of the simulations done with the model to investigate the major effect caused by SOL inhibition, TA activation and little variation of these perturbations in time and amplitude.

In Figure 30, the displacements of the CoP produced in anterior-posterior and lateral direction were shown for each kind of perturbation.

A simplified shape of the foot was gathered from the position of the three contact points of the foot with the ground, to make easier the observation of the displacement respect to position of the feet during standing. With an arrow, it was indicated the orientation of the acceleration imprinted to the CoM by the CoP displacement.

It is possible to observe that the posterior displacement of the CoP produced with the simulation of the sole inhibition of the SOL was inferior to that obtained with a greater dorsiflexion which simulated the activation of the TA. When there was a delay between the SOL inhibition and the TA activation the, the posterior displacement was comparable to that produced without the delay, but was achieved in a longer time.

51
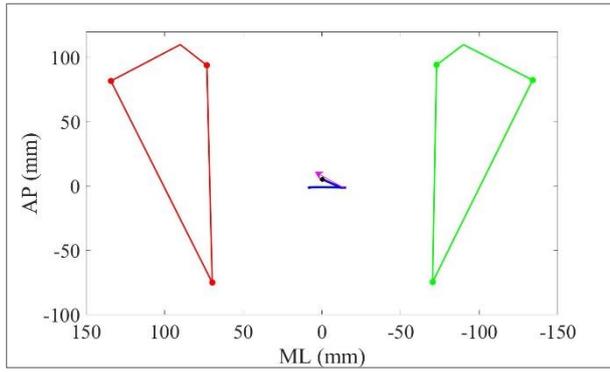
1. left soleus inhibition
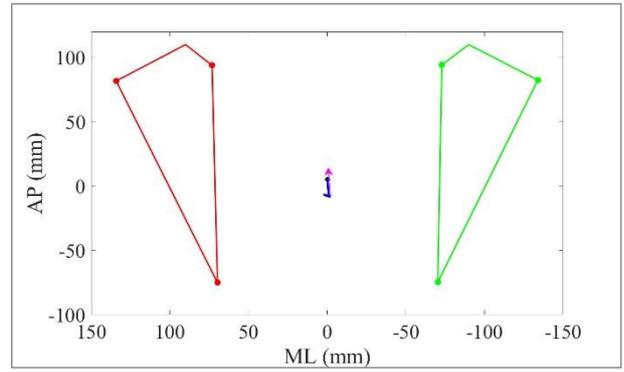
2. bilateral inhibition of soleus
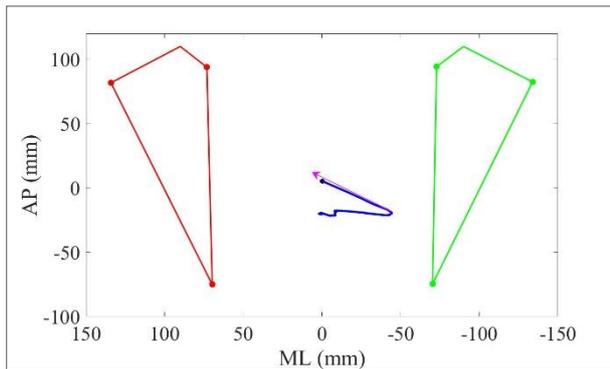

3. dorsiflexion of left ankle
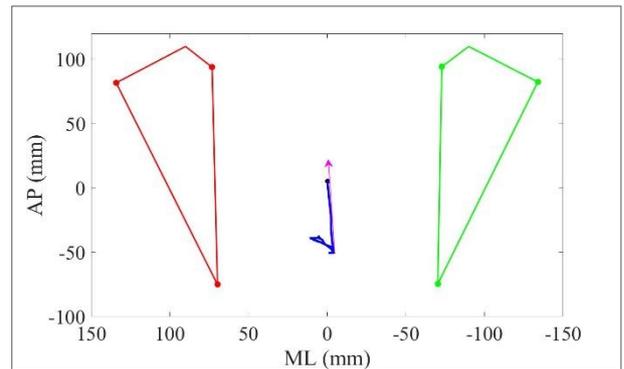
4. bilateral dorsiflexion of the ankles
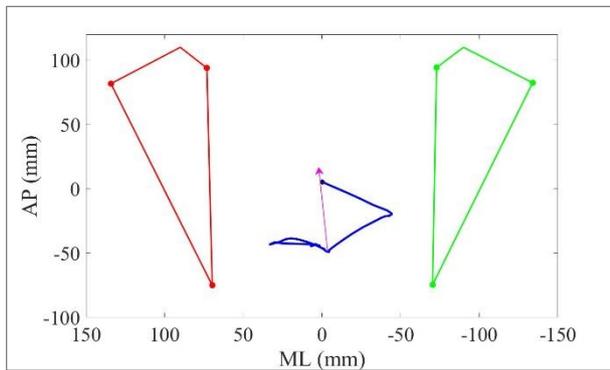
5. delayed dorsiflexion of right ankle
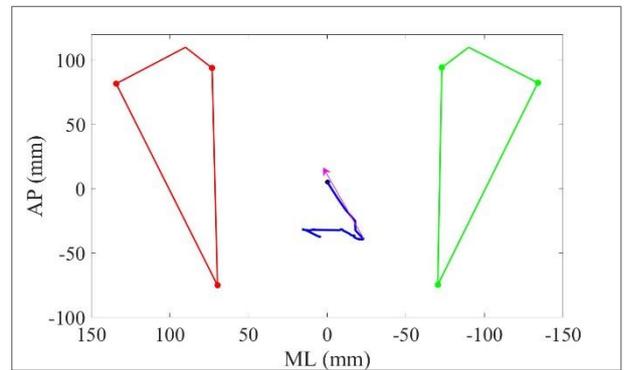
6. reduced dorsiflexion at right ankle
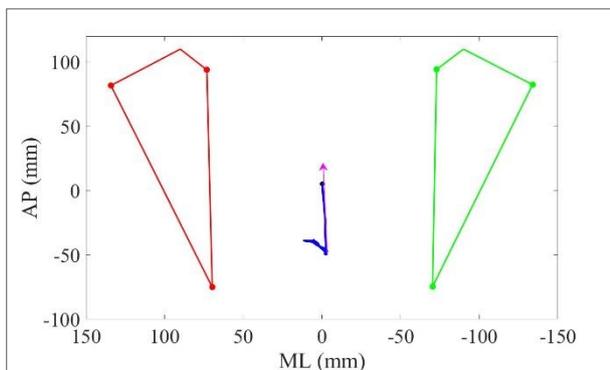
7. delay between soleus inhibition and tibialis anterior activation

Figure 30. The displacement of the CoP in anterior-posterior and lateral direction was shown for each kind of perturbation.

52

When the perturbation was different in the two legs, the CoP displacement laterally toward the side in which dorsiflexion moment was lower.

The dorsiflexion of the ankles produced effects also on the CoM displacement. In Figure 31, the forward and lateral displacements of the CoM were compared among all the perturbation simulated with the model described in this work.

It is possible to observe that the better strategy to push forward the CoM is the simultaneous dorsiflexion action at both ankles (*line 4*) that correspond to the simultaneous inhibition of both SOL and the activation of TA muscles, perturbed with the same amplitude of torque.

Immediately after the perturbation at time 0.02 s, the second more efficient perturbation in displacing forward the CoM was that one in which the amplitude of the dorsiflexion was different between legs (*line 6*). This kind of action is used in human strategy because it is useful to push forward the CoM but giving it also a direction toward the stance leg, and corresponds to the simultaneous inhibition of both SOL and the activation of both TA but with a reduced amplitude of activity in the swing limb (Figure 6). As observed in Figure 31.B, the more the ankles' torques were different, the more the CoM displaced laterally toward the foot more dorsiflexed. Introducing a little delay between the dorsiflexion of one foot respect to the other, and maintaining the same amplitude of perturbation in both legs (*line 5*), the CoM was less displaced forward in the first instants after 0.02 s, while then reached a displacement greater than those produced with the other combination of actions.
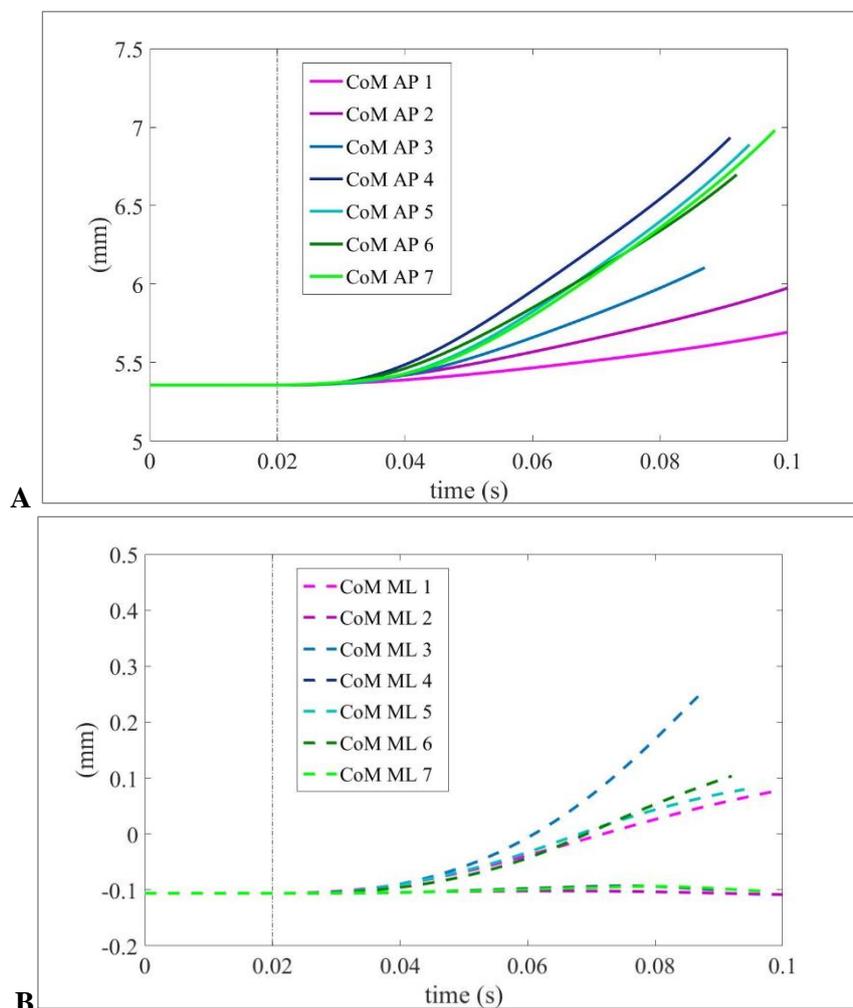
Figure 31. *The forward (**A**) and the lateral (**B**) CoM displacement obtained with the different combination of muscles activity for dorsiflexion action were compared: lines 1: one soleus inhibition; line 2: bilateral soleus inhibition; line 3: dorsiflexion of one single foot; line 4: simultaneous dorsiflexion of both feet with the same torque; line 5: delayed dorsiflexion of both feet with the same torque; line 6: simultaneous dorsiflexion of both feet with different torque; line 7: delay between bilateral soleus inhibition and bilateral dorsiflexion torque.*

Effects of altered pattern of dorsiflexion on the displacement of CoP and CoM

In this section, the results related to the simulation of two pathological pattern of muscular activity were reported. In particular, the patterns observed in the anticipatory postural adjustments of patients with Parkinson disease were reproduced.

The first simulation was inspired to the pattern reported in Figure 7, related to the anticipatory postural synergy of the gait initiation of a parkinsonian patient at a mild stage of his disease (PD_M). In this patient, a reduced velocity of dorsiflexion in the stance ankle respect to the swing one was seen.

In the model, the dorsiflexion was obtained with the *step* command, and a different slope was given to the left and the right ankles. The torque at the left foot started to be changed before and slowly respect to the torque at the right foot (Figure 32.A).

The second simulation inspired to a pathological muscular pattern activity reproduced the delayed and reduced dorsiflexion of the swing ankle respect to the stance ankle, seen in subjects with severe Parkinson disease (Figure 8). When the dorsiflexion torque in one of the feet was delayed and reduced in amplitude as shown in Figure 32.B, the combination of the effect produced by the delay of the dorsiflexion between feet and the effect caused by a difference in amplitude between torques were summed.

Regarding the simulation of the PD_M pattern of activation, the effect produced was the displacement of the CoP in the transverse plane comparable to that produced when the ankle dorsiflexion were just delayed. In particular, there was a backward displacement of the CoP toward the ankle less dorsiflexed (right foot), and then gradually toward the left foot, when the torque increased also at the right ankle (Figure 33).

Regarding the simulation of the PD_S pattern of activation, the action of the two dorsiflexions could be evidenced in the displacement of the CoP both in anterior posterior and lateral directions (Figure 34). Compressively, the CoP displacement produced was less backward oriented respect to the pattern of activation obtained with just a delay between the torques at the ankle. Thus, it would expected a reduced push of the CoM anteriorly, but also a greater acceleration laterally toward the foot more dorsiflexed.

In Figure 35, the components of the CoM displacement obtain from the simulations of the pathological synergies were shown and comparing to the pattern of muscular activation *6*, chosen as the best simulation for a HC subject's synergy. It is possible to observe that the simulation of the PD_M like synergy, (*line 8* in Figure 35), produced a reduced forward displacement of the CoM compared to the pattern of activation in HC subjects, (*line 6*), immediately after the first perturbation. However, at 60 ms the CoM displaced more forward being comparable to the displacement shown with *line 6*. On the other hand, the PD_M synergy produced a lacking displacement toward the left foot.

The simulation of the PD_S like synergy, (*line 9* in Figure 35), produced a backward displacement of the CoP constantly reduced respect to that shown by the *line 6*. On the other hand, the pattern of activation shown in Figure 32.B, produced a more lateral displacement of the CoM toward the left foot, that was the foot more dorsiflexed, suggesting that the synergy simulated has the effect to push the CoM more laterally then forward.
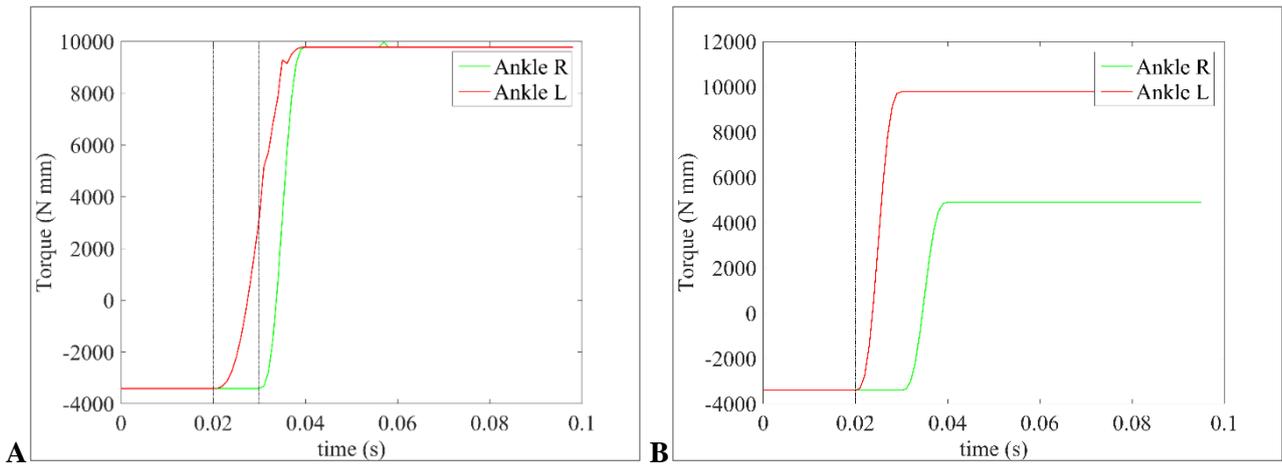
Figure 32. *Torque at ankle joints to simulate the pathological pattern of a PD_M subject (**A**) and of a PD_S subject (**B**). The negative sign of the torque represent a plantarflexion the positive sign represents a dorsiflexion. Dotted vertical black lines indicate the time of the perturbation: one at 0.02 s and the other at 0.03 s.*
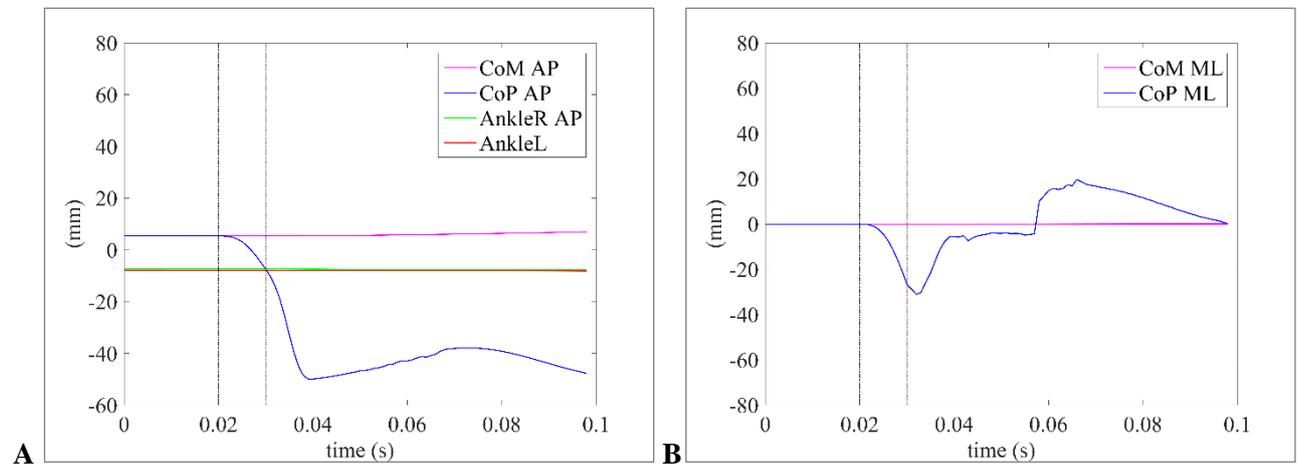

Figure 33. A. *The anterior posterior displacement of the CoP respect to the position of the CoM and the ankles position.* **B.** *The lateral displacement of the CoP respect to the CoM. The displacement was considered negative if posterior and toward the right foot.*
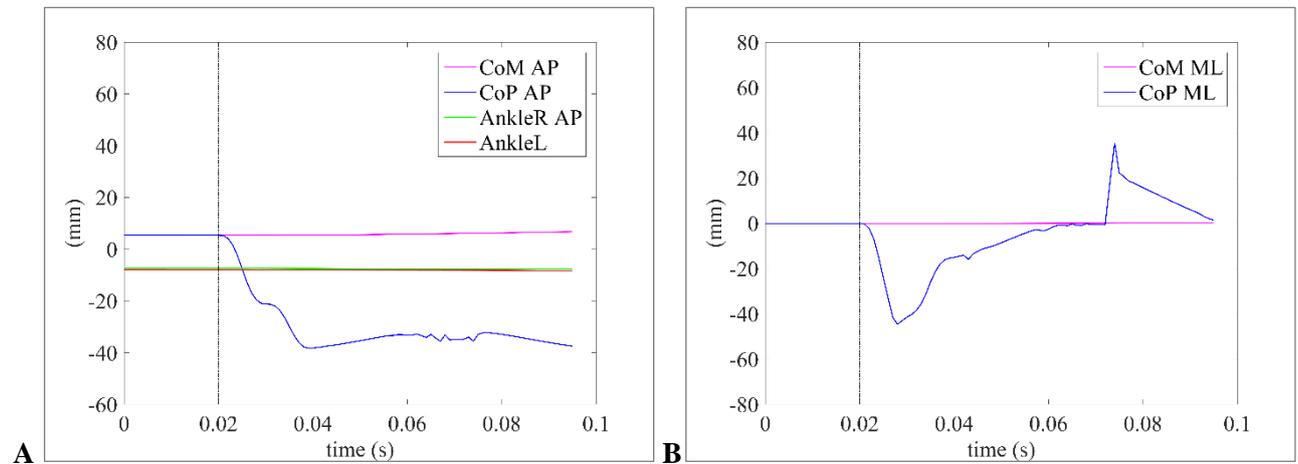
Figure 34. A. *The anterior posterior displacement of the CoP respect to the position of the CoM and the ankles position.* **B.** *The lateral displacement of the CoP respect to the CoM. The displacement was considered negative if posterior and toward the right foot.*
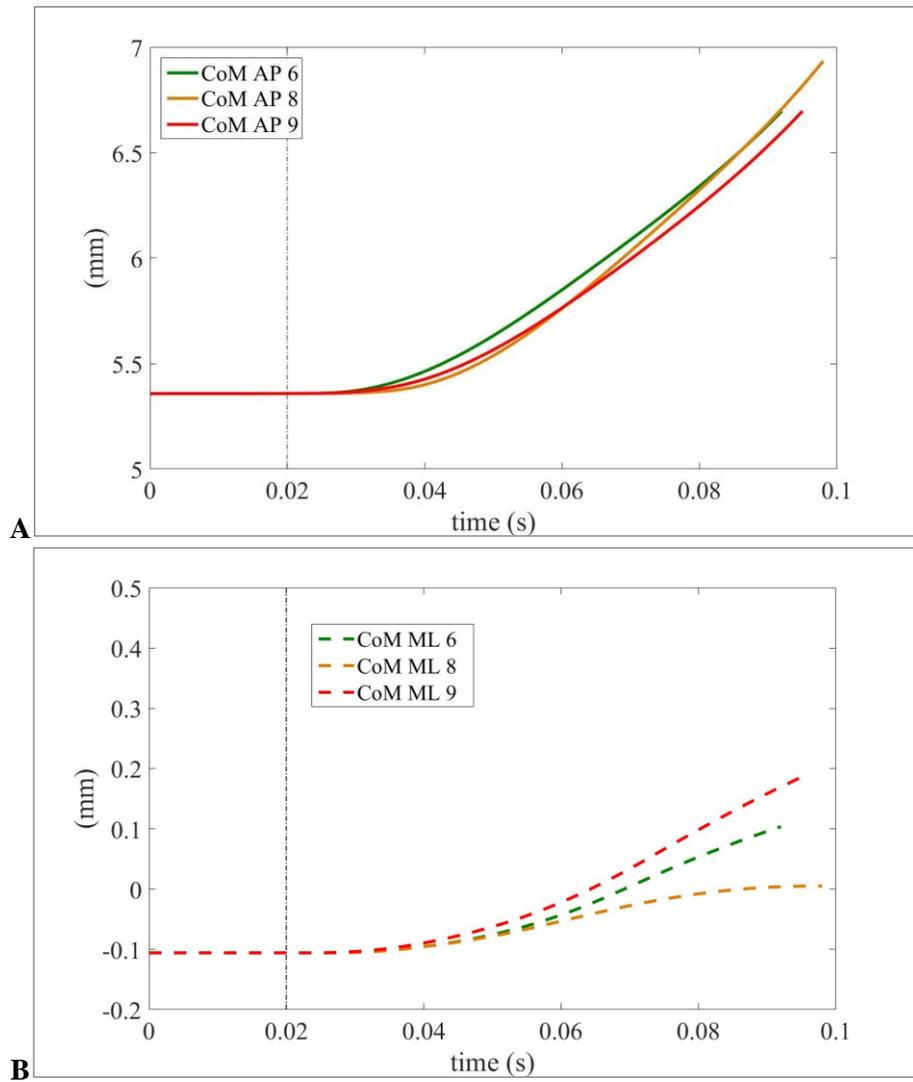
Figure 35*. The forward (**A**) and the lateral (**B**) CoM displacement obtained from a muscle activation pattern similar to the pattern of the healthy control subjects line 6, to the pattern of a PD_M subject line 8 and to the pattern of a PD_S subject line 9.*

CONCLUSIONS AND FUTURE SCENARIOS

The present work aimed to investigate the APAs of gait initiation, establishing first which parameters are influenced by the position of the feet before starting to walk. In fact, a preliminary study comparing subjects with PD_M, PD_S or PSP showed that patients greatly differ for the width of their base of support.

To address this question we first carried out a study on gait initiation in healthy subjects taking into account especially the distance between the feet (expressed as distance between anterior superior iliac spines, IFD%). We found that the parameters most influenced by the variation of the IFD% are the lateral displacements of the CoP during all APAs phases, the distance between CoP and the CoM during APAs, the orientation of the CoP-CoM vector at the end of APAs and the first step length. The values of all these measurements increased when the IFD% also increased. The variation of the initial conditions had no effect on the position of the CoP with respect to the heels during standing and on the posterior displacement of the CoP during APAs. While both magnitude and orientation of CoP-CoM vector at the end of unloading phase were significantly dependent on ankle distance, the orientation of CoP-CoM vector at the end of imbalance phase and the CoM forward acceleration were not. These results suggests that only these two parameters are independent parameters and could be taken into account to evaluate gait initiation independently from the base of support.

We, then, re-evaluated the gait initiation abnormalities in subjects with neurodegenerative diseases (i.e. PD and PSP) and this time patients were compared with different cohorts of healthy controls matched for IFD%. For PD, we identified two groups of patients at two different stages of the disease (mild PD_M and severe PD_S). The detailed evaluation of APAs parameters, also including measurements of the interplay between CoP and CoM, allowed us to describe several abnormalities in temporal and spatial scaling of APAs as well as to identify the related strategies to initiate walking. In particular, PD_M relied mostly on the ankle plantarflexion/dorsiflexion muscles at gait initiation (i.e. ankle strategy). Along with disease progression and possibly an increased in (axial) rigidity, PD_S developed APAs predominantly along the sagittal axis, thus suggesting a great impairment of the hip in the frontal plan and a desynchronization of ankle and hip strategies. These findings were also corroborated by an abnormal muscular activation pattern characterized by dis-synergistic or fragmented activity of pairs of postural muscles (i.e. tibialis anterior and soleus muscles).

PSP patients presented a combination of difficulties in mastering the hip and, even more, the ankle strategy as well as aberrant muscular activities, characterized mostly by a tonic activation of the TA. These measurements well correlated with the clinical picture of a devastating disease mainly characterized, at least at an early stage, by an impairment of balance with back falling. Despite we enrolled only patients able to stand and start walking unassisted; the neurodegenerative process involved in all subjects cortical and subcortical brain areas. Therefore, not only the execution of a coherent set of motor commands (i.e. APAs), but also the production (*feedforward* organization) of such commands was abnormal.

Finally, a musculoskeletal model for simulations of muscular activation and different type of synergies of the muscles of the lower limbs in standing position was described. This tool was used to provide some interpretation on the cause-effect relationships between the altered muscles pattern activation and the impairments observed in pathological subjects. It was found that the better strategy to push the CoM forwards was the simultaneous dorsiflexion of both ankles with comparable intensity of the torque between legs. A difference in the amplitude of the torque applied to each ankle reduced the forward push given to the CoM. On the other hand, it introduced a lateral displacement of the CoP toward the ankle on which the smaller torque acted, that caused a displacement of the CoM toward the more dorsiflexed leg. This kind of action is the strategy present in human anticipatory postural adjustments of gait initiation, when it is necessary to orient the displacement of the CoM on the stance foot (Figure 6).

Through the model was possible to simulate a delay between the dorsiflexion applied on one foot with respect to the other one, maintaining the same amplitude of perturbation in both legs, and in reverse, differentiate the amplitudes maintaining the same timing. The effect of the delay was to fragment the displacement of the CoP and delayed the displacement of the CoM. The main effect of the difference in amplitude between ankles dorsiflexion was to change the lateral displacement of the CoP, and consecutively of the CoM.

Of great relevance, the model allowed simulating two conditions similar to the altered muscular synergies observed respectively in PD_M and in PD_S subjects, and presented in this work.

In fact, the electromyography recorded in PD_M subjects during APAs at gait initiation showed that the TA of the stance (left) foot started its burst of activity before the TA of the swing (right) foot, but the peak of activity were reached in the same instant in both legs (Figure 7).

This muscles activation was reproduced in the model by varying the torque at each ankle with different times and with different velocities. This simulation showed a reduced forward and lateral displacement of the CoM compared to the pattern of activation usual in HC subjects.

In PD_S instead, the pattern visible from experimental results and reproduced with the model was characterized by delayed and reduced amplitude of the TA activity in the swing (right) leg before the displacement of the CoP during the imbalance phase (Figure 8). In the model, this was simulated with a delayed and reduced dorsiflexion torque at the right ankle. This action produced a displacement of the CoP backwards and towards the right foot, and accelerated the CoM forwards and towards the left leg. Comparing the forward displacement of the CoM with the healthy one, it was evident the poor efficacy of this synergy in displace the CoM forward while introduce a greater displacement in lateral direction toward the stance foot.

These results are in line with those observed in the experimental results and support a larger use of the musculoskeletal models in the study of biomechanics of human motion, in particular for helping the interpretation of altered pattern of movement related to neurodegenerative disease.

Despite the simplicity of the model used in this work to simulate muscular activation by the variation of dorsiflexion torque at the ankle joints, it allows a clear understanding of muscular functions and synergies and provides further understandings on the cause-effect relationships between the altered muscles pattern activation and the displacement of CoP and CoM.

However, the musculoskeletal model implemented, although quite effective for our purposes, has several limitations.

First of all, the development of this model was done with a simple anatomical architecture obtained through geometrical solids with mass and dimensions extracted from anthropometrical tables.

This computation model is highly dependent on the accuracy of the muscles reproduction, in particular their insertion points and their elastic characteristics. Moreover, the equilibrium of the model in upright standing position was obtained with only 12 muscles represented by spring damper elements, while many more are the muscles involved in this task, included those of the upper body. In this model, the movements permitted were in the sagittal plane, although also the ab-adduction of the hips was simulated. In particular, the flexion extension of the hip, the knee and the ankle joints were considered. Contrarily to the functional inclination angle of the rotation axis of anatomical joints, the axes of flexion extension movement of the joints simulated were oriented horizontally and parallel to the frontal plane.

Another important argument is the contact between surfaces, in particular of feet and ground. In this model, the foot was simulated as a rigid element of simple geometry, whose contact with the ground is rigidly transmitted through three spheres that interact with the ground with impulsive contact, and simulate the contact on the foot in just three point contacts, reducing the complexity and the errors of the computation. Therefore, with this model, it was not possible to simulate the soft tissue beneath the foot that could produce a delay in the transmission of the motor command from muscles to the measured variables, as the CoP displacement.

The use of the MRI images for the reconstruction of geometries with shapes closer to humans and to better simulate the contact of the foot with the ground could help in obtaining more reliable results. The introduction of a closed loop control system could provide also the opportunity to control more muscles, for example varying their stiffness or better their rest length, to find the muscular force necessary to perform a prescribed movement or maintain the upright standing position.

Despite these limitations, the results obtained should encourage the use dynamic musculoskeletal models to face clinical problems and pathophysiological questions. This kind of model could provide the opportunity to go deeper into the interpretation of the effect produced by a rehabilitation program, a pharmacological treatment, or a surgical procedure on the muscular activation patterns, the displacement of a body segment or of the whole body CoM during a prescribed movement, such as the gait initiation.

BIBLIOGRAPHY

Amano, S., Skinner, J. W., Lee, H. K., Stegemöller, E. L., Hack, N., Akbar, U., … Hass, C. J. (2015). Discriminating features of gait performance in progressive supranuclear palsy. *Parkinsonism & Related Disorders*, *21*(8), 888–93. http://doi.org/10.1016/j.parkreldis.2015.05.017

Belen'kii, V. E., Gurfinkel, V. S., & Pal'tsev, E. I. (1967). On the control elements of voluntary movements. *Biofizika*.

Breniere, Y., & Do, M. C. (1986). When and how does steady state gait movement induced from upright posture begin? *Journal of Biomechanics*, *19*(12), 1035–1040. http://doi.org/10.1016/0021-9290(86)90120-X

Carlsöö, S. (1966). The initiation of walking. *Acta Anatomica*, *65*, 1–9.

Carpinella, I., Crenna, P., Calabrese, E., Rabuffetti, M., Mazzoleni, P., Nemni, R., & Ferrarin, M. (2007). Locomotor function in the early stage of Parkinson's disease. *IEEE Transactions on Neural Systems and Rehabilitation Engineering : A Publication of the IEEE Engineering in Medicine and Biology Society*, *15*(4), 543–551. http://doi.org/10.1109/TNSRE.2007.908933

Carpinella, I., Crenna, P., Rabuffetti, M., & Ferrarin, M. (2010). Coordination between upper- and lower-limb movements is different during overground and treadmill walking. *European Journal of Applied Physiology*, *108*(1), 71–82. http://doi.org/10.1007/s00421-009-1168-5

Cavagna, G. A., Heglund, N. C., & Taylor, C. R. (1977). Mechanical work in terrestrial locomotion: two basic mechanisms for minimizing energy expenditure. *American Journal of Physiology - Regulatory, Integrative and Comparative Physiology*, *233*, R243–R261.

Christiansen, C. L., Schenkman, M. L., McFann, K., Wolfe, P., & Kohrt, W. M. (2009). Walking economy in people with Parkinson's disease. *Movement Disorders*, *24*(10), 1481–1487. http://doi.org/10.1002/mds.22621

Cook, T., & Cozzens, B. (1976). Human solutions for locomotion: the initiation of gait. In *Neural Control of Locomotion* (Vol. 61, pp. 65–76).

Crenna, P., Carpinella, I., Rabuffetti, M., Rizzone, M., Lopiano, L., Lanotte, M., & Ferrarin, M. (2006). Impact of subthalamic nucleus stimulation on the initiation of gait in Parkinson's disease. *Experimental Brain Research. Experimentelle Hirnforschung. Experimentation Cerebrale*, *172*(4), 519–532.

Dalton, E., Bishop, M., Tillman, M. D., & Hass, C. J. (2011). Simple Change in Initial Standing Position Enhances the Initiation of Gait. *Medicine & Science in Sports & Exercise*, *43*(12), 2352–2358.

Dariush, B., Parnianpour, M., & Hemami, H. (1998). Stability and a control strategy of a multilink musculoskeletal model with applications in FES. *IEEE Transactions on Bio-Medical Engineering*, *45*(1), 3–14. http://doi.org/10.1109/10.650346

Delp, S. L., Anderson, F. C., Arnold, A. S., Loan, P., Habib, A., John, C. T., … Thelen, D. G. (2007). OpenSim: Open-source software to create and analyze dynamic simulations of movement. *IEEE Transactions on Biomedical Engineering*, *54*(11), 1940–1950. http://doi.org/10.1109/TBME.2007.901024

Elble, R. J., Moody, C., Leffler, K., & Sinha, R. (1994). The initiation of normal walking. *Movement Disorders : Official Journal of the Movement Disorder Society*, *9*(2), 139–46. http://doi.org/10.1002/mds.870090203

Ferrarin, M., Lopiano, L., Rizzone, M., Lanotte, M., Bergamasco, B., Recalcati, M., & Pedotti, A. (2002). Quantitative analysis of gait in Parkinson's disease: a pilot study on the effects of bilateral sub-thalamic stimulation. *Gait & Posture.*, *16*(2), 135–148.

Ferrarin, M., Rizzone, M., Bergamasco, B., Lanotte, M., Recalcati, M., Pedotti, A., & Lopiano, L. (2005). Effects of bilateral subthalamic stimulation on gait kinematics and kinetics in Parkinson's disease. *Experimental Brain Research*, *160*(4), 517–527. http://doi.org/10.1007/s00221-004-2036-5

Hill, E., Stuart, S., Lord, S., Del Din, S., & Rochester, L. (2016). Vision, visuo-cognition and postural control in Parkinson's disease: An associative pilot study. *Gait and Posture*, *48*, 74–76. http://doi.org/10.1016/j.gaitpost.2016.04.024

Hunter, I. W., & Kearney, R. E. (1982). Dynamics of human ankle stiffness: Variation with mean ankle torque. *Journal of Biomechanics*, *15*(10), 747–752. http://doi.org/10.1016/0021-9290(82)90089-6

Kimmeskamp, S., & Hennig, E. M. (2001). Heel to toe motion characteristics in Parkinson patients during free walking. *Clinical Biomechanics*, *16*(9), 806–812. http://doi.org/10.1016/S0268-0033(01)00069-9

Kirker, S. G., Simpson, D. S., Jenner, J. R., & Wing, A. M. (2000). Stepping before standing: hip muscle function in stepping and standing balance after stroke. *Journal of Neurology, Neurosurgery, and Psychiatry*, *68*(4), 458–464. http://doi.org/10.1136/jnnp.68.4.458

Maggioni, M. A., Veicsteinas, A., Rampichini, S., Cé, E., Nemni, R., Riboldazzi, G., & Merati, G. (2012). Energy cost of spontaneous walking in Parkinson's disease patients. *Neurological Sciences*, *33*(4), 779–784. http://doi.org/10.1007/s10072-011-0827-6

Mann, R. A., Hagy, J. L., White, V., & Liddell, D. (1979). The initiation of gait. *The Journal of Bone and Joint Surgery. American Volume*, *61*(2), 232–239. http://doi.org/10.1016/0966-6362(94)90064-7

Michalowska, M., Fiszer, U., Krygowska-Wajs, A., & Owczarek, K. (2005). Falls in Parkinson's disease. Causes and impact on patients' quality of life. *Funct Neurol*, *20*(4), 163–168.

Mickelborough, J., Van Der Linden, M. L., Tallis, R. C., & Ennos, A. R. (2004). Muscle activity during gait initiation in normal elderly people. *Gait and Posture*, *19*(1), 50–57. http://doi.org/10.1016/S0966-6362(03)00016-X

Mitoma, H., Hayashi, R., Yanagisawa, N., & Tsukagoshi, H. (2000). Characteristics of parkinsonian and ataxic gaits: A study using surface electromyograms, angular displacements and floor reaction forces. *Journal of the Neurological Sciences*, *174*(1), 22–39. http://doi.org/10.1016/S0022-510X(99)00329-9

Morasso, P. G., & Sanguineti, V. (2002). Ankle muscle stiffness alone cannot stabilize balance during quiet standing. *Journal of Neurophysiology*, *88*(4), 2157–2162. http://doi.org/10.1152/jn.00719.2001

Morasso, P. G., & Schieppati, M. (1999). Can Muscle Stiffness Alone Stabilize Upright Standing ? *Journal of Neurophysiology*, *82*, 1622–1626. http://doi.org/10.1016/S0268-0033(01)00090-0

Morris, M. E., Huxham, F., McGinley, J., Dodd, K., & Iansek, R. (2001). The biomechanics and motor control of gait in Parkinson disease. *Clinical Biomechanics*, *16*(6), 459–470. http://doi.org/10.1016/S0268-0033(01)00035-3

Morris, M. E., Iansek, R., Matyas, T. A., & Summers, J. J. (1994a). The pathogenesis of gait hypokinesia in Parkinson's disease. *Brain : A Journal of Neurology*, *117*(5), 1169–81. http://doi.org/10.1093/brain/117.5.1169

Morris, M. E., Iansek, R., Matyas, T. A., & Summers, J. J. (1994b). Ability to modulate walking cadence remains intact in Parkinson's disease. *Journal of Neurology, Neurosurgery, and Psychiatry*, *57*(12), 1532–1534. http://doi.org/10.1136/jnnp.57.12.1532

Morris, M. E., Iansek, R., Matyas, T. A., & Summers, J. J. (1996). Stride length regulation in Parkinson's disease. Normalization strategies and underlying mechanisms. *Brain : A Journal of Neurology*, *119 (Pt 2*, 551–568. http://doi.org/10.1093/brain/119.2.551

Morris, M. E., McGinley, J., Huxham, F., Collier, J., & Iansek, R. (1999). Constraints on the kinetic, kinematic and spatiotemporal parameters of gait in Parkinson's disease. *Human Movement Science*, *18*(2-3), 461–483. http://doi.org/10.1016/S0167-9457(99)00020-2

Morris, M., Iansek, R., McGinley, J., Matyas, T., & Huxham, F. (2005). Three-dimensional gait biomechanics in Parkinson's disease: Evidence for a centrally mediated amplitude regulation disorder. *Movement Disorders*, *20*(1), 40–50. http://doi.org/10.1002/mds.20278

Nieuwboer, A., De Weerdt, W., Dom, R., Peeraer, L., Lesaffre, E., Hilde, F., & Baunach, B. (1999). Plantar force distribution in Parkinsonian gait: a comparison between patients and age-matched control subjects. *Scandinavian Journal of Rehabilitation Medicine*, *31*(3), 185–92.

Perry J. (1992) Gait Analysis: Normal and Pathological Function *(14th Ed.) Slack Incorporated, Thorofare* .

Player, J. R. (2001). Falls and Parkinson's disease. *Age and Ageing*, *30*(1), 3–4. http://doi.org/10.1093/ageing/30.1.3

Roaas, A., & Andersson, G. B. (1982). Normal range of motion of the hip, knee and ankle joints in male subjects, 30–40 years of age. *Acta Orthopaedica Scandinavica, 53*(2), 205-208.

Rocchi, L., Chiari, L., Mancini, M., Carlson-Kuhta, P., Gross, A., & Horak, F. B. (2006). Step initiation in Parkinson's disease: Influence of initial stance conditions. *Neuroscience Letters*, *406*(1-2), 128–132. http://doi.org/10.1016/j.neulet.2006.07.027

Vieregge, P., Stolze, H., Klein, C., & Heberlein, I. (1997). Gait quantitation in Parkinson's disease--locomotor disability and correlation to clinical rating scales. *Journal of Neural Transmission (Vienna, Austria : 1996)*, *104*(2-3), 237–248. http://doi.org/10.1007/BF01273184

Weiss, P. L., Hunter, I. W., & Kearney, R. E. (1988). Human ankle joint stiffness over the full range of muscle activation levels. *Journal of Biomechanics*, *21*(7), 539–544. http://doi.org/10.1016/0021-9290(88)90217-5

Winter, D. A. (1990). *Biomechanics and Motor Control of Human Movement. Processing* (Vol. 2nd). http://doi.org/10.1002/9780470549148

Winter, D. A. (1995). Human balance and posture control during standing and walking. *Gait and Posture*. http://doi.org/10.1016/0966-6362(96)82849-9

Winter, D. A., MacKinnon, C. D., Ruder, G. K., & Wieman, C. (1993). An integrated EMG / biomechanical model of upper body balance and posture during human gait. *Prog Brain Res*, *97*, 359–367.

Winter, D. A., Patla, A. E., Prince, F., Ishac, M., Gielo-perczak, K., Jc, Q., … Ishac, M. (1998). Stiffness Control of Balance in Quiet Standing. *Journal of Neurophysiology*, *80*, 1211–1221.

Winter, D. A., Patla, A. E., Rietdyk, S., & Ishac, M. G. (2001). Ankle muscle stiffness in the control of balance during quiet standing. *Journal of Neurophysiology*, *85*(6), 2630–2633. http://doi.org/Pdf/Winter_etal_2001.pdf

Winter, D. A., Prince, F., Frank, J. S., Powell, C., & Zabjek, K. F. (1996). Unified theory regarding A/P and M/L balance in quiet stance. *Journal of Neurophysiology*, *75*(6), 2334–2343. http://doi.org/http://www.ncbi.nlm.nih.gov/entrez/query.fcgi?cmd=Retrieve&db=PubMed&dopt=Citation&list_uids=8793746

Winter, D. A., & Yack, H. J. (1987). EMG profiles during normal human walking: stride-to-stride and inter-subject variability. *Electroencephalography and Clinical Neurophysiology*, *67*(5), 402–411. http://doi.org/10.1016/0013-4694(87)90003-4

Zatsiorsky, V., & Seluyanov, V. (1983). The mass and inertia characteristics of the main segments of the human body. *Biomechanics VIII-B: Proceedings of the Eight International Congress of Biomechanics*, 1152–1159.

APPENDIX A

MECHANICAL ENERGY RECOVERY DURING WALKING IN PATIENTS WITH PARKINSON DISEASE

Dipaola, M., Pavan, E. E., Cattaneo, A., Frazzitta, G., Pezzoli, G., Cavallari, P., Frigo, C. A. and Isaias, I. U.

Mechanical Energy Recovery during Walking in Patients with Parkinson Disease

Mariangela Dipaola[1,2], Esteban E. Pavan[2], Andrea Cattaneo[1,3], Giuseppe Frazzitta[4], Gianni Pezzoli[5], Paolo Cavallari[1], Carlo A. Frigo[2], Ioannis U. Isaias[3,5,6]*

1 Department of Pathophysiology and Transplantation, Human Physiology Section, Università degli Studi di Milano, Milan, Italy, 2 Movement Biomechanics and Motor Control Lab, Dipartimento di Elettronica, Informazione e Bioingegneria, Politecnico di Milano, Milan, Italy, 3 Department of Neurology, University Hospital of Würzburg and Julius Maximilian University of Würzburg, Würzburg, Germany, 4 Moriggia-Pelascini Hospital, Gravedona ed Uniti, Italy, 5 Parkinson Institute, Pini-CTO (ex ICP) Milan, Italy, 6 Fondazione Europea di Ricerca Biomedica FERB Onlus, Milan, Italy

* Isaias_I@ukw.de

Abstract

The mechanisms of mechanical energy recovery during gait have been thoroughly investigated in healthy subjects, but never described in patients with Parkinson disease (PD). The aim of this study was to investigate whether such mechanisms are preserved in PD patients despite an altered pattern of locomotion. We consecutively enrolled 23 PD patients (mean age 64±9 years) with bilateral symptoms (H&Y ≥II) if able to walk unassisted in medication-off condition (overnight suspension of all dopaminergic drugs). Ten healthy subjects (mean age 62±3 years) walked both at their 'preferred' and 'slow' speeds, to match the whole range of PD velocities. Kinematic data were recorded by means of an optoelectronic motion analyzer. For each stride we computed spatio-temporal parameters, time-course and range of motion (ROM) of hip, knee and ankle joint angles. We also measured kinetic (W_k), potential (W_p), total (W_{totCM}) energy variations and the energy recovery index (ER). Along with PD progression, we found a significant correlation of W_{totCM} and W_p with knee ROM and in particular with knee extension in terminal stance phase. W_k and ER were instead mainly related to gait velocity. In PD subjects, the reduction of knee ROM significantly diminished both W_p and W_{totCM}. Rehabilitation treatments should possibly integrate passive and active mobilization of knee to prevent a reduction of gait-related energetic components.

Introduction

Gait disturbance is a relevant component of motor disability in subjects with Parkinson disease (PD) and a large amount of experimental work has been dedicated to investigate biomechanical abnormalities in these patients. While PD patients at an early disease stage can show exclusively a reduction of gait velocity and stride length [1–3], along with disease progression they usually exhibit shortened stride length, prolonged stance and double support phases [4,5] and reduced velocity [3–6]. Gait cadence might not be altered [7,8] or, in some cases, it appears to be increased as a possible adaptation to stride length reduction [6,8–10]. The range-of-motion

(ROM) at lower limb joints is also usually reduced [8,11–15]. Very few studies, with unclear results, investigated energetic expenditure in PD patients. In particular, patients were investigated in unspecified meds-on state [16], or while walking on a treadmill [17], a condition which has been shown to alter the gait pattern with respect to over-ground walking [18,19]. In addition, PD patients were never compared to healthy subjects walking at similar velocities. Last but not least, the role of mechanical energy recovery was never taken into account in the analysis of energy expenditure along a stride cycle of PD patients.

In normal walking, the gravitational potential energy (E_p) of the center of mass (CM) is at maximum level during mid stance, when the kinetic energy (E_k) of the CM is minimum. From mid stance, the CM descends, and E_p is partially converted into E_k; forward acceleration occurs and the body lands on the contralateral limb. After this foot-ground contact, the CM again moves upward (as long as the limb remains relatively straight extended) and decreases its forward velocity. As a consequence, E_p increases again and E_k decreases [19–21]. Energy variation corresponds to mechanical work, so that $\Delta E_k = W_k$ and $\Delta E_p = W_p$. In an ideal energy recovery mechanism, the work associated to changes of potential energy is exactly the same as the work associated to kinetic energy changes, but with different sign: $W_p = -W_k$. That means that work produced to increase the potential energy can be obtained by reducing the kinetic energy, and can again be returned to increase the kinetic energy at the next step-to-step transition. Actually, the conversion between E_p and E_k does not occur completely, but it is about 70% during normal walking at preferred speed [21].

Several studies have separately indicated that the metabolic cost of walking is primarily allocated towards raising the CM throughout the gait cycle [22–24]. Therefore, the mechanism of exchanging E_k and E_p aims to reduce the metabolic cost of locomotion by lowering the muscular effort required to accelerate and decelerate the CM [25].

Aim of this study was to investigate changes in the mechanical energy recovery, and its correlations with spatio-temporal gait parameters, in a carefully selected cohort of PD patients at different disease stages.

Materials and Methods

Subjects

We consecutively enrolled 23 PD patients with bilateral symptoms (Hoehn and Yahr, HY stage ≥II) if able to walk unassisted in medication-off condition (overnight suspension of all dopaminergic drugs). All patients had stable dopaminergic treatment for at least six months and no levodopa-related motor fluctuations (e.g., dyskinesia). Ten age-matched healthy subjects (HC, mean age 62±3 years) also took part in the study. The diagnosis of PD was made according to the UK Brain Bank criteria and patients were evaluated with the Unified Parkinson Disease Rating Scale motor part (UPDRS-III). All PD patients improved (>20% at UPDRS-III score) after intake of 150–200 mg of L-Dopa (acute challenge test), thus further supporting the clinical diagnosis of idiopathic PD. Patients were not suffering from freezing of gait and did not show any freezing episodes during the acquisitions. No patients showed any atypical features of parkinsonism. Patients with cognitive decline (Mini-Mental State Examination <27) or any other signs of neurological or psychiatric disease other than PD were excluded. All patients did not suffer from any other disease than PD nor underwent any major surgery (e.g. orthopedic surgery). Patients were divided into two groups according to the HY stage: mild group (PD$_M$: HY stage II), and severely affected group (PD$_S$: HY stage III or IV). The local institutional review board (Section of Human Physiology, Department of Pathophysiology and Transplantation, University of Milan) approved the study and the consent procedure. All participants signed a written informed consent. All efforts were made to protect patient privacy and anonymity.

Experimental Setup and Protocol

Kinematic data were recorded using an optoelectronic system (SMART-E, BTS Bioengineering, Italy), consisting of six video cameras (sampling rate: 60 Hz; calibrated volume 4x2x1.5m). The position of the subjects' main body segments was determined by means of 29 retro-reflective markers (diameter: 15 mm) according to a published protocol [1]. During the static calibration trial, eight additional "technical" markers were attached on the following bony landmarks, on both sides of the body: greater trochanter, medial femoral condyle, medial malleolus, and first metatarsal head. The position of these points, not visible to the cameras during gait, was computed offline by means of technical reference systems, assuming their relative position in relation to local reference frames was fixed. Anthropometric parameters of each subject were computed from the markers' positions recorded during the calibration trial, and used for the estimation of internal joint centers, thus enabling calculation of lower limb kinematics. Subjects were asked to walk barefoot along a straight trajectory about 11.5 m long. All subjects started to walk from at least two strides behind the calibrated volume, without any starting command. Trials were repeated three to five times, according to patients' capabilities. All PD patients were evaluated after overnight suspension of all dopaminergic drugs (meds-off).

HC did two sets of eight walking trials at 'preferred' (HC_N) and 'slow' (HC_S) speeds, in random order, following verbal instructions in the absence of external feedback. The consistency of the two datasets was verified on the basis of the actual measured speeds.

Data Analysis and energy calculation

We used ad-hoc algorithms to compute the CM trajectory all along the gait cycle and to measure spatio-temporal gait parameters (i.e. walking speed, stride length and period, stance phase and double support phase duration), time courses of hip, knee and ankle joints angles during the stride cycle and their ROM.

For each subject, spatial parameters were normalized as a percentage of the body height (BH). Temporal parameters and all curves representing the time-course of kinematic variables were time normalized as a percentage of the stride duration (defined from heel contact of one foot to next heel contact of the same foot).

Subsequently, the mean values and the standard deviation (SD) for corresponding normalized time intervals were calculated for each variable of each subject. ROM values were computed as the difference between the maximum and the minimum values reached by each joint angle, within the stride.

The whole body center of mass (CM) was computed by estimating the displacement of the center of mass of each body segment (CM_j), and then implementing the general formula:

$$Y_{CM} = \frac{\sum_j y_j m_j}{M} \tag{1}$$

where, Y_{CM} is the generic coordinate of CM; y_j is the generic coordinate of center of mass of each anatomical segment (j), m_j is the mass of each body segment (j) and M is the mass of the whole body. The position of CM_j within each anatomical segment, as well as the mass of each body segment were obtained from the anthropometric tables and regression equations provided by Zatsiorsky and Seluyanov [26].

The kinetic energy associated to CM displacements was computed as follows:

$$E_{k,CM} = \frac{1}{2} M \left(v_x^2 + v_y^2 + v_z^2 \right) \tag{2}$$

where M is the whole body mass, v_x, v_y, v_z are the three components of the velocity of CM.

The potential energy associated to CM was calculated as:

$$E_{p,CM} = Mgh \tag{3}$$

where g is the gravitational acceleration (m/s^2) and h is the vertical distance of CM from the ground.

The total energy associated to CM was computed as function of time (t) as:

$$E_{tot,CM}(t) = E_{k,CM}(t) + E_{p,CM}(t) \tag{4}$$

Over the stride period, the positive variations (difference between maximum and minimum) of respectively $E_{p,CM}$, $E_{k,CM}$, and $E_{tot,CM}$ were identified and calculated. They were named respectively W_p, W_k, and W_{totCM}. Then the energy recovery index (ER) was computed according to Cavagna et al. [21]:

$$ER = \frac{(W_p + W_k) - W_{totCM}}{(W_p + W_k)} \times 100 \tag{5}$$

All energetic parameters were computed for each stride collected from our subjects and averaged over the strides (left and right pooled together) for each gait velocity command and for each group of subjects. Energetic parameters were divided by the mass (M) of the subject.

Statistics

Statistical analysis was performed using JMP statistical package (version 12.0, SAS Institute, Inc., Cary, NC, USA). ROMs of left and right hemibodies were compared by means of matched pairs analysis. Differences between PD and HC groups were analyzed by means of Kruskal-Wallis and Steel-Dwass tests. To look for measurements that were predictive of energetic parameters, we used the Spearman correlation coefficient. Variables were then included in stepwise multiple linear regression. Strength of the correlations was defined according to the absolute value of ρ as "very weak" (.00-.19), "weak" (.20-.39), "moderate" (.40-.59), "strong" (.60-.79) and "very strong" (.80–1.0). A $p<0.05$ was considered to be statistically significant.

Results

Demographic and clinical data are listed in Table 1. As expected, PD_S showed higher scores at UPDRS-III in meds-off and higher L-Dopa Equivalent Daily Dose (LEDD) [27] compared to PD_M ($p<0.05$, in both cases). No significant differences were found for age and body mass index among PD sub-groups and HC. No difference was also found when comparing ROMs of the right and left hemibodies, both for HC and PD, and data were then pooled together.

Spatio-temporal, kinematic and energetic parameters are listed in Table 2. Average gait velocity of HC_N matched the homologous data of PD_M, and the same hold true concerning HC_S and PD_S. Of relevance, PD_S showed a significant reduction of stride length and knee ROM when compared to HC_S, which was due to a more flexed knee in the stance phase (Fig 1). The average knee joint angles measured during terminal stance were: 12.74±5.32° and 6.22±4.62° for PD_M and HC_N ($p<0.05$), and 13.52±8.24° and 5.19±4.42° for PD_S and HC_S ($p<0.05$). Lastly, in PD_S hip and ankle ROMs were reduced in comparison to PD_M and both negatively correlated with UPDRS-III scores (hip ROM: $\rho = -0.56$, $p<0.05$ and ankle ROM: $\rho = -0.54$, $p<0.05$).

In Table 2 we listed all energetic measurements. Fig 2 shows time courses of kinetic, potential and total energy associated to CM during the stride cycle. As expected, we found low values of ER and W_k in slow walking subjects (i.e. PD_S and HC_S) being both measurements strictly

Table 1. Demographic and clinical data.

	PD$_M$	PD$_S$	HC
N. (male/female)	10 (8/2)	13 (7/6)	10 (8/2)
Age (years)	62 ± 9	65 ± 8	62 ± 3
Weight (kg)	80.2 ± 14.6	65.0 ± 13.7	80.8 ± 9.5
Height (m)	1.7 ± 0.1	1.6 ± 0.1	1.7 ± 0.1
BMI	27.7 ± 5.2	24.5 ± 4.7	26.9 ± 3.1
Disease duration (years)	5 ± 2	12 ± 3	
UPDRS-III	20 ± 9	28 ± 9	
L-Dopa daily dose	325.0 ± 143.6	557.1 ± 225.0	
LEDD	443.3 ± 142.4	690.4 ± 205.6	

LEDD = L-Dopa Equivalent Daily Dose; UPDRS-III = Unified Parkinson's Disease Rating Scale motor part (III) in meds-off state; BMI = Body mass index. Disease duration was from motor symptoms onset. Values are means and standard deviation.

doi:10.1371/journal.pone.0156420.t001

related to gait velocity. Indeed, ER and W_k correlated with stride velocity in HC ($\rho = 0.82$, p<0.0001 and $\rho = 0.88$, p<0.001, respectively) and in PD patients ($\rho = 0.69$, p<0.001 and $\rho = 0.91$, p<0.0001, respectively).

PD$_S$ showed lower W_p values in comparison with PD$_M$ and, more interestingly, with HC$_S$, although walking at comparable velocities. W_p positively correlated with hip ROM in HC ($\rho = 0.73$, p<0.01) while with knee ROM in PD ($\rho = 0.68$, p<0.01). W_k values were lower in PD$_S$ than HC$_S$. Besides the aforementioned correlation with stride velocity, in PD patients W_k also correlated with hip ROM ($\rho = 0.79$, p<0.001). W_{totCM} matched closely with W_p findings. All mean data per subject were listed in S1 Table.

Discussion

The main finding of our study was a reduction of W_{totCM} and W_p along with PD progression. These changes were greatly dependent on knee ROM reduction and in particular on knee extension in the terminal stance phase of the stride. W_k was also reduced in advanced PD

Table 2. Energetic, spatio-temporal and kinematic parameters.

Parameters	HC$_N$	HC$_S$	PD$_M$	PD$_S$
Stride Velocity (%BH/s)	67.4±6.0 [1*]	43.3±8.1 [1]	64.2±5.6 [2*]	41.1±8.7 [2]
Stride Period (s)	1.1±0.1 [1*]	1.4±0.2 [1]	1.1±0.1 [2]	1.2±0.1 [2]
Stride Length (%BH)	71.6±5.2 [1]	59.3±5.9 [1, 3]	68.8±5.8 [2*]	49.0±6.6 [2, 3]
% Stance Phase	61.8±2.1 [1*]	66.5±2.8 [1]	61.1±1.8 [2]	64.7±3.4 [2]
% Double Support Phase	12.1±2.2 [1]	16.4±3.2 [1]	11.4±1.9 [2*]	16.0±2.5 [2]
Hip ROM (°)	40.9±2.9 [1*]	35.8±2.1 [1]	38.0±6.6 [2*]	31.0±8.2 [2]
Knee ROM (°)	56.0±4.7	53.8±3.8 [3]	49.6±8.3	42.0±9.3 [3]
Ankle ROM (°)	24.5±4.3	22.1±5.1	26.8±4.7 [2*]	20.4±6.2 [2]
ER index (%)	65.4±5.7 [1]	49.1±10.2 [1]	68.2±4.3 [2]	52.5±12.13 [2]
W_{totCM} (J/kg)	0.36±0.08	0.37±0.05 [3*]	0.34±0.05 [2*]	0.24±0.04 [2, 3]
W_p (J/kg)	0.57±0.14	0.47±0.09 [3]	0.57±0.06 [2*]	0.33±0.09 [2, 3]
W_k (J/kg)	0.51±0.08 [1*]	0.32±0.07 [1, 3]	0.5±0.09 [2*]	0.21±0.06 [2, 3]

Superscript numbers indicate statistically significant differences (p<0.05 or p<0.01 when * is present) between HC$_N$ and HC$_S$ (1), PD$_S$ and PD$_M$ (2), HC$_S$ and PD$_S$ (3). We did not find any statistical difference between HC$_N$ and PD$_M$. Values are means and standard deviation. See text for statistical analysis.

doi:10.1371/journal.pone.0156420.t002
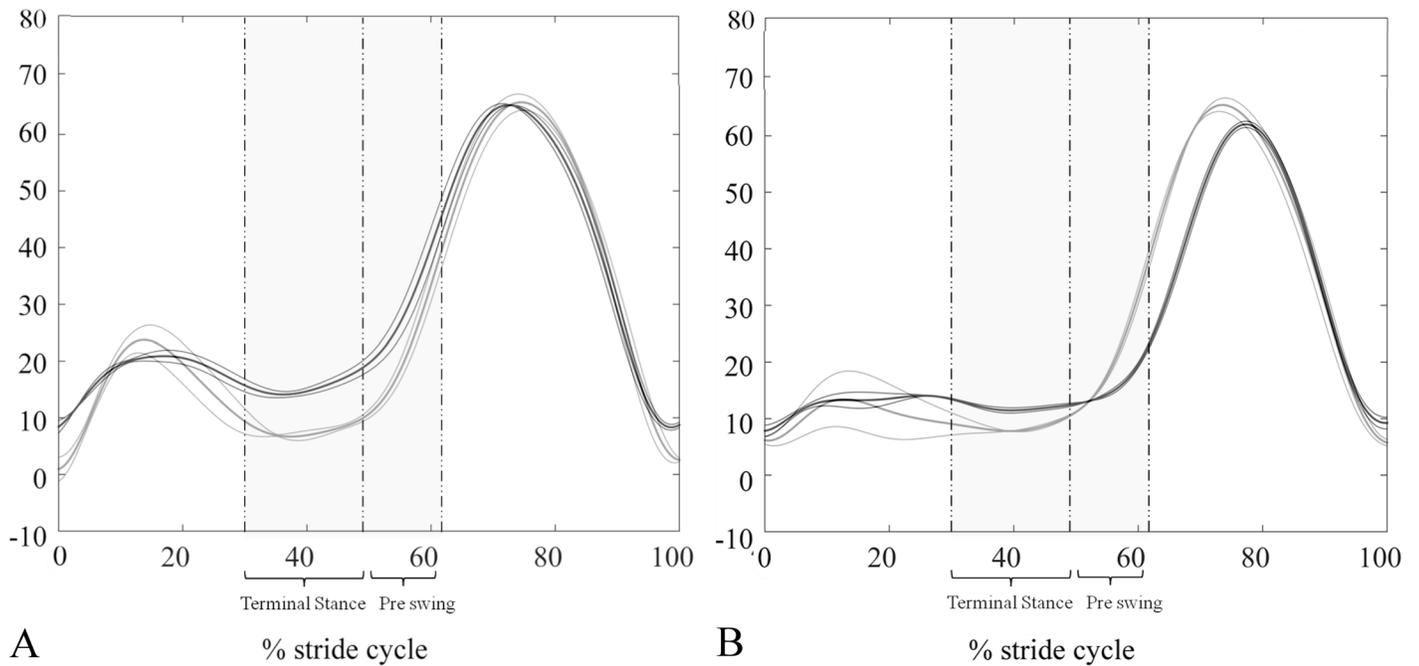
Fig 1. Time courses of knee flexion/extension angles. (A) Comparison between one representative PD$_M$ (black lines) and one HC$_N$ (grey lines). (B) Comparison between one representative PD$_S$ (black lines) and one HC$_S$ (grey lines). Thick and thin lines refer to the average time courses ±SD of different trials, respectively. The intervals of maximum knee extension, reached during the stance phase, are highlighted in grey.

doi:10.1371/journal.pone.0156420.g001

patients primarily due to low gait velocities, but also due to a reduction of hip ROM, possibly reflecting a greater rigidity and stopped posture in more advanced stages of the disease (i.e. PD$_S$).
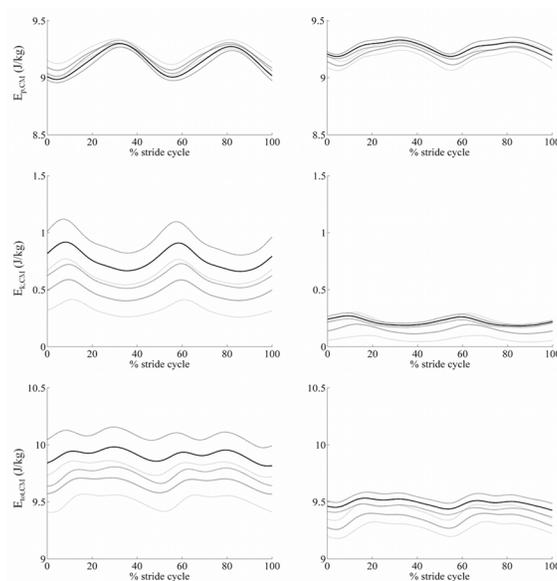

Fig 2. Energy components. Left column: PD$_M$ and HC$_N$. Right column: PD$_S$ and HC$_S$. Black lines refer to one representative PD and grey lines to one HC. Thick and thin lines refer to the average time courses ±SD of different trials, respectively.

doi:10.1371/journal.pone.0156420.g002

The direct correlation of all energetic parameters with gait velocity [28,29], as seen also when comparing cohorts matched for gait velocity (Table 2), is reasonable if we consider that W_k is the variation of kinetic energy along the stride, and thus it depends on the square of velocity, and W_p is the variation of potential energy, which relies upon the vertical excursion of CM. Of note, the minimum height of CM excursion is reached during the double support phase, and depends on step length, which in turn is related to hip joint excursion and on gait velocity. The maximum height of CM excursion depends instead on how much the knee is extended in the mid stance phase.

In PD_S, we found two main conditions to justify a reduction of all energetic components. In particular, (i) a reduced gait velocity, mainly as a result of short stride length (stride time was even shorter than in HC_S) and (ii) a reduced hip and knee ROM, the latter resulting mainly from a lack of full extension in the terminal stance. Of note, in normal subjects the rate of knee extension in terminal stance should be approximately half that of flexion during limb loading [28]. In PD_S, a deeply flexed knee during stance resulted in a reduced rising and a more flat path of the CM [25] which in turns reduced the amount of stored gravitational E_p [25,29,30]. We speculate that such an increased knee flexion could be related to an altered activity of plantar flexors muscles [9], which normally play a role to accelerate the knee into extension [12]. Indeed, in terminal stance the triceps surae muscle increases its activity and contracts vigorously as an ankle stabilizer [28]. The lack of EMG recording prevents us from confirming this hypothesis, but a reduction in amplitude of gastrocnemius activity was previously described in PD patients [12,13].

Of relevance, the finding that W_k, W_p, and W_{totCM} were reduced in PD_S in comparison to both patients walking faster (i.e. PD_M) and control subjects walking at a similar velocity (i.e. HC_S) suggests that such a reduction is mainly related to different kinematic patterns (such as altered ROMs) rather than to gait velocity *per se*.

At this point, it was quite unexpected that, despite a considerable reduction of all energetic parameters, the ER index itself was not reduced in PD_S when compared to HC_S subjects. This may suggest that the basic energy recovery mechanism, as adopted by normal subjects, which is an efficient way to reduce the energetic cost of walking, is still exploited in PD patients, also at advanced disease stages. Still, in PD_S the ER was relatively low when compared to subjects walking faster (both PD_M and HC_N). Therefore, it can be argued that any intervention aimed at increasing gait velocity would be beneficial from the energetic point of view. However, it must be considered that lower limb can only roughly be approximated to an inverted pendulum for which perfect out-of-phase kinetic and potential energy variations occur. Actually, among the many factors that can reduce energy cost during walking, the knee flexion-extension at load acceptance, the ankle plantarflexion-dorsiflexion at early stance phase and pelvis tilt in the frontal plane in mid stance are the most important [31,32]. They all must be regarded with great attention if walking efficiency, as manifested by the ER index, is to be preserved.

A limitation of our study is the relative low number of patients recruited. This relied mainly upon our inclusion criteria. In particular, only few PD patients at HY stage III or IV were willing and able to suspend overnight all dopaminergic medications and even fewer were able to complete unassisted all walking trials in meds-off state. In this study, we recruited solely subjects with PD at HY stage II or higher as patients with mild motor symptoms can show normal ROM of hip, knee and ankle joints during linear walking at preferred speed ([1] and Table 2).

At last, our findings could help developing a tailored rehabilitation treatment of gait in PD subjects. Indeed, PD patients could benefit from passive and active mobilization of the knee to possibly normalize knee extension and consequently improve W_{totCM} and W_p. Knee extension should be also monitored and possibly reinforced during treadmill training, which has been

proved useful in the rehabilitation of gait disorders in PD, in particular at an early stage of the disease [33–35].

Supporting Information

S1 Table. Demographic, clinical, energetic, spatio-temporal and kinematic mean data of each subject.
(PDF)

Author Contributions

Conceived and designed the experiments: IUI CF PC. Performed the experiments: MD IUI AC. Analyzed the data: MD EEP IUI. Contributed reagents/materials/analysis tools: MD EEP IUI. Wrote the paper: MD IUI CF EEP GP GF PC.

References

1. Carpinella I, Crenna P, Calabrese E, Rabbuffetti M, Mazzoleni P, Nemni R, et al. Locomotor function in the early stage of Parkinson's disease. IEEE Trans Neural Syst Rehabil Eng. 2007; 15(4):543–551. doi: 10.1109/TNSRE.2007.908933 PMID: 18198712

2. Shulman LM, Gruber-Baldini AL, Anderson KE, Vaughan CG, Reich SG, Fishman PS, et al. The evolution of disability in Parkinson disease. Mov Disord. 2008; 23(6):790–796. doi: 10.1002/mds.21879 PMID: 18361474

3. Morris ME, Iansek R, Matyas TA, Summers JJ. The pathogenesis of gait hypokinesia in Parkinson's disease. Brain. 1994; 117(5):1169–1181.

4. Ferrarin M, Lopiano L, Rizzone M, Lanotte M, Bergamasco B, Recalcati M, et al. Quantitative analysis of gait in Parkinson's disease: a pilot study on the effects of bilateral sub-thalamic stimulation. Gait Posture. 2002; 16(2):135–148. PMID: 12297255

5. Vieregge P, Stolze H, Klein C, Heberlein I. Gait quantitation in Parkinson's disease—locomotor disability and correlation to clinical rating scales. J Neural Transm. 1997; 104(2–3):237–248. PMID: 9203085

6. Morris ME, Iansek R, Matyas TA, Summers JJ. Stride length regulation in Parkinson's disease. Normalization strategies and underlying mechanisms. Brain. 1996; 119(2):551–568.

7. Morris ME, McGinley J, Huxham F, Collier J, Iansek R. Constraints on the kinetic, kinematic and spatio-temporal parameters of gait in Parkinson's disease. Hum Mov Sci. 1999; 18(2–3):461–483.

8. Morris M, Iansek R, McGinley J, Matyas T, Huxham F. Three-dimensional gait biomechanics in Parkinson's disease: Evidence for a centrally mediated amplitude regulation disorder. Mov Disord. 2005; 20 (1):40–50. PMID: 15390033

9. Kimmeskamp S, Hennig EM. Heel to toe motion characteristics in Parkinson patients during free walking. Clin Biomech. 2001; 16(9):806–812.

10. Morris ME, Iansek R, Matyas TA, Summers JJ. Ability to modulate walking cadence remains intact in Parkinson's disease. J Neurol Neurosurg Psychiatry. 1994; 57(12):1532–1534. PMID: 7798986

11. Ferrarin M, Rizzone M, Bergamasco B, Lanotte M, Recalcati M, Pedotti A, et al. Effects of bilateral sub-thalamic stimulation on gait kinematics and kinetics in Parkinson's disease. Exp Brain Res. 2005; 160 (4):517–527. PMID: 15502989

12. Mitoma H, Hayashi R, Yanagisawa N, Tsukagoshi H. Characteristics of parkinsonian and ataxic gaits: A study using surface electromyograms, angular displacements and floor reaction forces. J Neurol Sci. 2000; 174(1):22–39. PMID: 10704977

13. Dietz V, Zijlstra W, Prokop T, Berger W. Leg muscle activation during gait in Parkinson's disease: adaptation and interlimb coordination. Electroencephalogr Clin Neurophysiol. 1995; 97(6):408–415. PMID: 8536593

14. Morris ME, Huxham F, McGinley J, Dodd K, Iansek R. The biomechanics and motor control of gait in Parkinson disease. Clin Biomech. 2001; 16(6):459–470.

15. Delval A, Salleron J, Bourriez JL, Bleuse S, Moreau C, Krystkowiak P, et al. Kinematic angular parameters in PD: Reliability of joint angle curves and comparison with healthy subjects. Gait Posture. 2008; 28(3):495–501. doi: 10.1016/j.gaitpost.2008.03.003 PMID: 18434159

16. Maggioni MA, Veicsteinas A, Rampichini S, Cè E, Nemni R, Riboldazzi G, et al. Energy cost of spontaneous walking in Parkinson's disease patients. Neurol Sci. 2012; 33(4):779–784. doi: 10.1007/s10072-011-0827-6 PMID: 22042531

17. Christiansen CL, Schenkman ML, McFann K, Wolfe P, Kohrt WM. Walking economy in people with Parkinson's disease. Mov Disord. 2009; 24(10):1481–1487. doi: 10.1002/mds.22621 PMID: 19441128

18. Carpinella I, Crenna P, Rabuffetti M, Ferrarin M. Coordination between upper- and lower-limb movements is different during overground and treadmill walking. Eur J Appl Physiol. 2010; 108(1):71–82. doi: 10.1007/s00421-009-1168-5 PMID: 19756711

19. Cavagna GA, Heglund NC, Taylor CR. Mechanical work in terrestrial locomotion: two basic mechanisms for minimizing energy expenditure. Am J Physiol—Regul Integr Comp Physiol. 1977; 233:R243–R261.

20. Margaria R. Biomechanics and Energetics of Muscular Exercise (Clarendon Press, Oxford).; 1976.

21. Cavagna GA, Thys H, Zamboni A. The sources of external work in level walking and running. J Physiol. 1976; 262(3):639–657. PMID: 1011078

22. Grabowski A, Farley CT, Kram R. Independent metabolic costs of supporting body weight and accelerating body mass during walking. J Appl Physiol. 2005; 98(2):579–583. PMID: 15649878

23. Duff-Raffaele M, Kerrigan DC, Corcoran PJ, Saini M. The proportional work of lifting the center of mass during walking. Am J Phys Med Rehabil. 1996; 75(5):375–379. PMID: 8873706

24. Neptune RR, Zajac FE, Kautz SA. Muscle mechanical work requirements during normal walking: The energetic cost of raising the body's center-of-mass is significant. J Biomech. 2004; 37(6):817–825. PMID: 15111069

25. Sparling TL, Schmitt D, Miller CE, Guilak F, Somers TJ, Keefe FJ, et al. Energy recovery in individuals with knee osteoarthritis. Osteoarthr Cartil. 2014; 22(6):747–755. doi: 10.1016/j.joca.2014.04.004 PMID: 24752039

26. Zatsiorsky V, Seluyanov V. The mass and inertia characteristics of the main segments of the human body. Biomech VIII-B Proc Eight Int Congr Biomech. 1983:1152–1159.

27. Isaias IU, Marotta G, Hirano S, Canesi M, Benti R, Righini A, et al. Imaging essential tremor. Mov Disord. 2010; 25(6):679–686. doi: 10.1002/mds.22870 PMID: 20437537

28. Perry J. Gait Analysis: Normal and Pathological Function. J Pediatr Orthop. 1992; 12:815.

29. Fisher NM, White SC, Yack HJ, Smolinski RJ, Pendergast DR. Muscle function and gait in patients with knee osteoarthritis before and after muscle rehabilitation. Disabil Rehabil. 1997; 19(2):47–55. PMID: 9058029

30. Stauffer RN, Chao EY, Györy a N. Biomechanical gait analysis of the diseased knee joint. Clin Orthop Relat Res. 1977;(126:):246–255. PMID: 598127

31. Inman VT, Ralson HJ, Todd F. Human Walking. Baltimore (MD): Williams & Wilkins. 1981.

32. INMAN VT. Human locomotion. Can Med Assoc J. 1966; 94(20):1047–1054. PMID: 5942660

33. Mehrholz J, Friis R, Kugler J, Twork S, Storch A, Pohl M. Treadmill training for patients with Parkinson's disease. Cochrane Database Syst Rev. 2010;(1:).

34. Frazzitta G, Maestri R, Uccellini D, Bertotti G, Abelli P. Rehabilitation treatment of gait in patients with Parkinson's disease with freezing: A comparison between two physical therapy protocols using visual and auditory cues with or without treadmill training. Mov Disord. 2009; 24(8):1139–1143. doi: 10.1002/mds.22491 PMID: 19370729

35. Frazzitta G, Maestri R, Bertotti G, Riboldazzi G, Boveri N, Perini M, et al. Intensive Rehabilitation Treatment in Early Parkinson's Disease: A Randomized Pilot Study With a 2-Year Follow-up. Neurorehabil Neural Repair. 2015; 29(2):123–131. doi: 10.1177/1545968314542981 PMID: 25038064

APPENDIX B

GAIT INITIATION IN CHILDREN WITH RETT SYNDROME

Isaias, I. U., Dipaola, M., Michi, M., Marzegan, A., Volkmann, J., Roidi, M. L. R., Frigo, C. A. and Cavallari, P.

Gait Initiation in Children with Rett Syndrome

Ioannis Ugo Isaias[1,2]*, Mariangela Dipaola[2,3], Marlies Michi[2], Alberto Marzegan[2], Jens Volkmann[1], Marina L. Rodocanachi Roidi[4], Carlo Albino Frigo[3], Paolo Cavallari[2]

1 Department of Neurology, University Hospital Würzburg, Würzburg, Germany, 2 Department of Pathophysiology and Transplantation, LAMB Pierfranco & Luisa Mariani, University of Milan, Milan, Italy, 3 Department of Electronic, Information and Bioengineering, Biomedical Technology Laboratory, TBM Lab, Politecnico di Milano, Milan, Italy, 4 Fondazione Don Carlo Gnocchi IRCSS, Milan, Italy

Abstract

Rett syndrome is an X-linked neurodevelopmental condition mainly characterized by loss of spoken language and a regression of purposeful hand use, with the development of distinctive hand stereotypies, and gait abnormalities. Gait initiation is the transition from quiet stance to steady-state condition of walking. The associated motor program seems to be centrally mediated and includes preparatory adjustments prior to any apparent voluntary movement of the lower limbs. Anticipatory postural adjustments contribute to postural stability and to create the propulsive forces necessary to reach steady-state gait at a predefined velocity and may be indicative of the effectiveness of the feedforward control of gait. In this study, we examined anticipatory postural adjustments associated with gait initiation in eleven girls with Rett syndrome and ten healthy subjects. Muscle activity (tibialis anterior and soleus muscles), ground reaction forces and body kinematic were recorded. Children with Rett syndrome showed a distinctive impairment in temporal organization of all phases of the anticipatory postural adjustments. The lack of appropriate temporal scaling resulted in a diminished impulse to move forward, documented by an impairment in several parameters describing the efficiency of gait start: length and velocity of the first step, magnitude and orientation of centre of pressure-centre of mass vector at the instant of (swing-)toe off. These findings were related to an abnormal muscular activation pattern mainly characterized by a disruption of the synergistic activity of antagonistic pairs of postural muscles. This study showed that girls with Rett syndrome lack accurate tuning of feedforward control of gait.

Introduction

Rett syndrome (RTT) is an X-linked neurodevelopmental condition. Mutations in the gene encoding Methyl-CpG-binding protein 2 (MECP2) can be found in 95 to 97% of individuals with typical RTT [1], [2]. The clinical picture is defined by loss of spoken language and a regression of purposeful hand use, with the development of distinctive hand stereotypies and gait abnormalities. Epilepsy, breathing irregularities and gastro-intestinal problems may be also present [3–6]. At a clinical level, gait in children with RTT is characterized by ataxia, apraxia and spasticity with and without clonus. Affected girls develop a preference for one leg, putting it forward at every step as the foremost leg, using the contralateral one just for support and balance [7]. Based on available data, 20–40% children with RTT will never be able to walk. Furthermore, of the girls who gain the ability to walk, up to 80% might lose it along with disease progression [5], [8]. Despite being one of the most life burdening symptoms, detailed data on motor derangements and locomotion in RTT are not available.

Gait initiation is the transition from quiet stance to steady-state condition of walking. The associated motor program seems to be centrally mediated [9–11] and includes preparatory adjustments (Anticipatory Postural Adjustments, APA) prior to any apparent voluntary movement of the lower limbs [11], [12]. APA contribute to postural stability [13] and to create the propulsive forces

necessary to reach steady-state gait at a predefined velocity [14], [15]. These propulsive forces are generated by producing a misalignment between the centre of pressure (CoP), which is the point in which the resultant ground reaction force is applied at the foot-ground interface, and the vertical projection of the body centre of mass onto the ground (CoM) [14]. The distance between these two points in the sagittal plane can be modulated by changing the activity of the ankle plantarflexion/dorsiflexion muscles, while in the frontal plane the hip adduction/abduction muscle play a major role, associated with the activity of inversion/eversion muscles at the ankle [16], [17]. The APA phase can be subdivided into two sub-phases called imbalance phase and unloading phase. During the imbalance phase, the CoP moves backwards and towards the swing (leading) foot to produce a forward acceleration of the CoM directed also towards the stance (trailing) limb [14], [18], [19]. During the unloading phase, the CoP moves toward the stance foot, so that the body weight can be supported on this side and the swing foot can clear the ground to execute the first step. At this time the CoM is in front of the CoP and a propulsion force is produced by contracting the calf muscles. As a consequence, the CoP moves forward along a typical trajectory (figure 1 left) [11], [14], [18], [20], [21]. In healthy subjects, the CoP displacement during APA is associated with a typical electromyographic sequence consisting in the reduction,
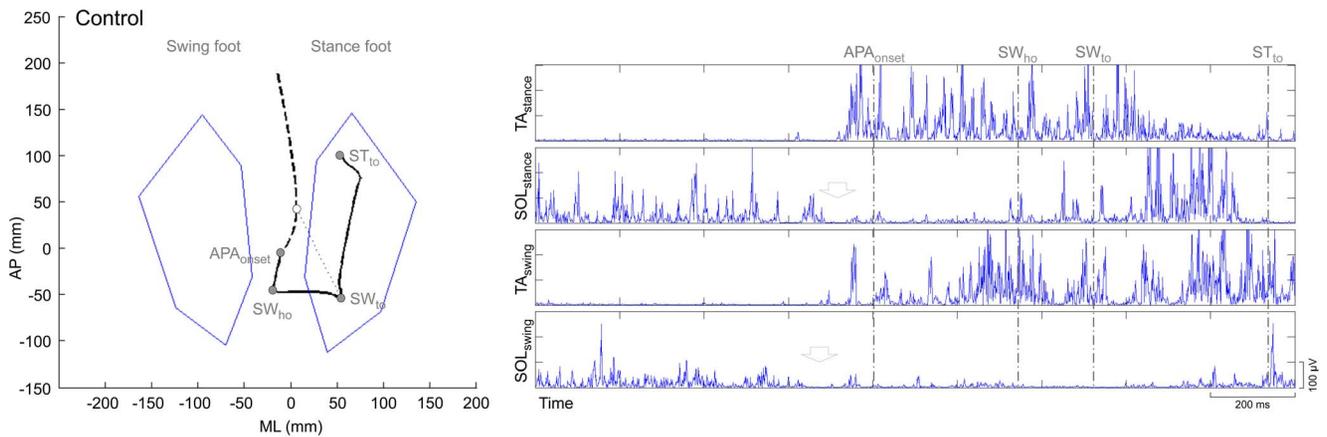
Figure 1. Recorded data at gait initiation. Centre of pressure (CoP, black line) and centre of mass (CoM, dashed line) displacement in a healthy subject (figure 1 left) and child with RTT (figure 2 left) with corresponding EMG activity of tibialis anterior (TA) and soleus muscles (SOL) of swing and stance foot (figure 1 right and 2 right). The dotted line (in figure 1 left and 2 left) shows CoP-CoM distance at toe-off of the swing foot (SWto). In figure 1 (right), arrows indicate bilateral suppression of the tonic activity of SOL which, together with the subsequent activation of TA, is responsible for the backward displacement of the CoP. This synergistic activity of pairs of postural muscles (i.e. TA and SOL) is not present in RTT girls (figure 2 right). *Imbalance phase*, from the instant APAonset, at which the CoP start moving backward, to the instant of heel-off of the swing foot (SWho). *Unloading phase*, from SWho to toe-off of the swing foot (SWto). STto is the instant of toe-off of the stance foot.
doi:10.1371/journal.pone.0092736.g001

mono- or bilateral, of the activity in the soleus muscles (SOL) normally present during standing, followed by activation of the tibialis anterior muscles (TA) (figure 1 right) [11].

The study of gait initiation can help understanding the control of balance [22] and, in this perspective, the APA may be indicative of the effectiveness of the feedforward control of gait [23]. Indeed, it is only when the child is able to display systematic anticipatory behavior that it starts organizing it in relation to the characteristics of the velocity [24]. Given the great difficulties in obtaining the execution of a task on command in children with RTT, gait initiation might be the only available task to investigate locomotor behavior in these children.

Patients and Methods

Subjects

Eighteen children with RTT participated in the study. Despite enrolling children that were anamnestically able to maintain an upright position and walk unassisted, only eleven children (mean age 9±3 years) were able to complete a gait initiation task. In particular, some girls were unable to walk barefoot, others were anxious and disoriented when left alone. Often, RTT girls made a lateral or back step, possibly to gain a more stable standing position, before start walking.

Ten healthy children (HC; 4 females and 6 males; mean age 10±3 years) served as control group. No difference in biomechanic measurements of gait initiation between healthy male and female children was described.

Clinical evaluation was performed according to the Rett Assessment Rating Scale (RARS) (table 1). The scale evaluates the specific phenotypic characteristics of RTT syndrome in five different domains (i.e. cognitive, sensory, motor, emotional, behavioral). Each of the 31 items is rated on a 4-point scale, where 1 = within normal limits, 2 = infrequent or low abnormality, 3 = frequent or medium-high abnormality, and 4 = strong abnormality. Intermediate ratings are also possible. A total score is computed by summing the ratings of all 31 items. The RARS was established by a standardization procedure, involving a sample of

220 subjects, and proved being a valid and reliable instrument to identify the level of severity of RTT syndrome [25].

All patients were found to have mutations of deletion in the MECP2 gene.

The local institutional review board (Section of Human Physiology, Department of Pathophysiology and Transplantation) approved the study and all parents (or guardians) provided written informed consent. Data are freely available upon request. Confidentiality rules related to human-subject research will apply.

Experimental protocol

Subjects were placed over a force platform upright, with feet parallel, and asked to start walking spontaneously as soon as they received a verbal cue; RTT children were called repeatedly by the parents seated at about 5 m distance in front of them. All children were not supported nor helped at any time during the gait initiation task. We evaluated only tasks when at least two strides after gait start were performed; this assured us that RTT children had elaborated a real intention to start walking.

Recording system

Movement kinematics were recorded using an optoelectronic system (SMART 1.10, BTS, Italy), consisting of six video cameras working at a sampling rate of 60 Hz and located around a calibrated volume of 5×3×2 m3. A full body markers dataset (29 retro-reflective markers with 12 mm diameter – LAMB protocol) [26] was used to analyze the motion of head, trunk, upper limbs and lower limbs in order to compute the global CoM. Anthropometric parameters of each subject were used for the estimation of internal joint centers. These, in turn, enabled us to calculate head, trunk, and lower limbs kinematics. Anthropometric data were obtained from Zatsiorski regression equations [27]. All recorded data were visually inspected, and trials performed incorrectly were rejected. Two specific sets of parameters were automatically extracted by using ad hoc algorithms.

Ground reaction forces and CoP position was obtained by means of a dynamometric platform (KISTLER 9286A, Winterhur, Switzerland) embedded in the floor (sampling rate 960 Hz).

Table 1. Demographic and clinical characteristics.

Patient n.	1	2	3	4	5	6	7	8	9	10	11
Genetic mutation	c.1327G>A	c.1156_1197del41	c.916C>T	c.763C>T	c.602_603insGGCC	c.455C>G	c.431delA	c.397C>T	c.1156del41	c.1052_188del37	c.808C>T
Age	10	6	7	7	7	15	7	7	12	8	15
RARS – Cognition	19	8	8	10.5	8.5	14	7	7	9	8	16
RARS – Sensory	2	2	2	2	2	2	2	2	2	2	4
RARS – Motor	7.5	4	4	6	5	7	5	5	5	4.5	7
RARS – Emotion	4.5	2	2	2	2	4	2	2	3	2.5	4
RARS – Indipendent activities	10	5	5	5	5	6	5.5	6	7	6	11
RARS – Typical features	30.5	21	19	17	18	24	23	21.5	23	21	33
RARS – Total score	73.5	42	40	42.5	40.5	57	44.5	43.5	49	44	75
Age of acquisition of independent gait (ms)	18	19	30	15	18	16	12	18	20	24	20
Age of appearance of stereotypies (ms)	12	39	24	30	24	40	24	18	9	36	18
Spasticity	No	No	No	No	No	LL-LR (mild)	No	LL-LR (mild)	No	No	UL-LL-LR (mild)
Dystonia	No	No	No	No	No	LL (mild)	No	No	No	LL-LR (mild)	No
Scoliosis	Mild	No	No	Mild	No	Mild	No	No	Moderate	Moderate	Mild
Microcephaly at the time of observation	No	No	Yes	Yes	Yes	No	Yes	No	Yes	Yes	Yes
Epilepsy	Yes	Yes	Yes	Yes	No	Yes	No	Yes	Yes	No	Yes

doi:10.1371/journal.pone.0092736.t001

3

Surface electromyographic (EMG) activity, during gait initiation trials, was recorded using a telemetric eight-channel system (TELEMG, BTS, Milan, Italy) from TA and SOL muscles of both legs. Myoelectric signals were collected by preamplified Ag/AgCl electrodes (diameter: 25 mm, bipolar configuration, inter-electrode distance: 20 mm), band-pass filtered ($f_{\text{high-pass}} = 10$ Hz, $f_{\text{low-pass}} = 200$ Hz) and acquired at a sampling frequency of 960 Hz and a resolution of 16 bit. A digital zero-phase shift eight-order Butterworth high-pass filter with a cutoff frequency of 20 Hz was applied in order to remove movement artifacts and finally the signals were rectified.

Events identification and parameters evaluated

The temporal transition between quiet standing and APAonset was defined as the first sample point in the CoP trajectory at which the CoP started moving backward and towards the swing limb (figure 1 left) [28].

SWho (heel-off of the swing foot) is the most lateral motion of the CoP towards the swing foot. SWto (toe-off of the swing foot) is the event when CoP shifts from lateral to anterior motion. STto (toe-off of the stance limb) is the event corresponding to the time when the stance limb breaks contact with the supporting surface [28], [29].

The parameters extracted to describe the APA phases were: 1) the duration of imbalance (from APAonset to SWho) and unloading phases (from SWho to SWto), 2) the antero-posterior (AP) and 3) medio-lateral (ML) shift of the CoP (normalized to the foot length, measured as the distance between lateral malleolar and fifth metatarsal markers), 4) the CoP length and 5) mean velocity. In addition, to evaluate the efficiency of gait start, we described the following parameters: 6) the magnitude of the CoP-CoM vector at SWto (i.e. CoP-CoM distance at SWto); 7) the orientation of the CoP-CoM vector with respect to the progression line at SWto; 8) the length and 9) the velocity of the first step. Spatial parameters were normalized on the basis of body height (%BH).

CoP–CoM vector magnitude and orientation

The CoP and CoM trajectory data were exported and time-synchronized with a frequency of 60 Hz. The superimposition of CoP and CoM in the ground level plane was obtained by removing the respective average values computed in the steady state time window, before any occurrence of voluntary movement. With a common time base and a common spatial origin, the quantity CoP-CoM distance was easily determined by applying a conventional geometric distance formula between the coordinates of CoP and the coordinates of CoM at distinct points in time t_i:

$$|\text{CoP} - \text{CoM}|(t_i) = \sqrt{\left[(X_{CoP}(t_i) - X_{CoM}(t_i))^2 + (Y_{CoP}(t_i) - Y_{CoM}(t_i))^2 \right]}$$

where $X_{CoP}(t_i)$ was the displacement of the CoP in AP direction at time t_i, $X_{CoM}(t_i)$ was the displacement of the CoM in AP direction at time t_i, and $Y_{CoP}(t_i)$ and $Y_{CoM}(t_i)$ are the corresponding values for the ML direction.

The orientation of the CoP-CoM vector was calculated with respect to the progression line at SWto. The vector joining CoP and CoM represents the direction of CoM acceleration according to the inverted pendulum model [17].

Length and velocity of first step

The length of the first step was defined as the measure of the anterior displacement of the ankle marker of the swing foot, from the initial standing position to next heel strike. The velocity of the first step was defined as the maximum value of the time derivative of the ankle marker displacement.

Data analysis

For each subject, variables were averaged over the trials (at least three for all subjects) of each test. Considering that data were not normally distributed, the differences between HC and RTT groups were analyzed non-parametrically by using the Wilcoxon-Mann-Whitney U Test. Spearman's rho was applied to investigate statistical dependence among APA variables and parameters describing the efficiency of gait start (see above). Level of significance was set to 0.05.

Results

Kinematic measurements are listed in table 2. Of relevance, in children with RTT a selective impairment of the velocity of CoP displacement was described during both the imbalance and unloading phase. Interestingly, besides AP displacement of the CoP during the unloading phase, spatial positioning as well as length of the CoP during APA was within the normal range (figure 2 left). Indeed, CoP-CoM distance at SWto was normal in girls with RTT, but not the velocity of CoM at SWto nor the orientation of the CoP-CoM vector. Lack of appropriate temporal scaling in RTT resulted in reduced impulse to move forward, as described by a reduction of length and velocity of the first step.

EMG recordings are listed in table 3. A lack of synergistic activity of SOL and TA was observed in all trials of RTT children. In particular, the burst of TA was reduced in amplitude, delayed and desynchronized (figure 2 right).

Several correlations were found in the HC cohort among the kinematic measurements of gait start efficiency. In particular, in the imbalance phase, AP displacement of CoP correlated with instant AP velocity of CoM at SWto ($\rho = 0.78$, $p = 0.003$) and CoP-CoM distance at SWto ($\rho = 0.82$, $p = 0.023$). In the unloading phase, ML displacement of CoP correlated with the CoP-CoM vector orientation ($\rho = 0.82$, $p = 0.036$). None of these correlations resulted statistically significant in the RTT cohort. On the contrary, in RTT children the length of the first step correlated with ML displacement and velocity of CoP, in the unloading phase ($\rho = 0.75$, $p = 0.052$; $\rho = 0.85$, $p = 0.013$, respectively). Also in this cohort, velocity of first step correlated with CoP-CoM distance at SWto ($\rho = 0.92$, $p = 0.002$).

Discussion

In children with RTT, investigation of APA revealed a distinctive impairment in timing rather than the spatial organization of gait initiation, particularly in the unloading phase. These findings may be related to an abnormal muscular activation pattern characterized by asynergistic activity of pairs of postural muscles (i.e. TA and SOL).

The deactivation of the plantarflexors, but more importantly the activation of the TA, [11] is responsible for the backward shift of the CoP which normally promotes the initial forward leaning of the body. The anticipatory behavior of the TA is an index of anticipatory scaling or feedforward control of movement [30], [31] and it is a prerequisite for the emergence of preparatory adjustments during gait initiation.

Table 2. Kinematic measurements.

	RTT		Healthy subjects		
	Median	Range	Median	Range	p value
Imb. phase duration (s)	0.47	0.13–0.51	0.37	0.24–0.46	0.36
Imb. phase AP displacement of CoP (%FL)	8.11	1.84–16.99	14.45	7.92–20.87	0.59
Imb. phase ML displacement of CoP (%FL)	9.82	2.69–35.36	13.03	6.7–23.57	0.23
Imb. phase CoP length (mm)	42.23	5.64–148.85	51.84	36.91–86.15	0.94
Imb. phase CoP mean velocity (mm/s)	87.16	21.60–137.43	127.42	103.23–279.54	0.01
Unl. phase duration (s)	0.81	0.61–1.12	0.33	0.24–0.59	0.006
Unl. phase AP displacement of CoP (%FL)	25.26	12.32–36.51	10.66	4.81–14.08	0.0004
Unl. phase ML displacement of CoP (%FL)	68.03	12.62–119.84	53.23	29.63–59.53	0.1385
Unl. phase CoP length (mm)	179.08	23.01–242.03	136.25	79.6–170.74	0.3671
Unl. phase CoP mean velocity (mm/s)	176.82	67.54–459.55	334.78	282.68–648.59	0.0056
Magnitude of CoP-CoM vector at SWto (%BH)	6.44	2.5–8.91	5.45	3.7–7.73	0.15
Orientation of CoP-CoM vector (deg) with respect to the progression line (at SWto)	48.66	20.4–71.73	30.41	22.04–33.77	0.02
Length of the first step (%BH)	19.8	11.35–40.5	31.13	27.25–32.85	0.04
Velocity of the first step (mm/s)	670.12	657.06–1115.70	1662.40	1458.35–1770.00	0.001

AP = Antero-posterior; ML = Medio-materal. Imb. = Imbalance; Unl. = Unloading; FL = foot length; BH = body height; SWto = Heel-off of the swing foot. p values refers to Wilcoxon-Mann-Whitney U Test.
doi:10.1371/journal.pone.0092736.t002

Girls with RTT showed a pattern similar to children with age of 4-year or below characterized, in the imbalance phase, by a predominant ML displacement of CoP and a low TA burst [32]. It is possible that children with RTT needed a greater effort to produce the disequilibrium required to initiate the single limb support phase. To simplify this task, RTT girls might produce such a disequilibrium predominantly in the ML direction, as this plane of movement involves fewer degrees of freedom [33]. A wider base of support, often seen in RTT girls, may also promote ML displacement by reducing the pelvic rotation that allows for rotatory movements of the trunk about the vertical axis [34–36]. Of relevance, in RTT children the length of the first step

correlated selectively with ML displacement in the unloading phase.

The magnitude of the initial TA burst, and concomitant backward shift of CoP, are normally associated with the forthcoming gait velocity [11]. In girls with RTT, the lack of the anticipatory activation of the TA may suggest that the control mechanisms of gait initiation are not integrated into a locomotor program. RTT children would be unable to adjust the magnitude of their anticipatory responses as a possible result of an impaired representation of their forthcoming velocity. It is worth mentioning that, as for spatial organization of APA, mastering of spatio-temporal characteristics of gait (e.g. tuning backward shift to desired forthcoming velocity), is already completed at the age of 6-
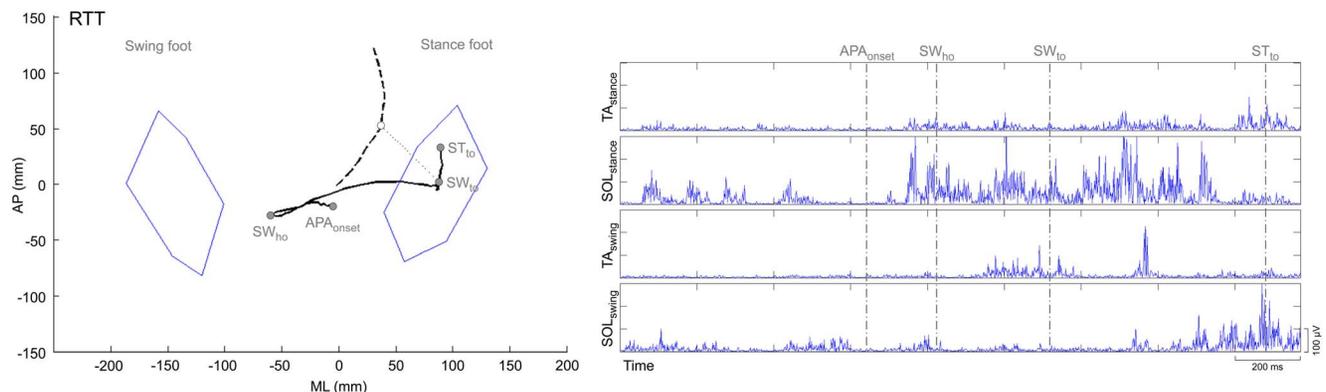

Figure 2. Recorded data at gait initiation. Centre of pressure (CoP, black line) and centre of mass (CoM, dashed line) displacement in a healthy subject (figure 1 left) and child with RTT (figure 2 left) with corresponding EMG activity of tibialis anterior (TA) and soleus muscles (SOL) of swing and stance foot (figure 1 right and 2 right). The dotted line (in figure 1 left and 2 left) shows CoP-CoM distance at toe-off of the swing foot (SWto). In figure 1 (right), arrows indicate bilateral suppression of the tonic activity of SOL which, together with the subsequent activation of TA, is responsible for the backward displacement of the CoP. This synergistic activity of pairs of postural muscles (i.e. TA and SOL) is not present in RTT girls (figure 2 right). *Imbalance phase*, from the instant APAonset, at which the CoP start moving backward, to the instant of heel-off of the swing foot (SWho). *Unloading phase*, from SWho to toe-off of the swing foot (SWto). STto is the instant of toe-off of the stance foot.
doi:10.1371/journal.pone.0092736.g002

Table 3. EMG recordings (RMS).

	RTT		Healthy subjects		
	Median	Range	Median	Range	p value
Imb. phase SOL stance foot	1.31	0.23–3.55	0.79	0.47–1.03	0.2135
Imb. phase TA stance foot	0.91	0.54–1.81	19.11	9.27–102.04	0.0004
Imb. phase SOL swing foot	0.78	0.41–2.83	0.95	0.6–1.56	0.8065
Imb. phase TA swing foot	0.9	0.33–2.79	20.91	5.97–33.25	0.0002
Unl. phase SOL stance foot	1.78	1.15–8.57	1.71	0.79–3.18	0.4772
Unl. phase TA stance foot	1.88	0.43–2.78	18.69	4.15–125.27	0.0005
Unl. phase SOL swing foot	1.64	0.46–5.78	0.93	0.51–1.46	0.1053
Unl. phase TA swing foot	2.47	0.57–10.52	17.13	8.80–42.88	0.0001

Imb. = Imbalance; Unl. = Unloading; SOL = Soleus muscle; TA = Tibialis anterior muscle; p values refers to Wilcoxon-Mann-Whitney U Test.
doi:10.1371/journal.pone.0092736.t003

year [24], [37]. Failure to develop a TA burst could also result from either a less efficient descending motor command (motor unit recruitment) or from immature muscle properties. However, both factors appear unlikely, since all children were able to develop a large phasic TA burst during the swing phase of the first three strides (data not shown).

We cannot exclude that abnormal standing posture, possibly related to dystonia or spasticity in few girls (table 1), could have been partly responsible for the observed changes in the APA phases. However, this would have influenced also spatial parameters of APA, which resulted within the normal range in our RTT cohort. Of relevance, in this study we only took into consideration recordings where children with RTT had a base of support similar to controls. Still, although in some cases imposed, it was not possible to standardize the base of support and corresponded of the preferred (natural) stance of the children. However, differences of anthropometric characteristic [32], [38]

or posture (e.g. forward leaning) [11] were reported not to account for a reduction of the initial TA burst and the concomitant smaller backward shift of the CoP.

Reduced TA activity, especially of the swing foot, has been previously described in hemiplegic children with cerebral palsy (CP) [39] and interpreted as anticipatory planning deficit, which may be caused by an impairment at the motor imagery level [40]. However, a direct comparison with our findings may not be possible since children with hemiplegic CP demonstrated a tendency to shift the CoP towards the less affected limb, which is usually their stance limb. This shift may determine a reduced TA activity of the swing foot as a results of an increased reliance upon the stance limb to create the posterior shift of the CoP and redirect the ground reaction force vector anteriorly to facilitate forward motion [39].

Taken together, our results suggest that girls with RTT might lack accurate tuning of feedforward control of movements at gait initiation. These findings may be relevant with regards to rehabilitation practice. Guidelines for motor rehabilitation in RTT consider intensely applied physical therapy [41]. Indeed, there is preliminary evidence of a protective effect of learning to walk on the risk of fracture in children with RTT [42]. Balance exercises, eye/feet coordination, walking on different surfaces and crossing obstacles are some of the goals in motor rehabilitation. A specific training on gait initiation and on practices to facilitate tuning of feedforward control of movements has never been described in motor rehabilitation protocols for RTT girls. Our preliminary results also suggest that motor intervention in girls with RTT should include preparatory adjustments of gait initiation inducing backward disequilibrium reactions and strengthening a TA activation in order to promote the initial forward leaning of the body which is necessary to initiate walking. Further research should be encouraged to obtain evidence based protocols of intervention, such as intensive models of motor intervention for short periods [43,44], and to investigate the relationships between specific motor exercises and quality of gait in RTT children.

Author Contributions

Conceived and designed the experiments: IUI. Performed the experiments: IUI MD MM AM. Analyzed the data: IUI MD MM AM CAF. Contributed reagents/materials/analysis tools: IUI MD MM AM. Wrote the paper: IUI JV MR CAF PC.

References

1. Amir RE, Van den Veyver IB, Wan M, Tran CQ, Francke U, et al. (1999) Rett syndrome is caused by mutations in X-linked MECP2, encoding methyl-CpG-binding protein 2. Nat Genet 23: 185–188.
2. Neul JL, Fang P, Barrish J, Lane J, Caeg EB, et al. (2008) Specific mutations in methyl- CpG-binding protein 2 confer different severity in Rett syndrome. Neurology 70: 1313–1321.
3. Rett A (1966) On a unusual brain atrophy syndrome in hyperammonemia in childhood. Wien Med Wochenschr 116: 723–726.
4. Hagberg B, Aicardi J, Dias K, Ramos O (1983) A progressive syndrome of autism, dementia, ataxia, and loss of purposeful hand use in girls: Rett's syndrome: report of 35 cases. Ann Neurol 14: 471–479.
5. Witt Engerström I (1990) Rett syndrome in Sweden. Neurodevelopment–disability–pathophysiology. Acta Paediatr Scand Suppl 369: 1–60.
6. Neul JL, Kaufmann WE, Glaze DG, Christodoulou J, Clarke AJ, et al. (2010) Rett Syndrome: Revised Diagnostic Criteria and Nomenclature. Ann Neurol 68: 944–950.
7. Dan B, Cheron B (2008) Postural control in children with Rett syndrome or Angelman syndrome. In: Hadders-Algra M, Brogren Carlberg E, Eds. Posture: A Key Issue in Developmental Disorders. London: Mac Keith Press. pp. 148–169.
8. Colvin L, Fyfe S, Leonard S, Schiavello T, Ellaway C, et al. (2003) Describing the phenotype in Rett syndrome using a population database. Arch Dis Child 88: 38–43.
9. Das P, McCollum G (1988) Invariant structure in locomotion. Neuroscience 25: 1023–1034.
10. Forssberg H (1985) Ontogeny of human locomotor control I. Infant stepping, supported locomotion and transition to independent locomotion. Exp Brain Res 57: 480–493.
11. Crenna P, Frigo C (1991) A motor programme for the initiation of forward-oriented movements in humans. J Physiol Lond 437: 635–653.
12. Massion J (1992) Movement, posture and equilibrium: interaction and coordination. Progr Neurobiol 38: 35–56.
13. McIlroy WE, Maki BE (1999) The control of lateral stability during rapid stepping reactions evoked by antero-posterior perturbation: does anticipatory control play a role. Gait Posture 9: 190–198.
14. Brenière Y, Do MC, Bouisset S (1987) Are dynamic phenomena prior to stepping essential to walking? J Mot Behav 19: 62–76.
15. Lepers R, Breniere Y (1995) The role of anticipatory postural adjustments and gravity in gait initiation. Exp Brain Res 107: 118–124.
16. Winter DA (1995) Human balance and postural control during standing and walking. Gait Posture 3: 193–214.
17. Winter DA, Patla AE, Ishac M, Gage WH (2003) Motor mechanisms of balance during quiet standing. J Electromyogr Kinesiol 13: 49–56.
18. Brenière Y, Do MC (1986) When and how does steady state gait movement induced from upright posture begin? J Biomech 19: 1035–1040.
19. Jian Y, Winter DA, Ishac MG, Gilchrist L (1993) Trajectory of the body COG and COP during initiation and termination of gait. Gait Posture 1: 9–22.

20. Mann RA, Hagy JL, White V, Liddell D (1979) The initiation of gait. J Bone Joint Surg 61: 232–239.

21. Nissan M, Whittle MW (1990) The initiation of gait in normal subjects: a preliminary study. J Biomed Eng 12: 165.

22. Carlsoo A (1966) The initiation of walking. Acta Anatomica 65: 1–9.

23. Hayes KC, Riach CL (1990) Preparatory postural adjustements and postural sway in young children. In: Woollacott M, Horak F, edotors. Posture and gait: control mechanisms, vol II. Portland: University of Oregon Books. pp. 255–258.

24. Ledebt A, Bril B, Brenière Y (1998) The build up of anticipatory behaviour: an analysis of the development of gait initiation in children. Exp Brain Res 120: 9–17.

25. Fabio RA, Martinazzoli C, Antonietti A (2005) Costruzione e standardizzazione dello strumento "R.A.R.S." (Rett Assessment Rating Scale). Ciclo Evol Disabil 8: 257–281.

26. Ferrari A, Benedetti MG, Pavan E, Frigo C, Bettinelli D, et al. (2008) Quantitative comparison of five current protocols in gait analysis. Gait Posture 28: 207–216.

27. Zatsiorsky V, Seluyanov V (1983) The mass and inertia characteristics of the main segments of the human body. In: H . Matsui & K . Kobayashi, Eds. Biomechanics VIII-B. Champaign, IL: Human Kinetics. pp. 1152–1159.

28. Martin M, Shinberg M, Kuchibhatla M, Ray L, Carollo JJ, et al. (2002) Gait initiation in community-dwelling adults with Parkinson disease: comparison with older and younger adults without the disease. Phys Ther 82: 566–577.

29. Carpinella I, Crenna P, Calabrese E, Rabuffetti M, Mazzoleni P, et al. (2007) Locomotor Function in the Early Stage of Parkinson's Disease. IEEE 15: 543–551.

30. Gahery Y (1987) Associated movements, postural adjustements and synergies: some comments about the historic and significance of the three motor concepts. Arch Ital Biol 125: 345–360.

31. Rosenbaum DA (1984) The planning and control of movements. In: Anderson JR, Kosslyn SM, Eds. Tutorials in learning and memory: essay in honor of Gordon. San Francisco: Freeman. pp. 219–233.

32. Malouin F, Rchards CL (2000) Prepartory adjustements during gait initiation in 4–6-year-old children. Gait Posture 11: 239–253.

33. Berstein N (1967) Coordination and Regulation of Movement. New York: Pergamon.

34. Forssberg H, Hirschfeld H, Stokes VP (1991) Development of human locomotor mechanisms. In: Shimamura M, Grillner S, Edgerton VR, Eds. Neurobiological Basis of Human Locomotion. Tokyo: Japan Scientific Society Press. pp. 259–273.

35. Malouin F, Menier C, Comeau F, Dumas F, Richards CL, et al. (1994) Dynamic Weight transfer during gait initiation in hemiparetic adults and effect of foot position. Soc Neurosci 241: 3.

36. Malouin F, Richards CL, Trahan J, Menier C, Dumas F, et al. (1996) Gait initiation in 4-6-year-old children. Soc Neurosci 802: 8.

37. Brenière Y, Bril B, Fontaine R (1989) Analysis of the transition from upright stance to steady state locomotion in children with under 200 days of autonomous walking. J Mot Behav 21: 20–37.

38. Caderby T, Dalleau G, Leroyer P, Bonazzi B, Chane-Teng D, et al. (2013) Does an additional load modify the anticipatory postural adjustments in gait initiation? Gait Posture 37: 144–146.

39. Stackhouse C, Shewokis PA, Pierce SR, Smith B, McCarthy J, et al. (2007) Gait initiation in children with cerebral palsy. Gait Posture 26: 301–308.

40. Mutsaarts M, Steenbergen B, Bekkering H (2005) Anticipatory planning of movement sequences in hemiparetic cerebral palsy. Motor Control 9: 439–458.

41. Lotan M, Hanks S (2006) Physical therapy intervention for individuals with Rett syndrome. ScientificWorldJournal 6: 1314–1338.

42. Downs J, Bebbington A, Woodhead H, Jacoby P, Jian L, et al. (2008) Early determinants of fractures in Rett syndrome. Pediatrics 121: 540–546.

43. Polovina S, Polovina TS, Polovina A, Polovina-Proloscić T (2010) Intensive rehabilitation in children with cerebral palsy: our view on the neuronal group selection theory. Coll Antropol 34: 981–988.

44. Sorsdahl AB, Moe-Nilssen R, Kaale HK, Rieber J, Strand LI (2010) Change in motor basic abilities, quality of movement and daily activities following intensive, goal-directed, activity-focused physiotherapy in a group setting for children with cerebral palsy. BMC Pediatr 27: 10–26.

APPENDIX C

FINDING A NEW THERAPEUTIC APPROACH FOR NO-OPTION PARKINSONISMS: MESENCHYMAL STROMAL CELLS FOR PROGRESSIVE SUPRANUCLEAR PALSY

Canesi M., Giordano R., Lazzari L., Isalberti M., Isaias I.U., Benti R., Rampini P., Marotta G., Colombo A., Cereda E., Dipaola M., Montemurro T., Viganò M., Budelli S., Montelatici E., Lavazza C., Cortelezzi A. and Pezzoli G.

RESEARCH

Open Access

CrossMark

Finding a new therapeutic approach for no-option Parkinsonisms: mesenchymal stromal cells for progressive supranuclear palsy

Margherita Canesi[1†], Rosaria Giordano[2*†], Lorenza Lazzari[2], Maurizio Isalberti[3], Ioannis Ugo Isaias[4,5], Riccardo Benti[6], Paolo Rampini[7], Giorgio Marotta[6], Aurora Colombo[1], Emanuele Cereda[8], Mariangela Dipaola[5], Tiziana Montemurro[2], Mariele Viganò[2], Silvia Budelli[2], Elisa Montelatici[2], Cristiana Lavazza[2], Agostino Cortelezzi[9] and Gianni Pezzoli[1]

Abstract

Background: The trophic, anti-apoptotic and regenerative effects of bone marrow mesenchymal stromal cells (MSC) may reduce neuronal cell loss in neurodegenerative disorders.

Methods: We used MSC as a novel candidate therapeutic tool in a pilot phase-I study for patients affected by progressive supranuclear palsy (PSP), a rare, severe and no-option form of Parkinsonism. Five patients received the cells by infusion into the cerebral arteries. Effects were assessed using the best available motor function rating scales (UPDRS, Hoehn and Yahr, PSP rating scale), as well as neuropsychological assessments, gait analysis and brain imaging before and after cell administration.

Results: One year after cell infusion, all treated patients were alive, except one, who died 9 months after the infusion for reasons not related to cell administration or to disease progression (accidental fall). In all treated patients motor function rating scales remained stable for at least six-months during the one-year follow-up.

Conclusions: We have demonstrated for the first time that MSC administration is feasible in subjects with PSP. In these patients, in whom deterioration of motor function is invariably rapid, we recorded clinical stabilization for at least 6 months. These encouraging results pave the way to the next randomized, placebo-controlled phase-II study that will definitively provide information on the efficacy of this innovative approach.

Trial registration ClinicalTrials.gov NCT01824121

Keywords: Progressive supranuclear palsy, Mesenchymal stem/stromal cells, Cell therapy, Regenerative medicine

Background

Progressive supranuclear palsy (PSP), Steele–Richardson–Olszewsky syndrome (SR) type, is a progressive neurodegenerative disorder belonging to the group of taupathies, with motor, cognitive and behavioral symptoms. Its prevalence is about 6.5 cases per 100,000 people and its incidence is about 5.3 new cases every 100,000

people [1–3]. Although distinctive signs of PSP may appear already within the first 2 years of disease after onset, its clinical heterogeneity makes early diagnosis a challenge [4–6] and no reliable biomarkers are available. Therefore postmortem neuropathology is the diagnostic gold standard of PSP [7, 8]. Motor symptoms include gait disturbances, early onset of postural instability, backward falls, axial rigidity and restriction of vertical eye movements [9]. Personality changes and cognitive impairment are other frequent invalidating symptoms [10]. Quality of life deteriorates rapidly and patients are confined to a wheelchair a few years after the onset of disease [11].

*Correspondence: rosaria.giordano@policlinico.mi.it
†Margherita Canesi and Rosaria Giordano contributed equally to this work
[2] Cell Factory, Unit of Cell Therapy and Cryobiology, Fondazione IRCCS Ca' Granda Ospedale Maggiore Policlinico, Via F Sforza 35, 20122 Milan, Italy
Full list of author information is available at the end of the article

Canesi *et al. J Transl Med* (2016) 14:127

Page 2 of 11

Disease duration is generally no longer than 9 years [4, 10, 12, 13]. Aspiration pneumonia and respiratory failure are frequent causes of death [14]. PSP has all the negative features of the most severe neurodegenerative disorders: its etiology is unknown, it is invariably progressive, it does not respond to any available therapy and it brings a huge human and economic burden to society. Despite healthy neural cell replacement is the ideal objective of any curative therapy for PSP, as in many other neurodegenerative disorders, up to now no approach can efficiently achieve this goal. Therefore, even treatment that could reduce neural cell loss and stabilize clinical symptoms would be a significant breakthrough in this field. The use of several new drugs, such as davunetide, a tau-directed therapeutic agent, and donezepil, failed to exert beneficial effects in PSP patients [15]. Only slight improvement was achieved with coenzyme Q10 [16]. On the other hand, both preclinical in vitro investigations as well as preliminary clinical studies have shown that bone marrow (BM) derived mesenchymal stromal cells (MSC) may offer a new strategy for several neurodegenerative disorders [17–19]. The biological hypothesis underlying this approach is that MSC can exert neuroprotective effects by reducing cell apoptosis and neural cell loss [17]. We specifically define in our work MSC as mesenchymal stromal cells since they completely fulfil the minimal requirements set by ISCT for mesenchymal stromal cells [18], while they only partially comply with the definition of stem cells [19]. With all this in mind and with no intention of actually replacing diseased neurons, we conceived a phase I study to test the safety of MSC intra-arterial infusion, as well as its effects in slowing down the rate of progression of the disease in PSP patients. We followed up the enrolled patients for 1 year, with the best available validated clinical rating scales for the assessment of Parkinsonism, neuroimaging procedures and an automated biomechanical evaluation. In the present report we describe the one-year follow-up results obtained in the first five PSP patients treated with autologous MSC.

Methods

Protocol approval, patient screening and cell manufacturing

The protocol was authorized by the local Ethics Committee of Fondazione IRCCS Cà Granda Ospedale Maggiore Policlinico (Italy), by the national competent authority for phase-I cell therapy at the National Health Institute (Istituto Superiore di Sanità) and approved by the Italian Medicines Agency (Agenzia Italiana del Farmaco, AIFA). The trial is registered at ClinicalTrials.gov (NCT01824121). All patients gave their written informed consent. A detailed description of the study design, inclusion and exclusion criteria, BM collection, MSC isolation

and administration along with clinical (motor and neuropsychological) and neuroimaging assessments have been previously reported [20]. In order to efficiently select the patients to be treated in the clinical trial, a pre-screening procedure was implemented. The patients who met the inclusion/exclusion criteria were therefore enrolled in a pre-clinical, validation study and underwent bone marrow aspiration to test the ability of their BM to give rise to MSC with the due quantitative and qualitative characteristics. In particular, the following specifications were set up to classify MSC cultures as compliant and therefore proceed towards expanding them for clinical use: (a) ≥1-fold expansion between passage 0 and 1 and between passage 1 and 2; (b) normal karyotype at passage 0, 1 and 2.

This validation study was implemented because there is sporadic evidence that MSC from patients affected by neurological diseases might differ somehow from those generated from normal healthy donors [21]. In this way we ensured that the patients were treated only with cells that could be identified as standard MSC complying with the universally recognized characteristics [18]. A maximum of 30 mL of BM was harvested. All the cell preparations passed the quality controls following good manufacturing practices (GMP) rules.

Clinical and neuropsychological assessment

The patients underwent neurological examinations to assess motor function using the following scales: unified Parkinson's disease rating scale [22] (UPDRS part-III, motor score), Hoehn and Yahr staging [23] (H&Y), PSP rating scale [12] (PSP-RS). These tests, together with mini mental state evaluation (MMSE, according to Folstein et al. [24]) were assessed at baseline and at each follow-up point (1, 3, 6 and 12 months after cell administration). The clinical conditions were classified as "stable" when the UPDRS and PSP-RS scores had not diminished by more than 30 % compared to baseline and the H&Y staging did not change at the defined time point.

Neuroimaging

All patients underwent longitudinal neuroimaging assessments, using brain magnetic resonance imaging (MRI) (baseline, 24 h after cell administration and after 1 year), striatal dopamine transporter single photon emission computed tomography (SPECT) and positron emission tomography (PET) (both at baseline and after 12 months). Tropanic tracers labeled with Iodine-123 (FP-CIT) and 18F-Fluoro-2-deoxyglucose (Beta-CIT) were used for SPECT imaging and for PET/TC imaging, respectively. For SPECT, intravenous administration of 110–140 MBq of [^{123}I] FP-CIT (Datscan, GE-Health,

Canesi *et al. J Transl Med* (2016) 14:127

Page 3 of 11

Amersham, UK) was performed 30–40 min after thyroid blockade (10–15 mg of Lugol solution per os) in all patients. The analysis was performed as already described [25]. A volumetric template of grey matter anatomic distribution, generated from the Montreal Neurological Institute MRI single participant brain atlas by applying a macroscopic anatomical method (automated anatomic labelling), was reoriented and reformatted to obtain a 2.64-cm-thick reference section. A template of eight irregular regions of interest (ROIs) was manually drawn on this section to assess the anatomical extent of striatal and occipital structures having both specific and nonspecific uptake of [123I] FP-CIT, respectively. This ROI template was also positioned on the reference SPECT section and adjusted on both striatal and occipital cortex. Moreover, striatal ROIs were also segmented into their anterior (caudate nucleus) and posterior (putamen) portions. Specific striatal dopamine uptake transporter (DAT) binding of [123I] FP-CIT was calculated in the whole striatum, putamen and caudate nucleus using the formula:

[(mean counts in specific ROI)

−(mean counts in occipital ROI)]

/(mean counts in occipital ROI).

We also calculated putamen/caudate ratios for each subject. All patients underwent [18] F-Fluoro-2-deoxyglucose positron emission tomography scanning (FDG-PET) at rest, after intravenous injection of 170 MBq. Each acquisition included a computed tomography (CT) transmission scan of the head (50mAs lasting 16 s) followed by a three-dimensional (3D) static emission of 15 min using a Biograph Truepoint 64 PET/CT scanner (Siemens). PET sections were reconstructed using an iterative algorithm (OS-EM), corrected for scatter and for attenuation, using density coefficients derived from the low dose CT scan of the head obtained with the same scanner, with the proprietary software. Images were reconstructed in the form of transaxial images of 128×128 pixels of 2 mm, using an iterative algorithm, ordered-subset expectation maximization (OSEM). The resolution of the PET system was 4–5 mm FWHM.

Biomechanical evaluation

Biomechanical evaluation was assessed at baseline and at six and 12 months after cell administration. Equipment and settings were previously described [26]. For this study in particular, two specific sets of parameters, one for standing and one for gait initiation, were automatically extracted by means of ad hoc algorithms. For standing, we measured the center of pressure (CoP) mean velocity and spatial displacement [27–31]. To examine gait initiation we focused on anticipatory postural adjustment [26, 32] (i.e. imbalance and unloading phases) and measured the following parameters: (1) the duration of both phases, (2) the antero-posterior (AP) and mediolateral (ML) shift and velocity of the CoP, (3) the CoP mean length and velocity. Finally, we also measured the (4) length and (5) velocity of the first step. Spatial parameters were normalized on the basis of body height (%BH).

Cell administration

The median cell dose was 1.7 (1.2–2.0) $\times$ 10E6 MSC/kg of body weight. One single administration was performed for each patient. Before cell administration, the patient underwent neuroleptoanalgesia and was monitored by an anaesthetist. MSC were administered by intra-arterial route [33], with modifications according to local equipment and local standards. Briefly: with Seldinger technique, catheterization was carried out via the right common femoral artery (or the left one in the event of difficulty in achieving arterial access) using a 6F Ultimum EV (St Jude Medical, MN, USA) introducer and a 5F Hinck or Simmons (Terumo Europe NV, Leuven, Belgium) diagnostic catheter. An angiographic study of the cervical and intracranial arteries was performed, with the support of an 0.035 in., 150 cm long hydrophilic guide (Terumo Europe NV, Leuven, Belgium). Subsequently, with or without an exchange manoeuvre, using a 260 cm exchange wire Easykit 0.35″ or 0.38″ (ab medica s.p.a., Lainate (MI), Italy), a 90 cm 6F Envoy XB guiding catheter (Miami Lakes, FL, USA) was used, after intravenous administration of heparin sodium (3000–5000 IU according to body mass) to reduce the risk of thromboembolism. The guiding catheter, flushed with heparinised saline, was positioned at the origin of both internal carotid arteries and at the origin of the widest vertebral artery. Once the guiding catheter was in place, a Rebar 027 (130 or 145 cm) or Rebar 018 (153 cm) microcatheter (ev3/Covidien, Irvine, CA, USA), steered by a 205 cm Transend EX 0.014 (Boston Scientific, Natick, MA, USA), was moved forward and upward into the internal carotid arteries just above the origin of the ophthalmic arteries and into the basilar artery. The MSC were then injected into the various districts, through the microcatheter, using a pump at 70 mL/h. The catheter was flushed periodically with heparinised normal saline solution.

Results

Five patients were included and treated in the study. Nine were pre-screened and seven tested positive in the validation study with a good rate of MSC expansion. As expected, in view of the severity of the disease, another two patients were not enrolled because one died before MSC administration and the other one rapidly worsened and was no longer eligible at the time of

Canesi *et al. J Transl Med* (2016) 14:127

Page 4 of 11

MSC treatment. Clinical and imaging data are listed in Tables 1 and 2, respectively. All the patients were alive at 12 months, except one, who died 9 months after cell administration for causes not related to the treatment: she fell accidentally before the six-month assessment and was not able to come for the follow-up visits. Also the last patient did not come for the 6 month assessment due to hospitalization for rehabilitation. Therefore the latest follow-up point was 12 months for three patients and 3 months for the remaining two. All the evaluable patients had stable UPDRS scores at the last follow-up. The PSP-RS also demonstrated disease stabilization at 6 and 12 months in all the evaluable patients, except one (PSP08). Another important positive effect was recorded by H&Y staging, which remained stable over time. The results of biomechanical evaluation are shown in Table 3.

Patient clinical presentation
Case I (PSP01)

The first patient enrolled was a male who noticed motor impairment in his right arm at the age of 52. Diagnosis of PSP was made two years after the onset of symptoms, when gait difficulty, instability with falls, dysarthria, dysphagia and vertical gaze appeared and motor symptoms worsened. Brain MRI and ECD SPECT were also compatible with PSP. Five years later he needed a walker due to postural instability and backward falls. Dysarthria and dysphagia worsened over time. The patient was enrolled in this study after 8 years of disease. At the time of enrollment, neuropsychological evaluation was in the normal range with the exception of mild depression, irritability and anxiety. Brain MRI showed slight subcortical, frontoparietal and mesencephalic atrophy. FDG PET showed bilateral hypometabolism in the frontal superior gyrus,

Table 1 Patients' description

	Case 1 (PSP01)	Case 2 (PSP02)	Case 3 (PSP06)	Case 4 (PSP08)	Case 5 (PSP09)
Demographic data and cell dose					
Gender	M	F	F	F	F
Age (years)	60	66	65	65	68
Disease duration (years)	8	7	4	6	5
Cell dose ($\times 10^6$/kg)	1.4	1.7	2	1.8	1.2
MMSE					
Baseline	27.49	28.27	25.49	24.27	25.53
1-month	27.49	25.27	26.49	24.27	28.53
12-month	26.49	25.03	na	21.27	na
H&Y					
Baseline	4/5	4/5	4/5	4/5	4/5
1-month	4/5	4/5	4/5	4/5	4/5
3-month	4/5	4/5	4/5	4/5	4/5
6-month	4/5	4/5	na	4/5	na
12-month	4/5	4/5	na	4/5	na
UPDRS III					
Baseline	47	38	47	31	42
1-month	45 (−4 %)	37 (−3 %)	36 (−23 %)	31 (0 %)	48 (+14 %)
3-month	47 (0 %)	49 (+29 %)	48 (+2 %)	39 (+26 %)	48 (+14 %)
6-month	45 (−4 %)	51 (+34 %)	na	40 (+29 %)	na
12-month	47 (0 %)	47 (+24 %)	na	40 (+29 %)	na
PSP-RS					
Baseline	37	53	52	36	57
1-month	41 (+11 %)	40 (−25 %)	46 (−12 %)	39 (+8 %)	n.a.
3-month	44 (+19 %)	39 (−26 %)	43 (−17 %)	46 (+28 %)	51 (−11 %)
6-month	47 (+27 %)	63 (+19 %)	na	52 (+44 %)	na
12-month	47 (+27 %)	57 (+8 %)	na	53 (+47 %)	na

Demographical data, cell dose, baseline and follow-up neuropsycological assessments by mini-mental state evaluation (MMSE) and clinical scoring using three different scales

For UPDRS and PSP-RS the values are reports as absolute value and percentage of variation from baseline (in brackets)

H&Y Hoehn-Yahr stage, UPDRS III Unified Parkinson's Disease Rating Scale part III, PSP-RS PSP rating score, na not available

Canesi *et al. J Transl Med* (2016) 14:127

Page 5 of 11

Table 2 SPECT and PET data

	Baseline	12-month
Case 1 (PSP01)	R striatum = 0.16	R striatum = 0.19
	L striatum = 0.14	L striatum = 0.16
	R caudate nucleus = 0.27	R caudate nucleus = 0.10
	L caudate nucleus = 0.17	L caudate nucleus = 0.23
	R putamen = 0.08	R putamen = 0.27
	L putamen = 0.10	L putamen = 0.09
Case 2 (PSP02)	R striatum = 0.49	R striatum = 0.34
	L striatum = 0.35	L striatum = 0.21
	R caudate nucleus = 0.59	R caudate nucleus = 0.48
	L caudate nucleus = 0.39	L caudate nucleus = 0.33
	R putamen = 0.42	R putamen = 0.1
	L putamen = 0.35	L putamen = 0.01
Case 3 (PSP06)	R striatum = 0.42	na
	L striatum = 0.60	
	R caudate nucleus = 0.54	
	L caudate nucleus = 0.73	
	R putamen = 0.30	
	L putamen = 0.43	
Case 4 (PSP08)	R striatum = 1.00	R striatum = 0.61
	L striatum = 1.15	L striatum = 0.72
	R caudate nucleus = 1.30	R caudate nucleus = 0.67
	L caudate nucleus = 1.46	L caudate nucleus = 0.72
	R putamen = 0.79	R putamen = 0.55
	L putamen = 0.86	L putamen = 0.65
Case 5 (PSP09)	R striatum = 0.37	na
	L striatum = 0.46	
	R caudate nucleus = 0.37	
	L caudate nucleus = 0.55	
	R putamen = 0.36	
	L putamen = 0.39	

Specific striatal dopamine uptake transporter (DAT) binding of [123 I] FP-CIT, calculated in the whole striatum, putamen and caudate nucleus using the formula: $[$(mean counts in specific ROI) − (mean counts in occipital ROI)$]$ / (mean counts in occipital ROI)

anterior cingulate, caudatus and midbrain. Severe reduction in dopamine transporter binding in the striatum was evident at FP-CIT SPECT. Biomechanical evaluation revealed normal measurements for standing, but several alterations of gait initiation.

Case II (PSP02)
Female, at the age of 63 she began to complain of rigidity, bradykinesia and unstable gait. She complained above all of neck pain that did not respond to any symptomatic therapy. Two years after the appearance of the first motor symptoms, clinical symptoms, brain MRI and FP-CIT SPECT supported the diagnosis of PSP. One year later she was still able to walk without assistance, but falls were more frequent and mild dystonic posture in the left leg was

evident. The patient took part in the study after 7 years of disease. Neuropsychological evaluation was in the normal range with the exception of a slight deficit in long-term verbal memory. FDG PET showed hypometabolism in the polar temporal area, and in the ponto-mesencephalic and midbrain areas. Severe reduction in dopamine transporter binding in the striatum was evident. The patient was unable to perform biomechanical analysis of movement because of apraxia involving her right leg.

Case III (PSP06)
The story of the third patient began at the age of 62 when she first noticed bradykinesia and mild depression. A few months later postural instability and falls appeared. Four years later she complained mainly of postural instability and difficulty in eye movements. The patient took part in the study after 4 years of disease. At the time of enrollment neuropsychological evaluations revealed mild depression and mild deficit in executive functions and visual-spatial abilities. Brain MRI showed mild encephalic and cerebellar cortical atrophy, and severe mesencephalic atrophy. Before MSC treatment, we were able to perform biomechanical measurement of standing only. In comparison to healthy controls, we found high values of ML displacement of CoP and high CoP velocity, thus suggesting great difficulties in maintaining the upright position.

Case IV (PSP08)
Female, at 61 years of age she complained of instability and occasional falls. Diagnosis of PSP was made 4 years later. The patient took part in the study after 6 years of disease. Neuropsychological evaluation showed deficit in cognitive and executive functions, visual-construction abilities and selective attention. Depression and anxiety were evident. Brain MRI showed fronto-parietal cortical atrophy, severe mesencephalic atrophy and mild cortical cerebellum atrophy. FDG PET showed severe hypometabolism in brainstem, moderate bilateral hypometabolism in the parietal lobe and slight bilateral hypermetabolism in fronto-orbital regions. Dopaminergic striatal innervation loss was remarkable bilaterally. Biomechanical evaluation performed before MSC infusion revealed only increased antero-posterior (AP) displacement of CoP, which was greater than normal values in the standing position. However, almost all parameters related to gait initiation were altered.

Case V (PSP09)
Female, at the age of 63 she began to complain of postural instability and retropulsion. Four years later, she presented with mild movement impairment, instability, akinesia at night, mild dysphagia, and irritability. She also

Canesi *et al. J Transl Med* (2016) 14:127

Page 6 of 11

Table 3 Biomechanical evaluation

(A)	Normal values (10°–90° percentile)	Case 1 (PSP01)			Case 4 (PSP08)		
		Basal	6-month	12-month	Basal	6-month	12-month
Standing							
Ellipse area (mm²) %BA	0.06–0.66	0.08	0.33	0.18	0.34	0.55	0.18
Ellipse eccentricity	0.62–0.97	0.97	0.92	0.8	0.98	0.99	0.80
Axis length AP avg. (mm) %FL	0.20–8.86	3.05	4.21	3.35	9.27[a]	3.73	3.35
Axis length ML avg. (mm) %FL	0.12–3.66	2.37	2.35	1.21	0.12	1.54	1.21
Sway path (CoP) velocity avg. (mm/s)	6.5–18.11	7.26	7.62	6.57	9.41	19.43	6.58
Gait initiation							
Imbalance phase							
Duration (s)	0.29–0.53	0.61[a]	0.84[a]	0.49	0.36	0.43	0.36
AP avg. (mm) %FL	9.58–17.26	0.86[a]	2.14[a]	1.04[a]	4.48[a]	1.73[a]	0.32[a]
AP vel. avg. (mm/s)	58.83–112.61	3.32[a]	13.68[a]	2.78[a]	22.33[a]	8.31[a]	1.01[a]
ML avg. (mm) %FL	4.6–19.21	5.13	6.61	3.55[a]	4.12[a]	3.18[a]	3.78[a]
ML vel. avg. (mm/s)	32.15–144.77	17.55[a]	43.53	23.1	24.78[a]	15.71[a]	27.22[a]
Sway path (CoP) velocity avg. (mm/s)	96.34–178.07	19.38[a]	46.99[a]	26.25[a]	36.17[a]	29.45[a]	28.74[a]
Sway path (CoP) length (mm)	36.73–63.60	14.29[a]	18.75[a]	11.69[a]	16.04[a]	11.12[a]	10.35[a]
Unloading phase							
Duration (s)	0.23–0.47	1.45[a]	0.83[a]	1.29[a]	1.09[a]	0.76[a]	1.36[a]
AP avg. (mm) %FL	3.9–14.44	7.94	8.73	8.79	11.48	12.28	8.21
AP vel. avg. (mm/s)	7.1–92.4	11.31	61.16	14.38	19.00[a]	37.42	10.71
ML avg. (mm) %FL	29.15–61.84	33.1	43.08	36.68	54.34	45.05	37.47
ML vel. avg. (mm/s)	265.14–481.64	78.31[a]	143.24[a]	85.81[a]	150.63[a]	151.28[a]	85.31[a]
Sway path (CoP) velocity avg. (mm/s)	269.18–510.98	108.73[a]	150.99[a]	95.58[a]	160.86[a]	163.10[a]	95.63[a]
Sway path (CoP) length (mm)	79.6–169.24	99.07	119.54	111.61	138.33	113.69	115.61
Step phase							
First step peak velocity (mm/s)	1475.4–1874.1	486.52[a]	783.05[a]	604.83[a]	714.70[a]	498.68[a]	566.64[a]
First step length (%BH)	26.27–33.63	21.04[a]	24.44[a]	17.08[a]	14.34[a]	8.21[a]	16.92[a]

(B)	Normal values (10°–90° percentile)	Case 3 (PSP06) Basal	Case 5 (PSP09) Basal
Standing			
Ellipse area (mm²) %BA	0.06–0.66	0.49	329.68[a]
Ellipse eccentricity	0.62–0.97	0.98	0.91
Axis length AP avg. (mm) %FL	0.20–8.86	6.78	5.16
Axis length ML avg. (mm) %FL	0.12–3.66	4.31[a]	4.13[a]
Sway path (CoP) velocity avg. (mm/s)	6.5–18.11	133.81[a]	12.69
Gait initiation			
Imbalance phase			
Duration (s)	0.29–0.53	ne	0.77[a]
AP avg. (mm) %FL	9.58–17.26	ne	6.01
AP vel. avg. (mm/s)	58.83–112.61	ne	16.70[a]
ML avg. (mm) %FL	4.6–19.21	ne	5.15
ML vel. avg. (mm/s)	32.15–144.77	ne	20.02[a]
Sway path (CoP) velocity avg. (mm/s)	96.34–178.07	ne	31.29[a]
Sway path (CoP) length (mm)	36.73–63.60	ne	22.06[a]
Unloading phase			
Duration (s)	0.23–0.47	ne	1.00[a]
AP avg. (mm) %FL	3.9–14.44	ne	5.63
AP vel. avg. (mm/s)	7.1–92.4	ne	8.63

Canesi *et al. J Transl Med* (2016) 14:127

Page 7 of 11

Table 3 continued

(B)	Normal values (10°–90° percentile)	Case 3 (PSP06) Basal	Case 5 (PSP09) Basal
ML avg. (mm) %FL	29.15–61.84	ne	54.85
ML vel. avg. (mm/s)	265.14–481.64	ne	129.37[a]
Sway path (CoP) velocity avg. (mm/s)	269.18–510.98	ne	132.25[a]
Sway path (CoP) length (mm)	79.6–169.24	ne	129.71
Step Phase			
First step peak velocity (mm/s)	1475.4–1874.1	ne	596.99[a]
First step length (%BH)	26.27–33.63	ne	12.78[a]

(A) Patients with complete follow-up; (B) patients with only basal evaluation. Case 2 (PSP 02) was not evaluable (ne) because of dystonia

For abbreviations: see text

[a] Patient's parameters outside the range between 10 and 90° percentile of healthy control subjects' values

reported hypothyroidism and had had left knee replacement. Diagnosis of PSP was made and the patient took part in the study after 5 years of disease. At the time of enrollment, brain MRI showed mild cortical, and severe subcortical and mesencephalic atrophy. Cerebellar cortical atrophy was also evident. FDG PET showed bilateral hypometabolism in frontal area, right insula and temporal area; mesencephalic and cerebellar hypometabolism was also evident. Neuropsychological evaluation showed normal cognition, but deficits in executive and attentional functions, and in visual-spatial ability. Biomechanical measurements during standing showed high values of CoP sway path, in particular in medio-lateral (ML) direction. Regarding gait initiation, the patient showed altered values of almost all parameters.

BM aspiration, cell administration and short term (24-hour) follow-up

All the patients underwent BM aspiration with no side effects. Cell administration was well tolerated in all patients. Neurological assessment remained stable after MSC administration in all patients, except one (Case V), in whom transient left hemiparesis was recorded. Also brain MRI performed 24 h after cell administration showed spotty ischemic lesions in all the patients (Fig. 1), while ischemic alterations in the posterior segment of the left inferior peduncle of the cerebellum and in the right mesencephalon were found in the last patient.

Clinical assessment
Case I (PSP01)
One month after MSC treatment the patient and caregiver reported improvement in balance and gait, and a slight improvement in dysphagia. Neuropsychological evaluation showed no cognitive changes with regards to pre-treatment values and an improvement in mood.

At three, six and 12 month follow-up, clinical conditions were stable and the improvement in balance and gait persisted. Neuropsychological evaluation remained unchanged, with the exception (at 1 year) of mild daytime somnolence and worsening in executive and long-term memory (at the lower limit of the normal range). Mood was always in the normal range.

Biomechanical measurements performed 6 and 12 months after MSC infusion showed a global improvement in balance and gait initiation. In particular, the duration of the imbalance phase and the relative ML velocity of CoP normalized after MSC infusion.

Case II (PSP02)
At 1 month follow-up there were subjective improvements in stability, eye mobility, tone of voice and significant reduction in painful neck rigidity. The patient and her caregiver noticed an improvement in gait, although assistance was still necessary. Motor function remained stable for six months. Thereafter the patient and her caregivers noticed worsening of apraxia in the right leg resulting in instability and gait difficulty. Neck pain was still present, but somewhat milder than before MSC administration. Neuropsychological evaluation described worsening of executive function and long-term verbal memory.

Brain MRI showed increased atrophy in the mesencephalon, but no modification in other areas.

FDG PET findings were almost unchanged, with mild worsening in the prefrontal cortical area. The striatal density of dopamine transporters also worsened.

Case III (PSP06)
At one-month follow-up the patient, and her caregivers, reported improvement in gait and stability. Although she was not self-sufficient, she needed less assistance

Canesi *et al. J Transl Med* (2016) 14:127

Page 8 of 11

Fig. 1 RMN study: representative figure of the RMN performed before **a** and 24 h after **b** cell administration. In **b** the *arrows* indicate several spotty lesions
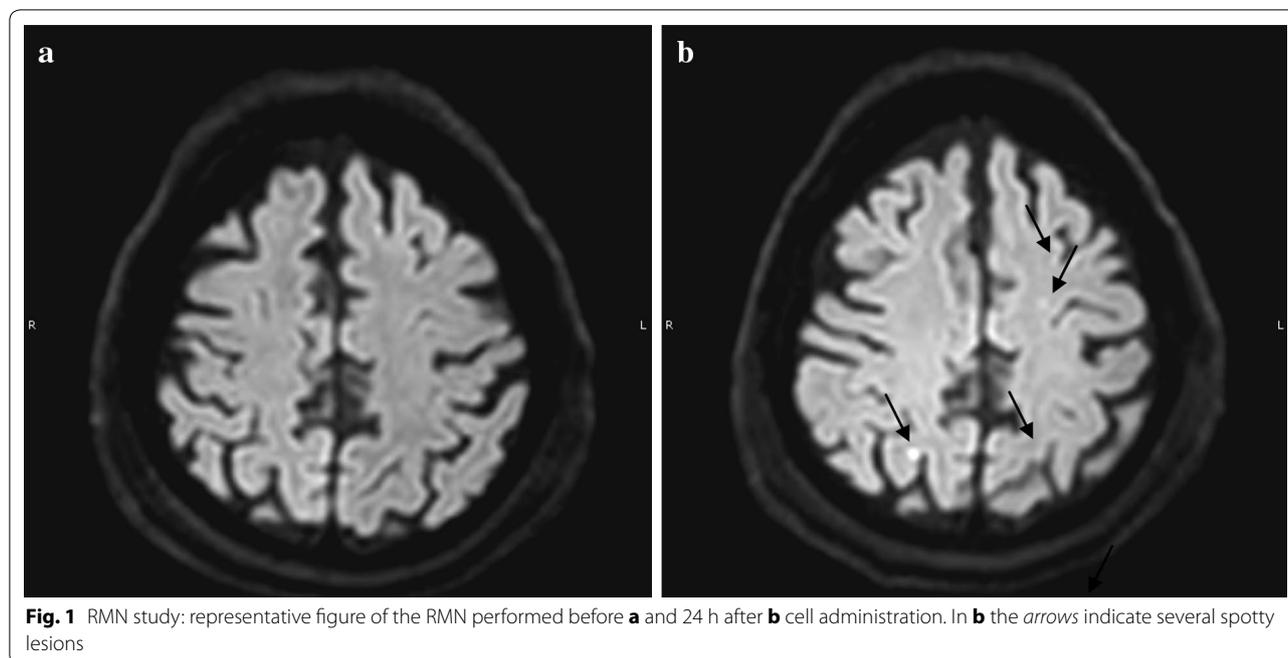
during daily activities, had improvement in ocular mobility mostly downward and reduction in photophobia. She also reported improvement in constipation. No changes for dysarthria and dysphagia were recorded. The improvement persisted at the 3 month follow-up visit.

Shortly before the 6 month follow-up evaluation, the patient fell and fractured her right foot. No biomechanical evaluation of posture and gait was thereafter attempted. Following this accident her clinical conditions worsened, the patient experienced depression and she refused food and drink. Renal function worsened and 9 months after MSC treatment the patient died in the emergency care unit due to cardiac arrest.

Case IV (PSP08)

One month after MSC administration neuropsychological evaluation showed global cognitive functions in the normal range, an increase in anxiety and depression. Her principal complaint was visual difficulty that was already present at the beginning of the disease. Three months after, improvement in global cognitive functions and increase in MMSE (from 24/26 to 27/30) was recorded. Nevertheless, depression and anxiety remained unchanged. Visual disturbances were still bothersome for the patient. Six months after MSC therapy subjective and objective evaluations were unchanged, the main complaint reported by the patient being ocular disturbances with photophobia and lacrimation, as at the onset of the disease. One year after MSC therapy, the clinical conditions of the patient were stable. FDG PET was

unchanged, whereas FP-CIT SPECT showed a greater reduction in dopamine transporter binding in the striatum. A biomechanical evaluation of posture and gait initiation was performed 6 and 12 months after MSC infusion and showed global worsening of maintenance of upright posture and walking planning.

Case V (PSP09)

In the last patient, sensory-motor facio-brachial-crural left hemisyndrome appeared 12 h after MSC administration. After 24 h hyposthenia of upper left arm, hemifacial paresis with severe dysarthria and dysphagia persisted. Brain MRI, performed 24 h after the procedure, showed ischemic alterations in the posterior segment of the left inferior peduncle of the cerebellum and in the right mesencephalon. During the following weeks, the neurological syndrome gradually improved with persistence of minor deficits (i.e. dysarthria, dysphagia and mild hyposthenia of the left arm). At 3 month-follow-up no sensory-motor deficits in the left arm were recorded. The patient did not attend the next follow-up visits, but information gathered on the telephone confirmed postural instability, whereas dysarthria was stable.

Discussion

The "Holy Grail" for cellular therapy of degenerative disorders is neural cell replacement. However, despite initial encouraging results with fetal dopaminergic neuron transplantation [34], the goal is still far away and, up to now, no feasible, safe and effective cell therapy is

Canesi *et al. J Transl Med* (2016) 14:127

Page 9 of 11

available. On the other hand, there are numerous severe and progressive neurodegenerative disorders, which do not respond to any available therapy, symptomatic therapy included, and invariably lead to disabilities with heavy individual and societal consequences. In consideration of these still unmet clinical needs, major efforts are to be made to find innovative approaches that can provide novel tools to contrast disease progression and, at the very least, reduce the consequences of progressive neural cell loss.

With this aim in mind, we designed a phase I study, to test the safety of MSC administration in patients affected by PSP and to collect preliminary data on its efficacy. Herein we describe the evidence that we have gathered through first-in-man experience in five patients treated in the open phase of our trial and the findings during a one-year follow-up. To our knowledge, this is the first clinical trial testing autologous bone marrow MSC in PSP. The subjects in our trial were patients with rapidly progressing, severe disease for which there are no therapeutic options. Therefore, even though this phase I trial was not designed to test the efficacy of MSC, the stabilization of the rating scale scores after the intervention and during one-year follow-up is of utmost importance. Actually, in this study all subjects were evaluated by means of the best available rating scales for the assessment of motor function in patients with Parkinsonism (i.e. PSP-RS, UPDRS motor score and H&Y staging), as well as by biomechanical evaluation of gait and posture at different time points. We report that all the patients at the last follow-up had stable clinical assessment scores related to at least two validated scales and one patient maintained this stabilization for 1 year. Regarding the biomechanical evaluation, as expected, it confirmed the presence of great difficulties in balance and planning of gait [35] in all patients. Despite being not applicable to severely impaired patients, such a biomechanical evaluation proved to be a reliable method to investigate motor and postural capabilities in PSP patients. We were also able to describe mild improvement in one subject (PSP01) 12 months after MSC infusion.

Regarding safety, it must not be left unsaid that intra-arterial administration of MSC is associated with important safety concerns because of the intrinsic risk of microembolization, which, in our experience was invariably present in all the treated patients. This risk had been already reported by Lee and co-workers, who treated patients affected by multiple system atrophy [36] and seems to depend, to some extent at least, on the intrinsic infusion technique. It was indeed present also in the placebo group and at a higher frequency compared to the treated group (35 vs 29 %). Other factors that may be involved in microembolization during MSC intrarterial

administration are cell size and type [37] and infusion velocity [38, 39]. In consideration of this risk and of its determinants, a stringent and accurate follow up was implemented, including frequent clinical assessments and the execution of MRI before and 24 h after intervention. An interdisciplinary evaluation of each single patient was performed jointly by the neurologist, the interventional radiologist and the anesthesiologist. In our study all the patients were alive 1 year after cell administration, except one, who died of the consequences of an accidental fall. To correctly interpret the significance of these findings, we analyzed the historical cohort of 455 PSP patients followed by our Center over the last years. In a subgroup of subjects (n = 118) with the same characteristics as the patients enrolled in the study, only 24 % of them were followed up for at least 1 year, the main causes of unavailability being death or severe disease progression (personal data, not shown). This makes the survival rate in our trial extremely significant.

Conclusions

Despite their preliminary nature, these first-in-man results with PSP patients are encouraging and can be easily transferred to several other neurodegenerative disorders. The approach followed in our study is, in fact, not to replace diseased neurons ("replacement" cell therapy) but to reduce the consequences and the rate of neural cell deterioration by using MSC as a medication. The intention is to exploit their well-known biological function in preserving cell homeostasis and maintaining a healthy microenvironment ("rescue" cell therapy). Due to the complexity and the specialization of the different types of neural cells, a specific replacement cell therapy should be developed for any single disease, while the "rescue" cell therapy may be suitable for many types of neurodegenerative disorders. For all these reasons the experience herein reported may be of general interest as a way to find suitable therapy for orphan neurologic disorders. Moreover, it paves the way to the next phase-II randomized, double-blind, placebo-controlled trial that may provide more valuable insights into the potential efficacy of MSC for neurodegenerative disorders.

Authors' contributions
MC: contributed to the conception, organization and execution of the research project, to the writing of the first draft of the manuscript and to its review and critique. Specifically she performed patient selection, clinical evaluation and follow-up. RG: contributed to the conception, organization and execution of the research project, to the writing of the first draft of the manuscript and to its review and critique. Specifically, she set up the procedures for MSC GMP validation, production and quality controls, wrote the protocols, performed the submission of the trial to the regulatory authorities and coordinated the project. LL: contributed to the conception and organization of the research project and to the review and critique of the manuscript. MI: contributed to the conception, organization and execution of the research project and to reviewing the manuscript. IUI: contributed to the conception, organization and execution of the research project and to writing and reviewing the

Canesi *et al. J Transl Med* (2016) 14:127

Page 10 of 11

manuscript. He also performed the multifactorial movement analysis. RB: contributed to the organization and execution of the research project. Specifically, he defined and performed the procedure for the SPECT and PET analysis. PR: contributed to the organization and execution of the research project and to reviewing the manuscript. Specifically, he monitored the patients just before, during and after (first 24 h) the treatment. GM: contributed to the organization and execution of the research project. Specifically, he defined and performed the procedure for the SPECT analysis. AC: contributed to the execution of the research project. Specifically, she performed neuropsychological assessments. EC: contributed to the evaluation of the results and revised the manuscript. MD: performed biomechanical evaluation of all patients. TM: contributed to the organization and execution of the research project. Specifically, she contributed to set up the procedures for MSC GMP validation and production. MV: contributed to the organization and execution of the research project. Specifically, she contributed to set up the procedures for MSC GMP validation and quality control. SB: contributed to the organization and execution of the research project. Specifically, she contributed to the preparation and the submission of the trial to the regulatory authorities and collected the patients' data patients during the study follow-up. EM: contributed to the organization and execution of the research project. Specifically, she contributed to MSC production. CL: contributed to the organization and execution of the research project. Specifically, she contributed to MSC quality controls. AC: contributed to the execution of the research project. Specifically, he took care of the bone marrow aspiration procedure and of the hematological patient assessment. GP: contributed to the conception, organization and execution of the research project, to the writing of the first draft of the manuscript and to its review and critique. Specifically, he conceived the clinical trial, contributed to study design and to write the research protocol. All authors read and approved the final manuscript.

Author details
[1] Parkinson Institute, G.Pini-CTO, exICP, Milan, Italy. [2] Cell Factory, Unit of Cell Therapy and Cryobiology, Fondazione IRCCS Ca' Granda Ospedale Maggiore Policlinico, Via F Sforza 35, 20122 Milan, Italy. [3] Interventional Neuroradiology Unit, Fondazione IRCCS Ca' Granda Ospedale Maggiore Policlinico, Milan, Italy. [4] Julius-Maximilians-Universität Würzburg and Neurologische Klinik, Universitätsklinik Würzburg, Würzburg, Germany. [5] Department of Pathophysiology and Transplantation, Human Physiology Section, Università degli Studi di Milano, Milan, Italy. [6] Nuclear Medicine Unit, Fondazione IRCCS Ca' Granda Ospedale Maggiore Policlinico, Milan, Italy. [7] Neurosurgery Unit, Fondazione IRCCS Ca' Granda Ospedale Maggiore Policlinico, Milan, Italy. [8] Fondazione IRCCS Policlinico San Matteo, Pavia, Italy. [9] Bone Marrow Transplantation Center, Fondazione IRCCS Ca' Granda Ospedale Maggiore Policlinico, Milan, Italy.

References
1. Bower JH, Maraganore DM, McDonnell SK, Rocca WA. Incidence of progressive supranuclear palsy and multiple system atrophy in Olmsted County, Minnesota, 1976 to 1990. Neurology. 1997;49:1284–8.
2. Schrag A, Ben-Shlomo Y, Quinn NP. Prevalence of progressive supranuclear palsy and multiple system atrophy: a cross-sectional study. Lancet. 1999;354:1771–5.
3. Nath U, Ben-Shlomo Y, Thomson RG, et al. The prevalence of progressive supranuclear palsy (Steele–Richardson–Olszewski syndrome) in the UK. Brain. 2001;124:1438–49.
4. Nath U, Ben-Shlomo Y, Thomson RG, Morris HR, Wood NW, Lees AJ, et al. Movement Disorders Society Scientific Issues Committee report: SIC task force appraisal of clinical diagnostic criteria for Parkinsonian disorders. Mov Disord. 2003;18:467–86.
5. Bensimon G, Ludolph A, Agid Y, Vidailhet M, Payan C, Leigh PN, et al. Riluzole treatment, survival and diagnostic criteria in Parkinson plus disorders: the NNIPPS study. Brain. 2009;132:156–71.
6. Hauw JJ, Daniel SE, Dickson D, Horoupian DS, Jellinger K, Lantos PL, et al. Preliminary NINDS neuropathologic criteria for Steele–Richardson–Olszewski syndrome (progressive supranuclear palsy). Neurology. 1994;44:2015–9.
7. Respondek G, Roeber S, Kretzschmar H, Troakes C, Al-Sarraj S, Gelpi E, et al. Accuracy of the National Institute for Neurological Disorders and Stroke/Society for Progressive Supranuclear Palsy and neuroprotection and natural history in Parkinson plus syndromes criteria for the diagnosis of progressive supranuclear palsy. Mov Disord. 2013;28:504–9.
8. Williams DR, Lees AJ. Progressive supranuclear palsy: clinicopathological concepts and diagnostic challenges. Lancet Neurol. 2009;8:270–9.
9. Burrell JR, Hodges JR, Rowe JB. Cognition in corticobasal syndrome and progressive supranuclear palsy: a review. Mov Disord. 2014;29:684–93.
10. Nath U, Ben-Shlomo Y, Thomson RG, Lees AJ, Burn DJ. Clinical features and natural history of progressive supranuclear palsy: a clinical cohort study. Neurology. 2003;60:910–6.
11. Litvan I, Kong M. Rate of decline in progressive supranuclear palsy. Mov Disord. 2014;29:463–9.
12. Golbe LI, Ohman-Strickland PA. A clinical rating scale for progressive supranuclear palsy. Brain. 2007;130:1552–65.
13. Burn DJ, Lees AJ. Progressive supranuclear palsy: where are we now? Lancet Neurol. 2002;1:359–69.
14. Papapetropoulos S, Singer C, McCorquodale D, Gonzalez J, Mash DC. Cause, seasonality of death and co-morbidities in progressive supranuclear palsy (PSP). Parkinsonism Relat Disord. 2005;11:459–63.
15. Boxer AL, Lang AE, Grossman M, Knopman DS, Miller BL, Schneider LS, et al. Davunetide in patients with progressive supranuclear palsy: a randomised, double-blind, placebo-controlled phase 2/3 trial. Lancet Neurol. 2014;13:676–85.
16. Stamelou M, Reuss A, Pilatus U, Magerkurth J, Niklowitz P, Eggert KM, et al. Short-term effects of coenzyme Q10 in progressive supranuclear palsy: a randomized, placebo-controlled trial. Mov Disord. 2008;23:942–9.
17. Cova L, Bossolasco P, Armentero MT, Diana V, Zennaro E, Mellone M, et al. Neuroprotective effects of human mesenchymal stem cells on neural cultures exposed to 6-hydroxydopamine: implications for reparative therapy in Parkinson's disease. Apoptosis. 2012;17:289–304.
18. Dominici M, Le Blanc K, Mueller I, Slaper-Cortenbach I, Marini F, Krause D, et al. Minimal criteria for defining multipotent mesenchymal stromal cells. The International Society for Cellular Therapy position statement. Cytotherapy. 2006;8:315–7.
19. Horwitz EM, Le Blanc K, Dominici M, Mueller I, Slaper-Cortenbach I, Marini FC, et al. Clarification of the nomenclature for MSC: The International Society for Cellular Therapy position statement. Cytotherapy. 2005;7:393–5.
20. Giordano R, Canesi M, Isalberti M, Isaias IU, Montemurro T, Viganò M, et al. Autologous mesenchymal stem cell therapy for progressive supranuclear palsy: translation into a phase I controlled, randomized clinical study. J Transl Med. 2014;12:14.
21. Bossolasco P, Cova L, Calzarossa C, Servida F, Mencacci NE, Onida F, et al. Metalloproteinase alterations in the bone marrow of ALS patients. J Mol Med (Berl). 2010;88:553–64.
22. Goetz CG, Tilley BC, Shaftman SR, Stebbins GT, Fahn S, Martinez-Martin P, et al. Movement Disorder Society-sponsored revision of the unified Parkinson's disease rating scale (MDS-UPDRS): scale presentation and clinimetric testing results. Mov Disord. 2008;23:2129–70.
23. Goetz CG, Poewe W, Rascol O, Sampaio C, Stebbins GT, Counsell C, et al. Movement Disorder Society Task Force report on the Hoehn and Yahr staging scale: status and recommendations. Mov Disord. 2004;19:1020–8.

Canesi *et al. J Transl Med* (2016) 14:127

Page 11 of 11

24. Folstein MF, Folstein SE, McHugh PR. "Mini-mental state". A practical method for grading the cognitive state of patients for the clinician. J Psychiatr Res. 1975;12:189–98.
25. Isaias IU, Benti R, Cilia R, Canesi M, Marotta G, Gerundini P, et al. [123I] FP-CIT striatal binding in early Parkinson's disease patients with tremor vs. akinetic-rigid onset. NeuroReport. 2007;18:1499–502.
26. Carpinella I, Crenna P, Calabrese E, Rabuffetti M, Mazzoleni P, Nemni R, et al. Locomotor function in the early stage of Parkinson's disease. IEEE Trans Neural Syst Rehabil Eng. 2007;15:543–51.
27. Winter DA, Patla AE, Frank JS. Assessment of balance control in humans. Med Prog Technol. 1990;16:31–51.
28. Prieto TE, Myklebust JB, Hoffmann RG, Lovett EG, Myklebust BM. Measures of postural steadiness: differences between healthy young and elderly adults. IEEE T Bio-Med Eng. 1996;43:956–66.
29. Duarte M, Zatsiorsky VM. Patterns of center of pressure migration during prolonged unconstrained standing. Mot Control. 1999;3:12–27.
30. Raymakers JA, Samson MM, Verhaar HJ. The assessment of body sway and the choice of the stability parameters. Gait Posture. 2005;21:48–58.
31. van der Kooij H, van Asseldonk E, van der Helm FC. Comparison of different methods to identify and quantify balance control. J Neurosci Meth. 2005;145:175–203.
32. Martin M, Shinberg M, Kuchibhatla M, Ray L, Carollo JJ, Schenkman ML. Gait initiation in community-dwelling adults with Parkinson disease: comparison with older and younger adults without the disease. Phys Ther. 2002;82:566–77.
33. Brazzini A, Cantella R, De la Cruz A, Yupanqui J, León C, Jorquiera T, et al. Intraarterial autologous implantation of adult stem cells for patients with Parkinson disease. J Vasc Interv Radiol. 2010;21:443–51.
34. Hauser RA, Freeman TB, Snow BJ, Nauert M, Gauger L, Kordower JH, et al. Long-term evaluation of bilateral fetal nigral transplantation in Parkinson disease. Arch Neurol. 1999;56:179–87.
35. Amano S, Skinner JW, Lee HK, Stegemöller EL, Hack N, Akbar U, et al. Discriminating features of gait performance in progressive supranuclear palsy. Parkinsonism Relat Disord. 2015;21:888–93.
36. Lee PH, Lee JE, Kim HS, Song SK, Lee HS, Nam HS, et al. A randomized trial of mesenchymal stem cells in multiple system atrophy. Ann Neurol. 2012;72:32–40.
37. Karlupia N, Manley NC, Prasad K, Schäfer R, Steinberg GK. Intraarterial transplantation of human umbilical cord blood mononuclear cells is more efficacious and safer compared with umbilical cord mesenchymal stromal cells in a rodent stroke model. Stem Cell Res Ther. 2014;5:45–63.
38. Cui L, Kerkelä E, Bakreen A, Nitzsche F, Andrzejewska A, Nowakowski A. The cerebral embolism evoked by intra-arterial delivery of allogeneic bone marrow mesenchymal stem cells in rats is related to cell dose and infusion velocity. Stem Cell Res Ther. 2015;6:11–9.
39. Janowski M, Lyczek A, Engels C, Xu J, Lukomska B, Bulte JWM, et al. Cell size and velocity of injection are major determinants of the safety of intracarotid stem cell transplantation. J Cereb Blood Flow Metab. 2013;33:921–7.

ACKNOWLEDGMENTS